

Influence of Increased Human Presence in the Mills River Basin on Water Availability
and Drought

by

Jared Lee Hodes

Department of Civil and Environmental Engineering
Duke University

Date: _____

Approved:

Ana P. Barros, Supervisor

Marc Jeuland

Mukesh Kumar

Thesis submitted in partial fulfillment of
the requirements for the degree of
Master of Science in the Department of
Civil and Environmental Engineering in the Graduate School
of Duke University

2016

ABSTRACT

Influence of Increased Human Presence in the Mills River Basin on Water Availability
and Drought

by

Jared Lee Hodes

Department of Civil and Environmental Engineering
Duke University

Date: _____

Approved:

Ana P. Barros, Supervisor

Marc Jeuland

Mukesh Kumar

An abstract of a thesis submitted in partial
fulfillment of the requirements for the degree
of Master of Science in the Department of
Civil and Environmental Engineering in the Graduate School of
Duke University

2016

Copyright by
Jared Lee Hodes
2016

Abstract

Periods of drought and low streamflow can have profound impacts on both human and natural systems. People depend on a reliable source of water for numerous reasons including potable water supply and to produce economic value through agriculture or energy production. Aquatic ecosystems depend on water in addition to the economic benefits they provide to society through ecosystem services. Given that periods of low streamflow may become more extreme and frequent in the future, it is important to study the factors that control water availability during these times. In the absence of precipitation the slower hydrological response of groundwater systems will play an amplified role in water supply. Understanding the variability of the fraction of streamflow contribution from baseflow or groundwater during periods of drought provides insight into what future water availability may look like and how it can best be managed. The Mills River Basin in North Carolina is chosen as a case-study to test this understanding. First, obtaining a physically meaningful estimation of baseflow from USGS streamflow data via computerized hydrograph analysis techniques is carried out. Then applying a method of time series analysis including wavelet analysis can highlight signals of non-stationarity and evaluate the changes in variance required to better understand the natural variability of baseflow and low flows. In addition to natural variability, human influence must be taken into account in order to accurately assess

how the combined system reacts to periods of low flow. Defining a combined demand that consists of both natural and human demand allows us to be more rigorous in assessing the level of sustainable use of a shared resource, in this case water. The analysis of baseflow variability can differ based on regional location and local hydrogeology, but it was found that baseflow varies from multiyear scales such as those associated with ENSO (3.5, 7 years) up to multi decadal time scales, but with most of the contributing variance coming from decadal or multiyear scales. It was also found that the behavior of baseflow and subsequently water availability depends a great deal on overall precipitation, the tracks of hurricanes or tropical storms and associated climate indices, as well as physiography and hydrogeology. Evaluating and utilizing the Duke Combined Hydrology Model (DCHM), reasonably accurate estimates of streamflow during periods of low flow were obtained in part due to the model's ability to capture subsurface processes. Being able to accurately simulate streamflow levels and subsurface interactions during periods of drought can be very valuable to water suppliers, decision makers, and ultimately impact citizens. Knowledge of future droughts and periods of low flow in addition to tracking customer demand will allow for better management practices on the part of water suppliers such as knowing when they should withdraw more water during a surplus so that the level of stress on the system is minimized when there is not ample water supply.

Contents

Abstract	iv
List of Tables	viii
List of Figures	ix
Acknowledgements	xix
1. Introduction	1
1.1 Statement of Problem	1
1.2 Research Objectives	2
1.3 Thesis Outline	3
2. Methodology and Preliminary Data Analysis	5
2.1 Study Region	7
2.2 Literature Review and Methods	13
2.2.1 Recession Curve	13
2.2.2 Baseflow Estimation	16
2.2.3 Instream Flow	18
2.3 Application to Mills River Basin	19
2.3.1 Recession Curve Constants	22
2.3.1.1 Baseflow Recession Constants and Streamflow	22
2.3.1.2 Extreme Baseflow Recession Constants	27
2.3.2 Baseflow Estimation	34
2.3.2.1 Streamflow Filtering	34

2.3.2.2 Time Series Analysis.....	36
2.3.3 Instream Flow and Combined Demand.....	44
3. Model Evaluation.....	47
3.1 Precipitation	49
3.2 Streamflow.....	51
3.3 Other Parameters.....	55
4. Evidence of Combined Natural and Human Systems.....	62
4.1 Sustainability.....	62
4.2 Streamflow and Baseflow Time Series Signatures.....	71
5. Characterization of Hydrogeological Heterogeneity based on Baseflow Variability ...	80
6. Conclusions.....	103
6.1 Limitations.....	104
6.2 Contributions	105
6.3 Recommendations for Future Work	106
AppendixA	107
AppendixB	110
Bibliography	112

List of Tables

Table 1: Percent population increase over select time periods for areas of interest. Note that Mills River has N/A for some because it did not exist prior to 2003. 9

Table 2: Specific of some of the DCHM runs with results present in this section. Lateral routing coefficients are used to change the rate of subsurface routing.....59

Table 3: Unsustainable days per year for (50 cfs, 7Q2, and 7Q10) in that order for each of the given time periods and different levels of human demand. Note that combined (both) takes into account both WTPs. HWTP data starts in the 1983 water year, AWTP in 2000, hence the N/A's in some places. Yellow highlighted periods is the actual combined demand during that given period. The orange highlighted period is the overall average for the entire period (all 3 yellow periods). All other values are what the numbers would have been if that level of human demand had theoretically occurred.....65

Table 4: USGS stream gauge stations used. Station number as seen in figures going forward, numbered from west to east. Start date is the start date used in the proceeding analysis for complete water years (October 1-September 30). End date used for all sites was 9/30/201582

List of Figures

- Figure 1: Buncombe and Henderson County populations since 1920. Note that data points on the decade are census data from April 1 of that year and data points in between decades are estimates for July 1 of that year (US Census Bureau, factfinder.census.gov).....8
- Figure 2: City of Asheville and Hendersonville populations since 1970. Note that data points on the decade are census data from April 1 of that year and data points in between decades are estimates for July 1 of that year (US Census Bureau, factfinder.census.gov).....9
- Figure 3: The MRB and Mills River stream network shown with Henderson, Buncombe, Transylvania, and Haywood counties. Asheville and Hendersonville are also shown because they are stakeholders in the basin.....10
- Figure 4: Mills River Basin elevation, stream network, stream gauge location, and the sites of water intakes for the two water municipalities in the basin.....11
- Figure 5: Section of the streamflow time series used to illustrate hydrograph recession limb separation. Q_0 is N days after the hydrograph peak and Q_t is $2N$ days after Q_015
- Figure 6: Two of the computerized hydrograph analysis methods (sliding interval on the left and fixed interval on the right) from White and Sloto (1990). Each takes the minimum value in the window and in the case of the sliding interval assigns that value to the middle point or in the case of fixed interval every point in the window.....18
- Figure 7: Log Pearson type III distribution fit annual minima from seven day mean streamflow. Desired return period (2, 5, 10, 25, and 50 years) streamflow estimates are circled in red.....20
- Figure 8: The lower end of the streamflow time series is shown to breach the 7Q50 threshold approximately once per 50 years (1954 and 2008), but with a couple of instances in the late 1990's/early 2000's where it was also very dry.....21
- Figure 9: 2008 water year (October 2007- September 2008) hydrograph displaying the 7-day mean streamflow along with the 2-year and 50-year return period 7-day mean

streamflow values. The onset of the extreme hydrological drought of 2008 in late summer is highlighted by the box in the figure.....21

Figure 10: Time series of calculated baseflow recession constants (n=1264). Mean=0.94, standard deviation=0.033.....23

Figure 11: The average hydrograph for the Mills River at USGS station 03446000. The top panel shows the average hydrograph by day of the year and the bottom panel is the top panel smoothed over a 31 day period (roughly a monthly moving average)....24

Figure 12: Monthly means of baseflow recession constants and the corresponding coefficient of variation.....25

Figure 13: Distribution of baseflow recession constants with respect to the peak of the hydrograph from which the constant was calculated.....26

Figure 14: Distribution of streamflow peaks associated with extreme baseflow recession constants (n=41). Note that the mean of the peaks associated with these extreme cases is three time as large as the mean of all hydrograph peaks.....28

Figure 15: Intra-annual distribution of extreme baseflow recession constants. Late summer and early fall months are the period of greatest occurrence.....29

Figure 16: An individual hydrograph from which the associated extreme baseflow recession constant was calculated (shown in blue) and the precipitation event that led to the hydrograph peak (shown in magenta).....30

Figure 17: Top panel shows the precipitation peak associated with each extreme ($k < 0.87$) baseflow recession constant event. The red line shows the mean+2*standard deviation of the non zero (rain occurring) days from the Hendersonville Rain Station. Bottom panel shows entire time series of Hendersonville precipitation for reference.....31

Figure 18: Distribution of streamflow peaks associated with high extreme baseflow recession constants (n=115).....32

Figure 19: Intra-annual distribution of high baseflow recession constants. Higher values are associated with shallower hydrograph recession limbs and lower hydrograph peaks, and we see this in the high frequency during the summer (lower flow) months.....33

Figure 20: Top panel shows the precipitation peak associated with each high baseflow recession constant event. The red line in the bottom panel shows the maximum of the top panel in reference to the Hendersonville Rain Station time series.....33

Figure 21: Example of a graphically estimated baseflow time series by hand (White and Sloto, 1990). The estimated baseflow does not have flashy peaks like the streamflow time series, but rather a much slower and gradual response.....35

Figure 22: Applying the first sliding filter to the Mills River streamflow data yields the time series in red. Compared with the shape of the estimated baseflow in Fig. 20, the new time series is not representative of a slow groundwater response, having distinct peaks under many of the streamflow hydrograph peaks, but rather interflow from surface-subsurface interactions. Y axis is in log scale for comparison to Fig. 21..35

Figure 23: The lower end of the streamflow time series and the progression going from streamflow to subsurface flow and to estimated baseflow.....36

Figure 24: Wavelet analysis of MRB baseflow anomaly. The main things to note are the global wavelet spectrum peak at 9.8 years and the variation of the scale averaged variance.....38

Figure 25: Wavelet analysis of MRB baseflow normalized by the standard deviation. Difference from Fig. 24 is in the scale average time series, split between 1-10 year and 10-20 year. 1-10 year accounts for nearly all of the variance.....39

Figure 26: Wavelet analysis of MRB subsurface flow anomaly. Note the global wavelet spectrum peaks at 1 and 6.9 years (annual variability and ENSO time scales) and the variation of the scale averaged variance.....40

Figure 27: Wavelet analysis of MRB streamflow normalized by the standard deviation. The main things to note are the global wavelet spectrum peak at 1 and 6.9 years (annual variability and ENSO time scales) and the variation of the scale average variance.....41

Figure 28: The 1-20 year scaled average variance of Mills River streamflow, subsurface flow, and baseflow.....42

Figure 29: Baseflow generally accounts for very little of the overall streamflow variance, but a few cases, it appears to peak when subsurface variance decreases and accounts for a more significant portion of the streamflow scale average variance.....42

Figure 30: MRB seasonal baseflow wavelet analysis. Seasons of April, May, June (amj), July, August, Spetember, October (jaso), and November, December, January, February, and March (ndjfm) were used to separate the hurricane season from typical weather in the spring and early summer. Baseflow was initially calculated on a monthly basis (via an altered Eq. 6 using monthly minimum instead of water year minimum) and then averaged according to the seasons just listed. An ENSO (6.9 years) associated peak in the global spectrum is very pronounced and especially strong in the second half of the time series, looking at 30(b).....43

Figure 31: The lower portion of the Mills River streamflow time series and three potential instream flow requirements (7Q10, 50cfs, and 7Q2). 50 cfs (1.416 m³/s) is the current threshold used by HWTP. Changing the instream flow requirement can change the appearance of how sustainable an area is.....46

Figure 32: Rain gauge locations. The northern station is in Asheville (<http://www.ncdc.noaa.gov/cdo-web/datasets/GHCND/stations/GHCND:USW00013872/detail>) and the southern station is in Hendersonville (<http://climate.ncsu.edu/cronos/?station=313976&temporal=D>)50

Figure 33: Cumulative precipitation over a single day during a large precipitation event in March 2008. Notice the gradient going from high precipitation to low as you go from high elevations to low (west to east). The general gradient is in line with what would be expected and has been observed (McGill Associates, 2012). If these values are overestimated from the observed it would explain the overestimation of hydrograph peaks that will be seen in section 3.2.....51

Figure 34: 2008 Water Year. 15 minute interval streamflow data from Mills River USGS station compared with 5 minute interval DCHM model output streamflow aggregated to 15 minute interval.....52

Figure 35: Residual of time series from figure 34. 1.58% of the residual is more than 5 m³/s away from the accepted value and 0.54% is more than 10m³/s away from the accepted value.....52

Figure 36: Shown are the USGS and DCHM time series resulting from the first filter application (Eq. 5), as well as the interflow from DCHM output. Interflow in the model output varies a great deal more than the filtered results in response to precipitation events. Looking at the shape of the peaks from the filtered time series they are still not indicative of a slow response, as they are still flashy.....53

Figure 37: Shown are the USGS and DCHM time series resulting from the second filter application (Eq. 6 using monthly minimum), as well as the baseflow output from DCHM. The DCHM baseflow output is still lower in most cases than the twice filtered time series.....54

Figure 38: Two sets of model outputs seen in magenta and blue. Decreasing the maximum channel width from 50m to 30m is correct in that it is a more accurate representation of the Mills River and as expected gives a higher peak streamflow.....56

Figure 39: Channel width distribution in MRB. Most of the basin is comprised of smaller headwater streams, only becoming larger once the topographic relief decreases in the eastern portion of the basin.....56

Figure 40: Changing the subsurface routing will have a significant effect on the location of the lower end of the hydrograph. There are three coefficients changed in each scenario (one for soil layer 2, one for soil layer 3, and one for soil layer 4). High (Run2) = 2000, 3, 0.5. Intermediate (Run4) = 1000, 1.5, 0.15. Low (Run 3) = 100, 0.5, 0.05. Runs are listed in Table 2 below.....57

Figure 41: The difference in soil moisture for each of the four soil layers (intermediate routing – low routing). Calculated as the basin average of soil moisture at each time step and then subtracted. Note that Tropical Storm Fay occurred in late August, which is the reason for the significant increase for layers 1, 2, and 3.....58

Figure 42: Varying soil moisture conditions after four spins using different lateral routing coefficients. High (Run 2), Intermediate (Run 4), Inter-Low (Run 5), and Low (Run 3) from Table 2. Notice how layer 4 is most noticeably different because the higher the lateral routing, the more water that will make its way to the stream network. The 4 years of spin prior to this figure is enough time to have differentiation between the base layers (layer 4).....60

Figure 43: Over the course of October there is a period of little to no rain (mid to late October) and then a noticeable rainfall/streamflow response event near the end of the month (see Fig. 34 for hydrograph response). The change from October 16 to October 27 is very noticeable in the first two layers, but there is no visible change in layers three or four. This is due to the fact that the upper layers respond at shorter time scales while lower layers respond at much longer time scales.....61

Figure 44: Daily Streamflow compared to natural and combined demand. Note that all values are aggregated to m³/day. Natural demand is defined by 50 cfs, which is the

value below which the HWTP alters its uptake pattern. Combined demand is defined as the amount of water withdrawn from the river downstream of the USGS gauge plus natural demand.....62

Figure 45: Introduction of human demand (HWTP only) in 1982 and increased human demand (HWTP&AWTP) in 2000 increases the number of unsustainable days within a given water year. Note that AWTP did not open until 2000 and HWTP data was not consistent until 1982. 2008 was an especially dry year and is reflected in the figure....63

Figure 46: The effect of combining human demand with natural demand can be seen in the difference between the blue, green, and red data points. Prior to 2000 the green and red points will be identical because there was no additional water treatment plant open yet. PDSI is the Palmer Drought Severity Index, calculated for NC climate division 1 for a four month period June-September (<http://www.ncdc.noaa.gov/cag/>).....64

Figure 47: Distribution of naturally occurring unsustainable days. Note that 2008 (severe drought) is the tallest peak. There appears to be a longer term trend getting wetter from 1940-1975 and then drier from 1975 on.....67

Figure 48: Distribution of naturally occurring unsustainable days. As expected the months with the higher frequencies occur during the lower values of streamflow on average.....67

Figure 49: Average number of days per year where observed mean daily streamflow is below the instream flow requirement threshold.....69

Figure 50: Distribution of naturally occurring unsustainable days. Two nearby precipitation station records (smoothed to six month average). Almost every multiyear trough in the precipitation data corresponds to a cluster of high frequency years of unsustainable days (meteorological drought conditions).....72

Figure 51: Two year running mean of Mills River streamflow to explore any differences before and after 1975 (4/1/1975 is the midpoint of the data). There is minimal difference in the mean before and after 4/1/1975 (4.80 vs 4.85), but there is a large change in variance (0.63 vs 1.40). This is evident in the much larger swings between periods of high and low streamflow post 1975.....72

Figure 52: Unsustainable days over time of the Mills River with different levels of human influence over time, first with the addition of HWTP and then AWTP. The

number of unsustainable days that would have occurred given zero human demand is shown in blue.....75

Figure 53: Fraction of unsustainable days attributed to natural demand only. Natural demand (50 cfs instream flow requirement) is still the main driver of unsustainability, but there are some years where that is not the case.....76

Figure 54: Contribution to streamflow by component of streamflow. It is evident that baseflow is consistently the overwhelming contributor to streamflow in the periods of low streamflow during the summer and fall. The baseflow time series used was calculated by Eq. 5 and 6. Interflow was calculated by Eq. 5. Runoff is the difference between streamflow and interflow.....77

Figure 55: Contribution to streamflow by component of streamflow. The difference from Fig. 54 is an alteration to Eq. 6. Instead of taking the minimum value for the entire water year, the minimum value per month was used instead. This takes away some of the previously calculated interflow and attributes it instead to baseflow.....78

Figure 56: USGS streamflow gauge sites with at least 54 years of data, divided by physiographic regions as defined by USGS (n=126 sites). Note that the stations are numbered from 1 to 126 by longitude (west to east).....85

Figure 57: Normalized baseflow variance for the 126 stations in question. Red denotes Plateau region, green Valley Ridge, blue Blue Ridge, magenta Piedmont, and cyan Coastal Plain. Note that Mills River is Station 42 (Blue Ridge).....86

Figure 58: Zones used to search for tracks of hurricanes and tropical storms through the National Hurricane Center (<https://coast.noaa.gov/hurricanes/>). 200 km radius (max), centered at 35.5 N, 80W and 35.5N, 84W.....88

Figure 59: Temporal distribution of tropical storm and hurricane tracks passing through the selected zone seen in Fig. 58.....88

Figure 60: Storm tracks of major hurricanes and tropical storms of 2004. Geographic location and thus proximity to storms can also help to explain differences in baseflow response.....89

Figure 61: The transect shown in white creates a set of stations such that the stations progress from one physiographic region to the next as you change longitude.....90

Figure 62: Normalized baseflow variance for the 53 stations within the transect defined in Fig. 61. Red denotes Plateau region, green Valley Ridge, blue Blue Ridge, magenta Piedmont, and cyan Coastal Plain.....91

Figure 63: Normalized scaled averaged variance of seasonal baseflow for the 126 stations in question. Red denotes Plateau region, green Valley Ridge, blue Blue Ridge, magenta Piedmont, and cyan Coastal Plain. Note that Mills River is Station 42 (Blue Ridge). The baseflow used here is seasonal as opposed to per water year (see Fig. 30 for explanation of seasonal baseflow calculation).....92

Figure 64: SE US precipitation anomaly (<http://www.ncdc.noaa.gov/cag/>) and PC 1. The anomaly was calculated from a two year average of precipitation. For example the precipitation anomaly for 1963 is from the two year mean precipitation for 10/1961 - 9/1963. PC 1 for 1963 is a measure of the 1963 water year (10/1962 - 9/1963). The two year precipitation average is important because large storms occurring in September will have significant impact on baseflow in October. This captures both precipitation during the respective water year as well as the antecedent precipitation that has a future impact on slow response baseflow.....94

Figure 65: Hurricane and tropical storm tracks during 1961-1975 plotted with EOF 2. Note that EOF 2 is calculated for the entire period (1961-2015). Notice the lack of storm tracks over the eastern Blue Ridge and western Piedmont Provinces. Scarcity of storm tracks during this generally wet period, especially the early 1970's, is in line with the idea that the wet early 1970's were a result of high precipitation, but not due to impact of tropical storms and hurricanes.....95

Figure 66: Hurricane and tropical storm tracks during 1976-1995 plotted with EOF 2. Note that EOF 2 is calculated for the entire period (1961-2015). Notice the lack of storm tracks over the eastern Blue Ridge and western Piedmont Provinces compared to the western Appalachians and Coastal Plain.....96

Figure 67: Hurricane and tropical storm tracks during 1996-2015 plotted with EOF 2. Note that EOF 2 is calculated for the entire period (1961-2015). Notice the lack of storm tracks over the eastern Blue Ridge and western Piedmont Provinces compared to the western Appalachians and Coastal Plain. Also this period has many more storms over the Appalachians than in Fig. 65 and 66. The higher number of large storms over the Appalachians during this period is in line with idea that some of the more recent wet years (2004 in particular) were heavily impacted by tropical storms and hurricanes...96

Figure 68: AMO 12 month running average SST anomaly and PC 2 for normalized baseflow. Inverse relationship both long and short term is evident. Monthly AMO data (unsmoothed) from <http://www.esrl.noaa.gov/psd/data/timeseries/AMO/>.....97

Figure 69: Time series of PC 1 and PC 2. PC 2 trending negatively over the length of the time series and becomes more extreme in most recent decades. Strong negative values of PC 2 can be associated with years heavily influenced by passing tropical storms and hurricanes.....98

Figure 70: Normalized baseflow EOF 3 spatial distribution. Blue is negative while black it positive and the size of the circle indicates magnitude of variability.....99

Figure 71: EOF 3 and elevation of 126 stations. Stations in the western portion that are mostly in mountainous terrain in the Blue Ridge and Valley and Ridge Provinces have non-stationarity and variability in the same direction, while stations 75 and above located in the eastern portion of the Piedmont Province and Coastal Plain exhibit non-stationarity in the same direction (opposite to that of the western stations).....99

Figure A1: Semi logarithmic plot of two example hydrographs (seen in Fig. 5). The red circle marks the second change in slope of the hydrograph after the peak. This marks the beginning of the baseflow recession curve. The red circles are also the points calculated as N days after the peak, which shows that the chosen recession period definition is in agreement with the graphical definition of the start of the baseflow recession curve.....107

Figure A2: Asheville Water Treatment Plant river uptake data. WTP daily quantity of water treated data available for length of record (2000-2015), but raw water withdrawn from Mills River only available for 2009-2015 (cyan color). Average ratio per day of year between treated and raw water for 2009-2015 was calculated and the applied to treated data for 2000-2009 to obtain an estimate for raw water (red color).....108

Figure A3: The principal components are calculated from the mean time series of normalized baseflow of all 126 stations. It is expected that PC 1 would be in agreement with most of the mean time series since it captures most of the variance. The regions where there is not perfect agreement can be explained by PC 2 and 3....108

Figure A4: Underlying geology (focusing on North Carolina here). Note that age increases as you go down the explanation of colors. Older rocks (more consolidated)

are in the western and central part of the state where the mountainous regions are. Younger rocks (less consolidated) are located in the eastern portion of the state. This accounts for some of the difference in variability and timing of baseflow at different stations throughout the region.....109

Acknowledgements

I am very grateful for my adviser Dr. Barros and all of the opportunities and guidance she has provided me with. Thank you to committee members Dr. Marc Jeuland and Dr. Mukesh Kumar for their participation on the committee. Thank you to former and current research group members Jing Tao, Lauren Lowman, and Malar Arulraj for their assistance. I would also like to thank the Duke CEE department for providing me with the opportunity to attend this institution. From the Mills River, North Carolina area I would like to thank April Graham and Jere Brittain of the Mills River Partnership, as well as Ron Reid of Hendersonville Water Treatment Plant and Reggie Widemon of Asheville Water Treatment Plant for assisting in data collection.

1. Introduction

1.1 Statement of the Problem

Approximately 60-70% of the world's population depends on mountains for freshwater needs including drinking water, water for food production, industrial use, and ecosystem services (Barros, 2013). Classical water infrastructure in these regions is primarily designed to meet human water demand associated with agriculture, tourism, and economic development. Often overlooked and ignored is the fundamental interdependence of human water demand, ecosystem water demand, water rights and allocation, and water supply (Gleick, 1998; Gossling, 2001; Wu et al., 2013). A truly sustainable system for water resources takes into account ecosystem demand along with human infrastructure and economic demand, as well as the feedbacks that exist between them (Loucks et al., 2000). Allocation policies should take into account basin resilience, that is the amount of stress the system can handle under varying future scenarios (Vorosmarty et al., 2000).

Mountain basins and the headwaters of river basins along the foothills of major mountain ranges are undergoing rapid environmental change due to urban development, land acquisition by investors, population increase, and climate change (Vorosmarty et al., 2000). These source regions of freshwater are of increasing interest as populations continue to increase and development begins to encroach upon previously undeveloped regions (Monticino et al., 2007). Changes in stress on the natural system

can be anthropogenic in the form of population increase, land use change, economic development, or may be due to the natural system in the form of natural variability and a decrease in water supply due to changes in precipitation. Climate change can lead to a shift in seasonality for both precipitation and runoff as well as changes in total streamflow, which will have consequences for future water availability (Viviroli et al., 2011). A change in water supply due to climate change or climate variability could potentially render traditional methods of water management obsolete if management is not adaptive (Hao et al., 2015).

1.2 Research Objectives

The overarching goal of this thesis is to investigate the impact of increased human presence on the availability of water for both natural and human systems with regard to periods of low flow and drought in the Mills River Basin (MRB), North Carolina as a case-study representative of ongoing processes in mountain watersheds anywhere. Focusing on baseflow, the slow, deep subsurface response of streamflow, long term regimes can be characterized and the impact of increased human activity in the region can be elucidated. Using the Duke Combined Hydrology Model (DCHM), the spatial and temporal basin response to precipitation events will be examined to understand the relationship between streamflow and distributed soil moisture which has implications for the typical streamflow response under wet and dry conditions and

as a function of season. This knowledge can be used to investigate what future responses might look like under varying conditions. Initial analyses led to three main hypotheses:

1. Increased human presence in the MRB leads to a decrease in sustainability of the combined natural-human system, but the main controller of the level of sustainability is determined by the qualification of natural demand.

2. Baseflow variations over time show long term natural variability with strong non-stationarity associated with years of frequent heavy precipitation events such as hurricanes.

3. Baseflow is the only resilient contribution to streamflow during drought. Therefore, hydroecological sustainability hinges on managing water demand using baseflow.

The first two hypotheses will be investigated using streamflow observations and water use records. The seasonality of baseflow and its implication for water resources management including ecological in-streamflow requirements will rely on the DCHM.

1.3 Thesis Outline

The presentation of the thesis is organized as follows. Chapter 2 describes the data used, provides a general description of the chosen study area, and presents some initial analysis. Chapter 3 includes results from the DCHM and a discussion of model implementation for this study. Chapter 4 presents findings that describe the impact of the combining human and natural systems and water demands. Chapter 5 looks at the

long term baseflow of the MRB in the context of regional hydrogeology and climate variability. Concluding remarks are given in Chapter 6.

2. Methodology and Preliminary Data Analysis

The purpose of this chapter is to describe the methodology used in this study, including literature review and initial results from the chosen methods. Some of the data used in modelling the study region include the DEM (Digital Elevation Model) of the MRB and surrounding regions, soil hydraulic property data, and meteorological forcing data. The DEM was obtained from the National Elevation Dataset provided by USGS at 3 arcsec resolution and was reprojected and spatially resampled to the model grid at 250m resolution (Tao and Barros, 2014). Soil hydraulic properties including saturated hydraulic conductivity, porosity, field capacity and wilting point were extracted from the State Soil Geographic (STATSGO) database provided by the US Geological Survey (Schwarz and Alexander, 1995) following the methods described by Tao and Barros (2014a) and can be found at <http://iphex.pratt.duke.edu/DataCenter/Time-invariantDatasets/SoilParameters>. Meteorological forcing data for the DCHM came from NCEP (National Centers for Environmental Prediction) North American Regional Reanalysis (NARR) products originally at 32 km spatial resolution and 3 hour temporal resolution (Mesinger et al., 2006), including air temperature, air pressure, wind velocity, downward shortwave and longwave radiation and specific humidity. Stage IV precipitation data was downscaled to 1 km using a transient multifractal downscaling method (Nogueira and Barros, 2014 and 2015). All the forcing data were spatially interpolated to 250 m using the nearest neighbor method, and landscape attribute data

were linearly temporally interpolated to 5 min resolution. The bilinear interpolation method was utilized to interpolate NARR fields to finer spatial resolution at 250 m, and linear interpolation was applied in time (Tao and Barros, 2014b).

The interest in baseflow and thus subsurface hydrology is due to the fact that during periods of drought or low flow it is the baseflow and subsurface hydrology that are the main controllers of water availability. Periods of low flow and drought are often the result of extended lack of water input to the basin in the form of precipitation (Dai et al., 2010). A lack of precipitation has a much more severe effect on surface runoff and subsurface flow in the upper soil layers, and thus leaves the long-term response of groundwater and baseflow contributions to streamflow as the primary contributions to streamflow during these periods (Priest, 2004). Characterizing the recession curve of a hydrograph many times over a streamflow time series can help characterize the hydrology of the basin of interest, specifically with regard to withdrawal of water from storage within the basin (Linsley, 1958). Methods that rely on various filter implementations to estimate baseflow from observed streamflow time series are available (Nathan and McMahon, 1990; Arnold and Allen, 1999; Eckhardt, 2008; Murphy et al., 2009) and will be employed here. From baseflow we look at how the natural and human system interaction impacts a basin's sustainability with regard to water availability in Section 4.1. To measure the level of sustainability or lack thereof we must determine what the demand of the combined system is, that is both human demand and

natural/ecosystem demand (Richter et al., 2003; Gleick, 1998). Determination of human demand can be relatively straightforward by water use and withdrawal data (if data is available), but natural/ecosystem demand is often ambiguous and can be defined by various methods, among which instream flow is a common metric (Richter et al., 2003; McKay, 2015). There are numerous definitions and applications of instream flow, which are probed in Sections 2.2.3 and 2.3.3.

2.1 Study Region

The MRB is located in western North Carolina within the southern Appalachian Mountain range. The 73.4 mi² drainage area of the basin encompasses the Mills River and its tributaries the North and South Fork Mills Rivers, all of which feed into the French Broad River at the outlet of the MRB. Of the land in the basin 92.5% is forest, 5.5% is agricultural, and less than 2% is classified as residential or high density (McGill Associates, 2012). The forested region is part of the Pisgah National Forest and the residential and high density sections are part of the Town of Mills River. 75% of the entire basin is controlled by the U.S. Forest Service. The basin itself is located near the expanding cities of Hendersonville and Asheville, serving as the sole provider of water for Hendersonville and as an additional source of water for Asheville. The recent development of high density land use in the MRB and associated land use land cover (LULC) change pressures makes the MRB representative of similar headwater basins in regions of complex terrain undergoing similar pressures including major mountain

ranges such as the Andes and Himalayas. Much of the basin is located in Henderson County, with some of the forested portion located in Transylvania County, and Buncombe County bordering the MRB to the north. It is evident that human influence in the surrounding region has been increasing and by all indications will continue to increase at a rapid pace (US Census Bureau, factfinder.census.gov).

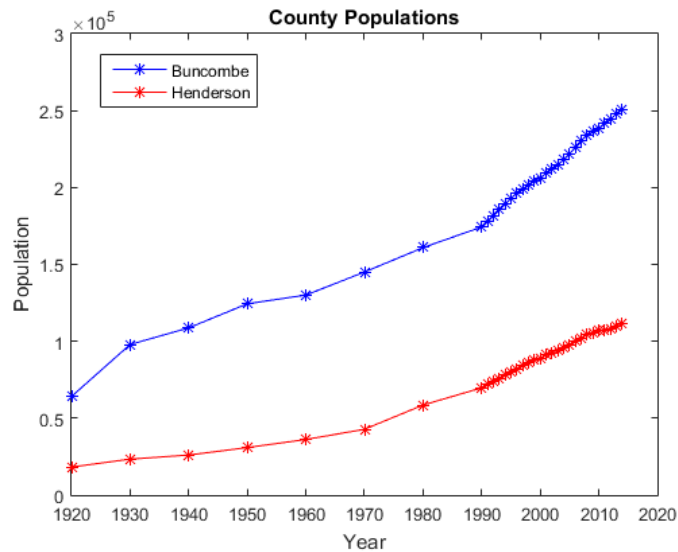


Figure 1: Buncombe and Henderson County populations since 1920. Note that data points on the decade are census data from April 1 of that year and data points in between decades are estimates for July 1 of that year (US Census Bureau, factfinder.census.gov).

Between 2010 and 2014 Asheville’s population increased 5.1% compared to the North Carolina state average of 4.3% (US Census Bureau, factfinder.census.gov). In addition to the rapid increase in population, another indication of recent development in

the area is the founding of the Town of Mills River in 2003. The town itself is located within the MRB in the downstream alluvial plain and foothill section of the basin.

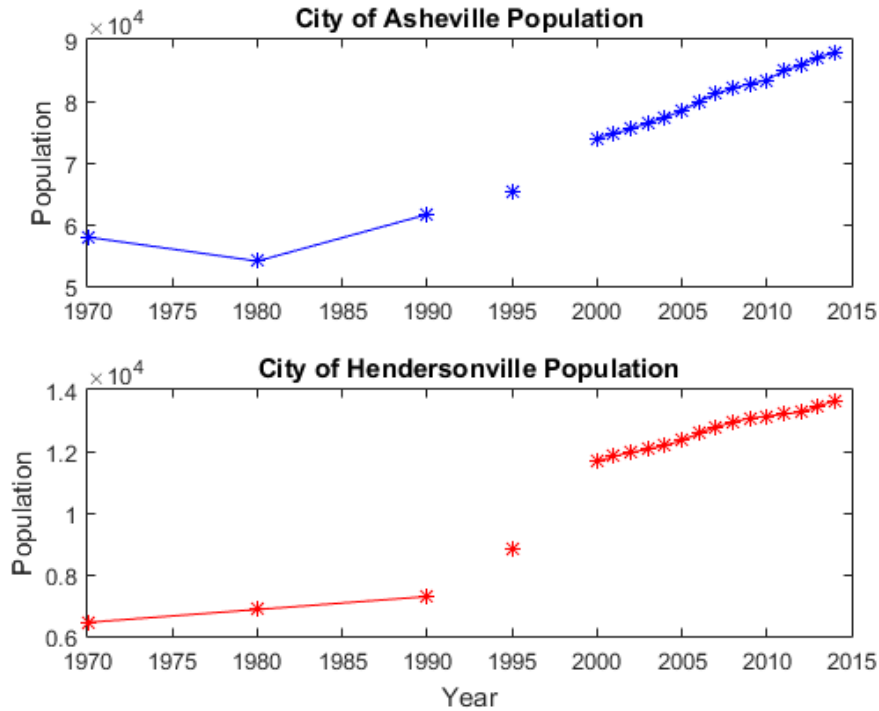


Figure 2: City of Asheville and Hendersonville populations since 1970. Note that data points on the decade are census data from April 1 of that year and data points in between decades are estimates for July 1 of that year (US Census Bureau, factfinder.census.gov).

Table 1: Percent population increase over select time periods for areas of interest. Note that Mills River has N/A for some because it did not exist prior to 2003.

	North Carolina	Henderson County	Buncombe County	Asheville	Hendersonville	Mills River
1970-2014	95.67	159.67	72.72	51.71	111.86	N/A
1970-2000	58.39	108.33	42.24	27.72	81.22	N/A
2000-2014	23.54	24.64	21.43	18.78	16.91	N/A
2003-2014	18.06	17.93	16.54	14.95	13.15	16.64

The increasing population of the area surrounding the MRB serves two purposes: first as an indicator of increased human presence and thus increased water demand in the region, and second as an example for the rest of North Carolina and other regions with similar population trends of how combined systems can be affected by such changes over time (Leu et al., 2008; Tao et al., 2011).

MRB Surrounding Counties and notable Cities

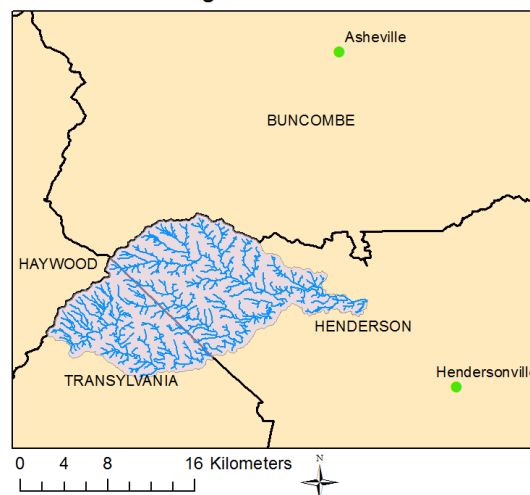


Figure 3: The MRB and Mills River stream network shown with Henderson, Buncombe, Transylvania, and Haywood counties. Asheville and Hendersonville are also shown because they are stakeholders in the basin.

In Table 1 Hendersonville and Asheville are also shown because both cities' municipalities have water treatment plants (WTPs) in the MRB located on the main stem of the Mills River. The Hendersonville Water Treatment Plant (HWTP) has three sources of water in the basin: one at the river intake near the treatment plant and two headwater catchment reservoirs on the tributaries of the Mills River, one on both the North and South Forks. The Asheville Water Treatment Plant (AWTP) has a river intake near the

treatment plant at the end of the Mills River, just before the confluence with the French Broad River. There is one USGS stream gauge on the Mills River (03446000) approximately four kilometers upstream of HWTP (see Fig. 4); this gauge has a contributing drainage area of 66.7 mi².

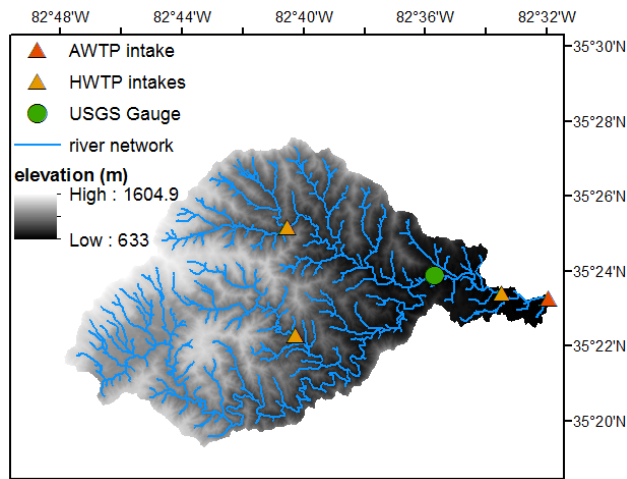


Figure 4: Mills River Basin elevation, stream network, stream gauge location, and the sites of water intakes for the two water municipalities in the basin.

Data for this USGS streamflow gauge (<http://waterdata.usgs.gov/nwis/>; <http://ida.water.usgs.gov/ida/>) includes daily mean streamflow starting in 1924, but 10/1/1934 is used as the start date due to significant missing data in the first portion of the record. Also available is 15 minute increment streamflow data starting from 10/1/1985. The daily data will be used for longer term analysis and the 15 minute increment data will be used to evaluate the DCHM, which has 5 minute temporal resolution.

The Mills River is not only used for potable water, but also for recreation, fishing, agriculture, aquatic life propagation and survival, and maintenance of biological integrity (McGill Associates, 2012). The basin is home to several threatened and endangered species most notably the Appalachian Elktoe mussel, which is considered endangered at both the state and federal levels (Jarvis, 2011). Siltation and erosion due to logging, agriculture, and human activity decrease viable habitat for the mussel (Neves et al., 1997; Fraly and Simmons, 2006). Freshwater mussels can serve as a proxy for freshwater quality because population stability is a good indicator of water quality and water pollution issues, as they are sensitive to changes in water quality and chemical composition. The mussel's dependence on a host fish in addition to its sensitivity to water quality makes it an even more vulnerable species, thus requiring increased awareness with regard to management practices (Jarvis, 2011). The presence of this endangered species and other at risk organisms in the Mills River has led to guidelines and policies for water management groups with regard to ecosystem demand (Mead, 2002).

Riparian rights, which is a common system of water allocation for many areas of the U.S., allows an owner of a plot of land to access the adjacent river or pump groundwater from the plot of land (Dellapenna, 2003). This differs from parts of the western U.S. where a method of prior appropriation is used allocating water to stakeholders and municipalities ahead of time (Hobbs Jr, 2013). Prior appropriation was

adopted in the more arid western U.S. due to the high variability and scarcity of water (Tarlock, 2001). Riparian rights favors those who live upstream such that they have first access to headwaters of rivers. The use of riparian rights appears to be working for the MRB as there is ample precipitation in the region and there are not many residents within the basin with just over 3,000 people (McGill Associates, 2012). If changes in future climate lead to a decreased amount of precipitation received or if the number of landowners in the region increases then a situation could occur where upstream stakeholders have first access to water at the detriment of those downstream (Dellapenna, 2003).

2.2 Literature Review and Methods

2.2.1 Recession Curve

The technique(s) of separating baseflow from the main hydrograph is still an inexact and non-trivial process due to complex and heterogeneous hydrogeology and subsurface processes that are often unique to a given watershed (White and Sloto, 1990; Szilagyi and Parlange, 1998). Immediately following the peak of a hydrograph, the runoff contribution is accounted for followed by interflow contribution and finally baseflow contribution to streamflow. The beginning of the baseflow period is marked by the second inflection point on the falling limb of the hydrograph if a graphical separation by hand were being performed (Linsley, 1958). This point can also be

identified as the point where the second change in slope following the hydrograph peak occurs if plotted on a log scale (see Fig. A1).

To come up with a repeatable definition for the end of direct runoff and beginning of baseflow, Linsley (1958) and subsequently White and Sloto (1990), Vogel and Kroll (1992), Tallaksen (1995), and Arnold et al. (1995) define the beginning of the baseflow recession as starting N days after the hydrograph peak, where:

$$N=bA^{0.2} \quad (\text{Eq. 1})$$

A=drainage area and b=0.8 if A is in units of km², or b=1 if A is in units of mi². White and Sloto (1990) define the length of the baseflow recession as starting N days after the hydrograph peak and ending 2N days after the start of the baseflow recession. Pettyjohn (1979) suggests that this calculation is not reliable for larger basins (A > 2000 mi²). Several basins used in White and Sloto (1990) were of similar size to the MRB, which would suggest the use of this separation technique for smaller basins is appropriate. A graphical representation to illustrate the definition of the baseflow recession period can be seen in Fig. 5 below.

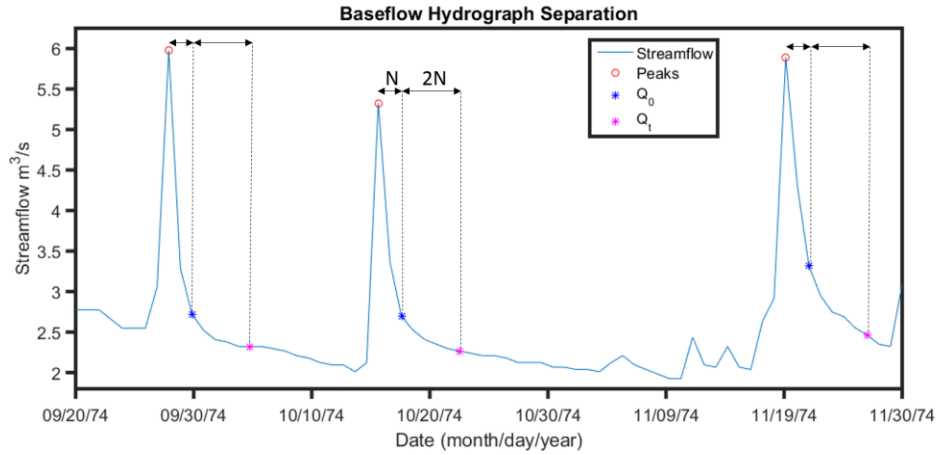


Figure 5: Section of the streamflow time series used to illustrate hydrograph recession limb separation. Q_0 is N days after the hydrograph peak and Q_t is $2N$ days after Q_0 .

Using the defined baseflow recession periods on the hydrograph the corresponding baseflow recession constants (k) were estimated following Linsley (1958):

$$Q_t = Q_0 k^t \quad (\text{Eq. 2})$$

Where Q_t is the streamflow at the end of the baseflow recession, Q_0 is streamflow at the beginning of the baseflow recession, and t is the time between Q_0 and Q_t in days.

Rearranging to isolate and parameterize k :

$$k = (Q_t / Q_0)^{(1/t)} \quad (\text{Eq. 3})$$

$$k = e^{-\alpha t} \quad (\text{Eq. 4})$$

The alpha value in Eq. 4 is commonly referred to as the baseflow recession coefficient and is used in some analyses and automated baseflow separation techniques (Arnold and Allen, 1999; Eckhardt, 2008). Higher values of k closer to 1 reflect a shallower slope of the recession curve on the hydrograph compared to that of a lower value of k . Baseflow recession constants reported in the literature above can range from

[0.7 .995], but typical values used for analysis and automated separation techniques usually range from [0.9 0.95] (Nathan and McMahon, 1990; Arnold and Allen, 1999).

2.2.2 Baseflow Estimation

There are a number of baseflow estimation techniques, some graphical, others employing digital filters (Murphy et al., 2009). The advantage of a graphical separation method is that it is specific to the individual recession curve and takes into account the uniqueness of the morphology of the baseflow hydrograph of the river basin at hand on an event by event basis as different events may engage different soil layers and parts of the aquifer. A drawback of graphical methods is that there is subjectivity on the part of the person carrying out the graphical analysis (Linsley, 1958), and they cannot be automated, therefore it is impractical to apply them to a long time series. Two commonly used recursive digital filters are from Chapman (1999) and Lyne and Hollick (1979). Both recursive digital filters use the baseflow recession constant to help characterize baseflow from streamflow, but while Lyne and Hollick's (1979) filter is commonly used, its criticism includes the fact that it has no true physical basis since it uses a fixed recession constant of 0.925 for best results (Arnold and Allen, 1999), and it further uses the assumption that baseflow is constant when there is no quickflow (surface runoff) (Murphy et al., 2009). Using a fixed recession constant value of 0.925 mitigates the impact of variability between and uniqueness of hydrologic conditions within each basin in question. On the other hand, Murphy et al. (2009) found that the

Chapman (1999) filtering method produced unrealistic baseflow hydrographs for baseflow recession constants less than 0.96. A computerized hydrograph analysis technique proposed by White and Sloto (1990) takes into account the physical characteristics of the hydrograph. White and Sloto's (1990) method, hereafter referred to as WS90, is seen as a valid and accurate method matching well with a baseflow estimation time series graphically calculated by hand, while having the advantage of being readily applied to a long time series, various basins, and eliminating the subjectivity of by hand separation. The WS90 method relies on the application of one of three filters: either a sliding interval minimum method, a fixed interval minimum method (see Fig. 6), or a local minima method. Here we use two filters: first, using one pass over the time series with a sliding interval minimum method, and then a second pass using a fixed interval minimum method, an estimate of groundwater contribution is obtained. The second pass was deemed necessary due to the shape of the time series resulting from the first filter, specifically the fact that the peaks of the once filtered time series are much flashier than one would expect from a slow response groundwater time series. This characteristic is seen in many methods illustrated in method comparison studies such as Eckhardt (2008), Murphy et al. (2009), and Nathan and McMahon (2009). Justification for the application of the second filter pass will be provided in subsequent sections.

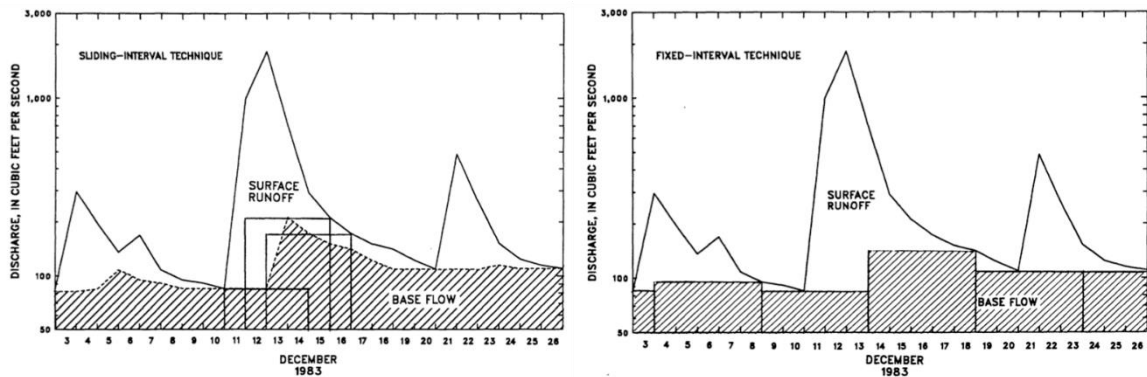


Figure 6: Two of the computerized hydrograph analysis methods (sliding interval on the left and fixed interval on the right) from White and Sloto (1990). Each takes the minimum value in the window and in the case of the sliding interval assigns that value to the middle point or in the case of fixed interval every point in the window.

2.2.3 Instream Flow

When assessing water availability, the standard for water requirements includes both human and ecosystem demand. In order to properly or sustainably manage a natural resource, there should be a balance and weight placed not only on the financial value of the natural resource, but also as a resource for society and common good, as well as an ecosystem service and the naturally provided benefits (Gleick, 1998; Grumbine, 1994; Raju, 2000). Instream flow or minimum ecological flow requirements are one such way of making sure combined demand is met, or at least monitored. An instream flow standard is a built in minimum ecosystem requirement that should be maintained to ensure ecosystem demand is met (Richter et al., 2003). To assess combined demand, human water demand is added on to this built in requirement. Instream flow standards were originally intended to protect water quality as a part of the Clean Water

Act of 1972, but have since been broadly adopted for establishing water availability standards (Richter, 2012). In the United States, the 7Q10 flow standard, that is the seven day minimum streamflow that happens on average once every ten years, was adopted by many states as the minimum instream flow requirement (Risley, 1994). As time went on, it became recognized that the 7Q10 threshold did not sufficiently protect aquatic habitats, which led to several states adopting thresholds such as the 30% mean annual flow, or more comprehensive individually basin based methods (Richter, 2009). A less talked about area of ecological requirement is with regard to groundwater and sustainable use. The complex interactions between surface and subsurface hydrology make it difficult to quantify subsurface demand and as a result either insufficient measures are put in place or subsurface demand is ignored altogether (Sophocleous, 1997).

2.3 Application to Mills River Basin

Drought for a region can be defined in many ways depending on whether it refers to rainfall anomalies (meteorological drought), streamflow anomalies (hydrological drought), or reduced soil moisture availability to crops (agricultural drought). There are also different alternative metrics of drought such as the widely used Palmer Drought Severity Index (PDSI) or the Standard Precipitation Index (SPI), the effectiveness of which is amply discussed in the literature (see for example Barros and Bowden (2008) and literature therein for a review of various metrics). Here, the focus is

on hydrological drought and the 7Q50 flow is used as the threshold standard for extreme drought. The 7Q50 flow is the seven day minimum flow that occurs on average once every 50 years. Thus, a drought event in this case means that the streamflow has been below 7Q50 levels for at least seven consecutive days. To determine the 7Q50 flow for the MRB, a seven day running mean streamflow time series was created from daily USGS streamflow data, and then a Log Pearson type III distribution was fitted on the annual minima from the seven day mean time series (Riggs, 1972; Risley, 1994). The streamflow associated with other particular return periods can be obtained from this fit, for example other commonly used values including 7Q10 or 7Q2 flows (Fig. 7).

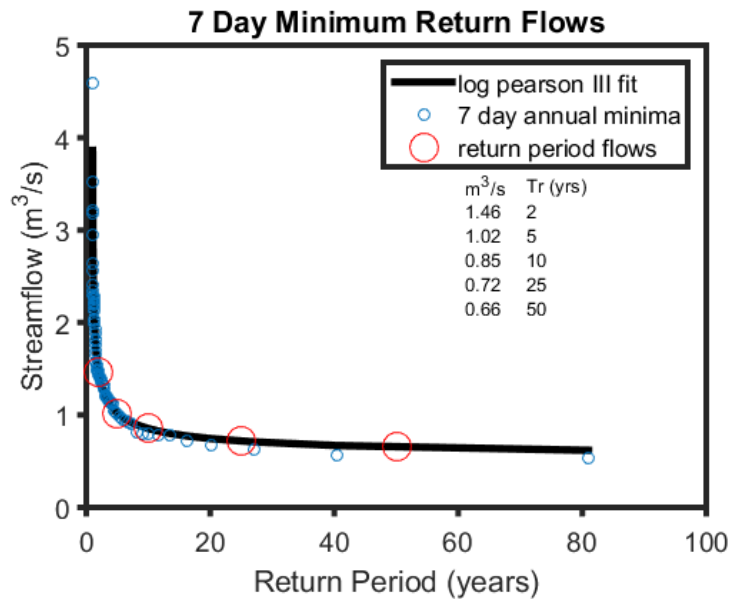


Figure 7: Log Pearson type III distribution fit annual minima from seven day mean streamflow. Desired return period (2, 5, 10, 25, and 50 years) streamflow estimates are circled in red.

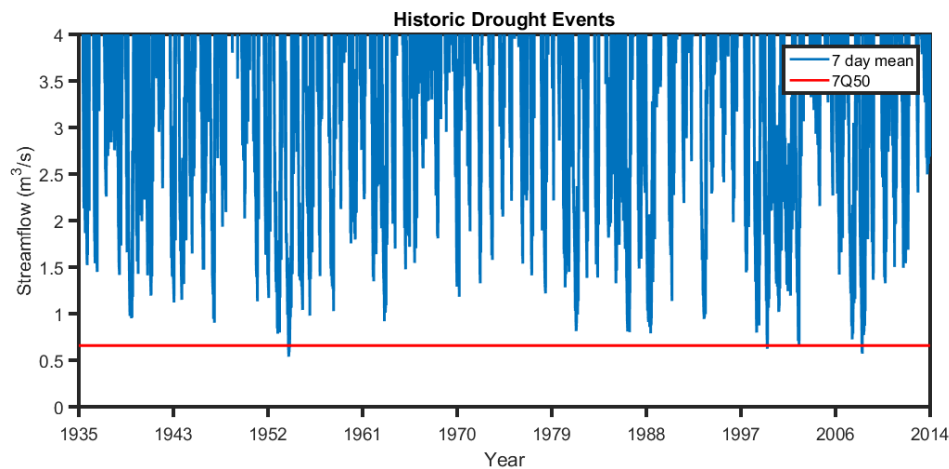


Figure 8: The lower end of the streamflow time series is shown to breach the 7Q50 threshold approximately once per 50 years (1954 and 2008), but with a couple of instances in the late 1990's/early 2000's where it was also very dry.

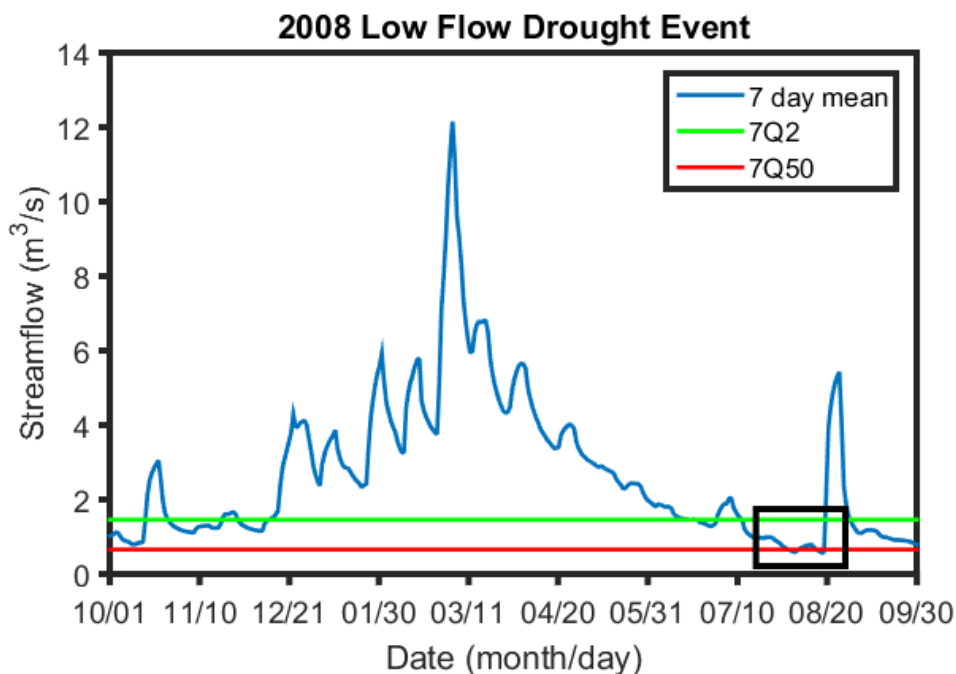


Figure 9: 2008 water year (October 2007- September 2008) hydrograph displaying the 7-day mean streamflow along with the 2-year and 50-year return period 7-day mean streamflow values. The onset of the extreme hydrological drought of 2008 in late summer is highlighted by the box in the figure.

During periods of drought or low flow, the baseflow becomes the main source of streamflow, and thus stream water availability (Priest, 2004), which is why much of the proceeding focus is on characterizing the nature of the MRB's subsurface behavior through hydrograph recession and subsequently investigating how baseflow varies on both intra- and inter- annual time scales.

2.3.1 Recession Curve Constants

2.3.1.1 Baseflow Recession Constants and Streamflow

The shape of the recession limb of a hydrograph can inform us about the behavior of water within the basin after the influx of water through precipitation ceases (Blume, 2007). A steeper recession limb indicates higher fraction of overall streamflow contribution from surface runoff and interflow, whereas a shallower recession limb indicates greater contribution from baseflow. As discussed earlier, the part of the hydrograph used to calculate the baseflow recession constant is defined as starting N days after the hydrograph peak and ending $2N$ days after the starting point, with N days defined by Eq. 1. For each pair of Q_0 and Q_t a baseflow recession constant is calculated using Eq. 3. A total of 1264 useable separate hydrographs were identified within the length of record of the USGS daily streamflow time series since 1934, and so there were 1264 calculated baseflow recession constants (Fig. 10).

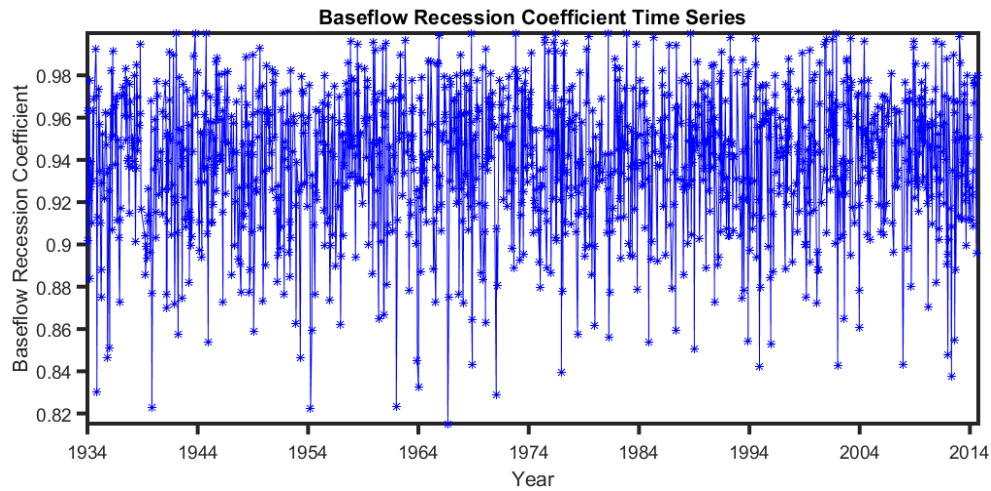


Figure 10: Time series of calculated baseflow recession constants (n=1264). Mean=0.94, standard deviation=0.033.

The range of recession constant values in the MRB [0.8-1.0] is consistent with the accepted literature values for baseflow recession constants, but begs the question of whether the low values periodically seen in Fig. 10 are related to extreme streamflow and/or precipitation events. This will be investigated later in the thesis.

The seasonality or intra-annual variability of the baseflow recession constant can provide insight into the seasonality of streamflow (Wittenberg, 2003). A typical hydrograph over the course of year has higher streamflow in the late winter and spring when soil moisture is high, and lower values during the summer and early fall (see Fig. 11).

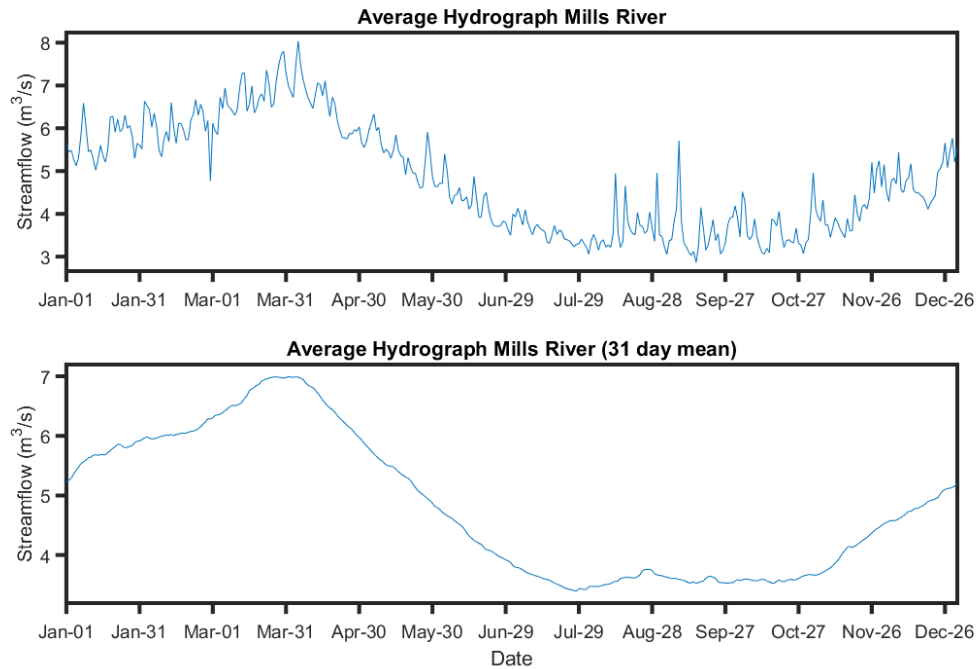


Figure 11: The average hydrograph for the Mills River at USGS station 03446000. The top panel shows the average hydrograph by day of the year and the bottom panel is the top panel smoothed over a 31 day period (roughly a monthly moving average).

The variability seen during the summer months in Fig. 11 can likely be attributed to isolated storms in the region, but otherwise one would expect low streamflow values for late summer and early fall. If the assumption of baseflow and groundwater being the major controlling factor in periods of drought and low streamflow is correct, then we should expect to see minimum values for the baseflow recession constants in the late summer and early fall.

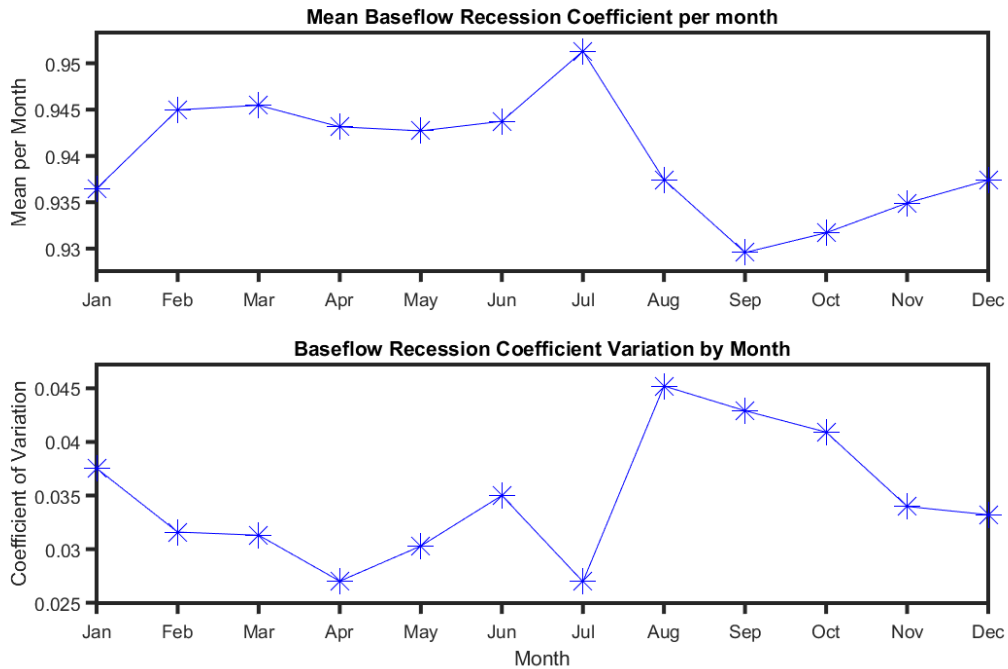


Figure 12: Monthly means of baseflow recession constants and the corresponding coefficient of variation.

The months of August, September, and October have lower mean baseflow recession constants as we would expect due to the tendency to have lower streamflow during these months, which is in agreement with Wittenberg’s (2003) findings. As previously stated and seen in Fig. 11, the high variability of streamflow in August and September can likely be attributed to isolated storms. Figure 12 strengthens this inference as August and September have the two highest coefficients of variation, suggesting that the individual hydrograph recession limbs in these months are either very steep (higher peak and low recession constant) or very shallow (lower peak and higher recession constant). To further explore the idea that the value of the baseflow

recession constant might be linked to the magnitude of the hydrograph peak we will compare the baseflow recession constants and their corresponding hydrograph peak.

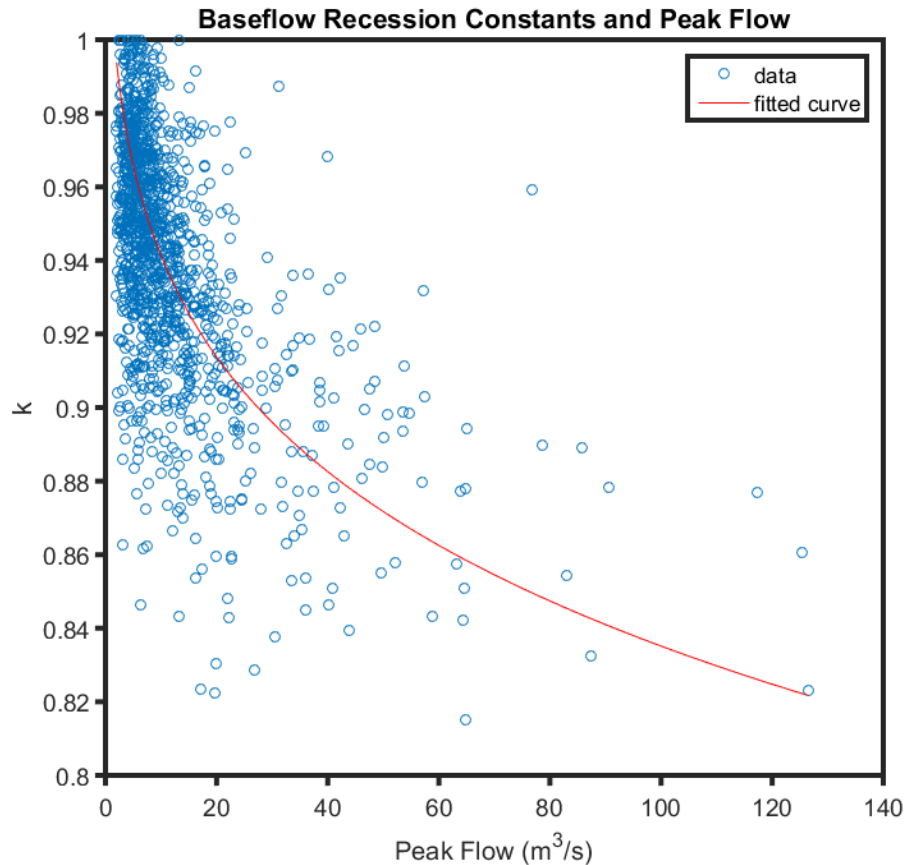


Figure 13: Distribution of baseflow recession constants with respect to the peak of the hydrograph from which the constant was calculated.

The fit of the data in Fig. 13 was obtained via power law distribution of the form $f(x)=ax^b+c$ ($a= -0.144$, $b=0.174$, $c=1.156$), with additional weight placed on the data points in the upper left cluster, and less weight placed on the data points toward the upper right section of the plot such that the distribution would place heavier weight on the main cluster of data points on the top left-hand side and less weight on outliers. The

scattered nature and high variance of the peak flow data makes it difficult to draw a final conclusion, but it does appear that in general the hydrographs with large peaks tend to result in lower baseflow recession constants. This is expected because hydrographs with abnormally high peaks (note that the mean peak value is 11.94 m³/s) would be the result of a larger precipitation event that would cause a greater portion of streamflow to be contributed by direct runoff and not from groundwater. The timing of extreme baseflow recession constants and extreme peak hydrograph values can help determine if these extreme values are linked to very wet and very dry conditions.

2.3.1.2 Extreme Baseflow Recession Constants

The time series of baseflow recession constants (Fig. 10) has a mean of 0.94 and standard deviation of 0.033. Extreme values (greater than 2 standard deviations from the mean) would be below ~0.87 or greater than 1.006 (not possible). Out of the 1264 calculated baseflow recession constants, 41 (3.24%) qualified as extreme. The stated hypothesis is that many of these extreme baseflow recession constants can be attributed to large hydrograph peaks as a result of large precipitation events, possibly a tropical storm or hurricane in the late summer or fall. The distribution of peak streamflow for these events can be seen in Fig. 14.

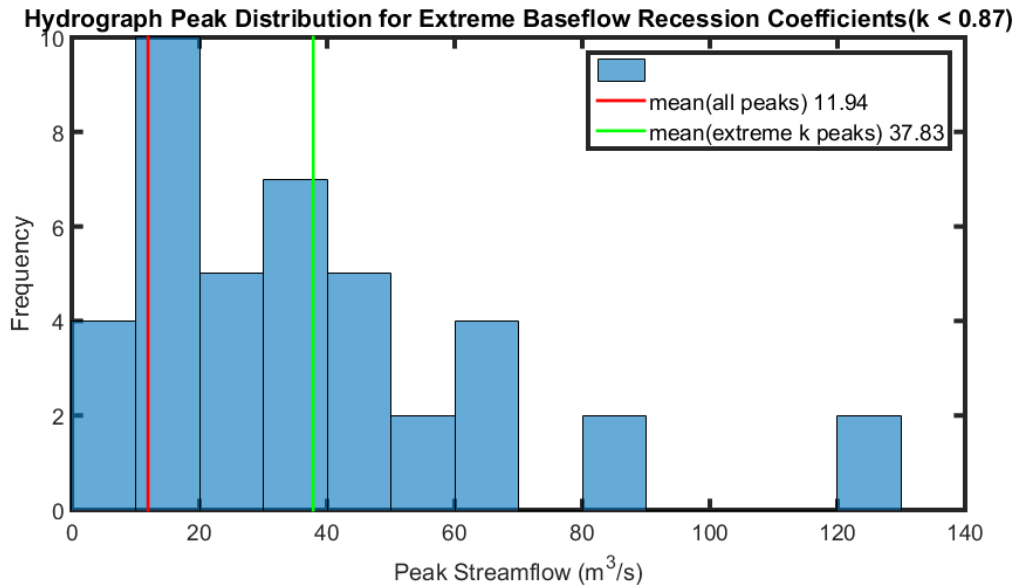


Figure 14: Distribution of streamflow peaks associated with extreme baseflow recession constants (n=41). Note that the mean of the peaks associated with these extreme cases is three time as large as the mean of all hydrograph peaks.

The case can be made between Fig. 13 and 14 that if there is an extremely large hydrograph peak, the resulting baseflow recession constant will be very low. Figure 13 shows that for unusually large peak flows (greater than 60 m³/s) in every instance except for one, the baseflow recession constant is less than 0.9. Focusing on Fig. 14, the distribution still favors seemingly smaller peak flows, but the new mean is actually quite large because of the smaller size of the Mills River itself (mean daily streamflow is 4.82 m³/s and mean hydrograph peak is 11.94 m³/s). The flows seen at the tail of the distribution are not commonly occurring. Of the two instances with values exceeding 120 m³/s, both are associated with hurricanes or tropical storms (Unnamed Hurricane in August 1940, and Tropical Storm Fay in August 2008). It is worth noting that the shift in

mean peak streamflow between all peaks and peaks associated with extreme baseflow recession constants is not insignificant. As previously stated, because of its small size, MRB peak streamflow is relatively low, and thus a tripling in the mean is meaningful when the new mean is above the 95th percentile of all peaks ($37.83 \text{ m}^3/\text{s} > 34.99 \text{ m}^3/\text{s}$).

Analysis of the seasonality of the extreme baseflow recession constants can provide further insight into the underlying hydrometeorological and hydrological regimes.

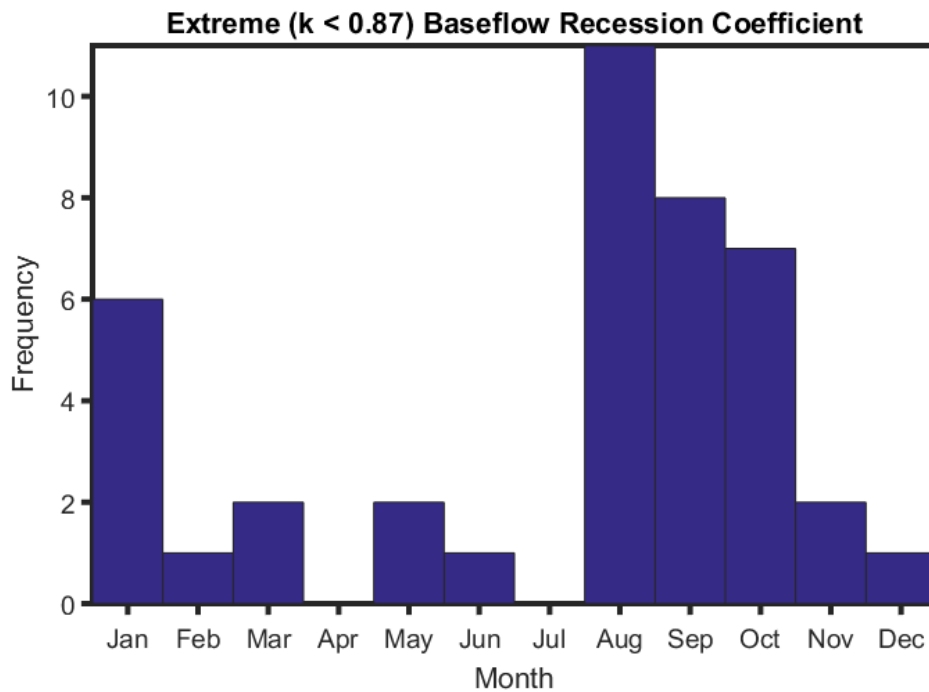


Figure 15: Intra-annual distribution of extreme baseflow recession constants. Late summer and early fall months are the period of greatest occurrence.

Of the 41 instances in Fig. 15, 26 occurred in the months most frequently associated with hurricanes and tropical storms (August, September, and October). The relatively large number in January could be attributed to cold front systems and rapid

snowmelt events that lead to larger streamflow. To determine if the extremely low baseflow recession constant is directly caused by a large precipitation event, the associated precipitation event occurring at the same time or just before the hydrograph peak must be identified. An example is shown in Fig. 16 (Unnamed hurricane from August 1940).

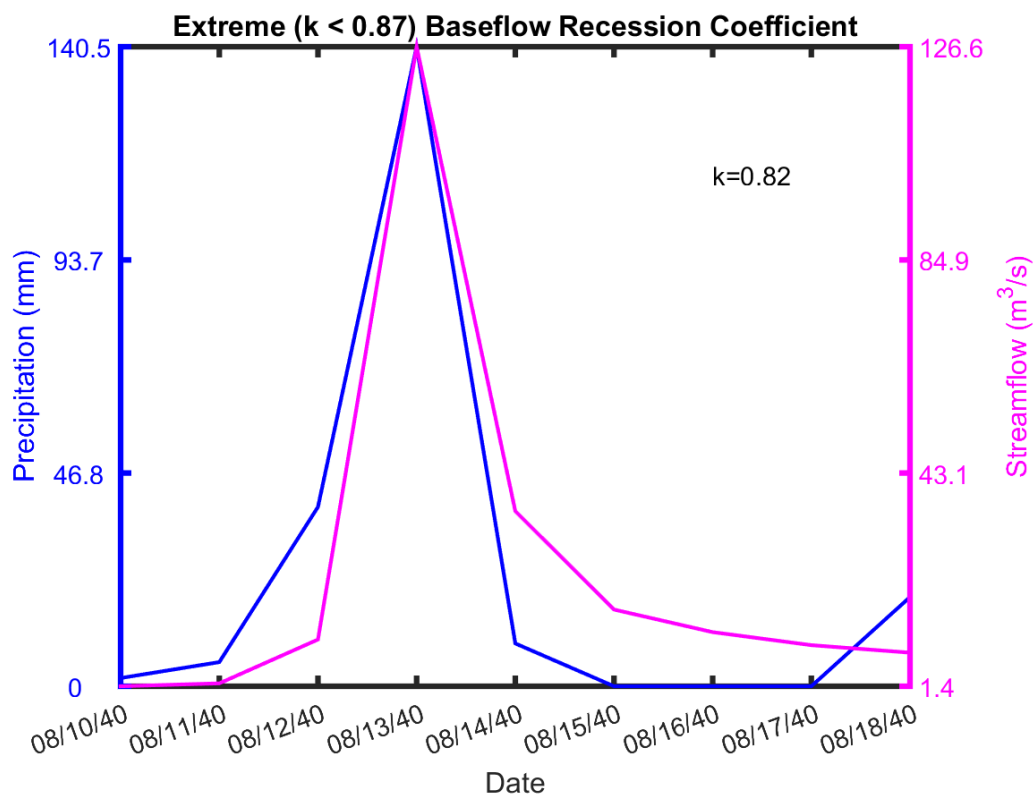


Figure 16: An individual hydrograph from which the associated extreme baseflow recession constant was calculated (shown in blue) and the precipitation event that led to the hydrograph peak (shown in magenta).

The relationship between large precipitation events and extreme baseflow recession constants is examined in Fig. 17. Note how all precipitation accumulations associated with extreme baseflow recession constants are close to or larger than the

mean plus two standard deviations of the precipitation time series only including days of non-zero precipitation so as not to skew the results due to numerous zeros (non-rain days) in the original time series.

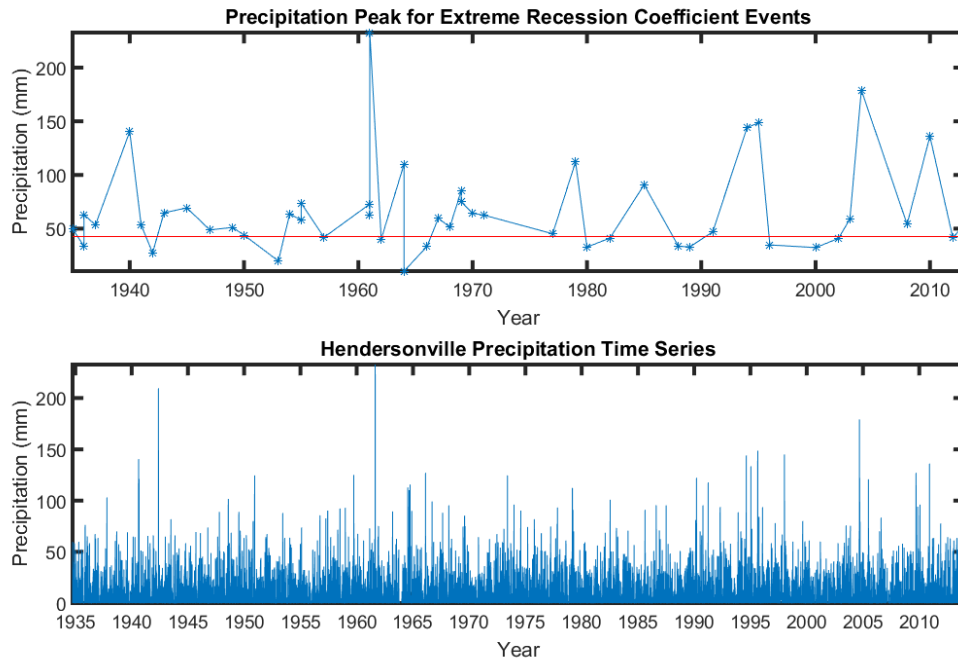


Figure 17: Top panel shows the precipitation peak associated with each extreme ($k < 0.87$) baseflow recession constant event. The red line shows the mean+2*standard deviation of the non zero (rain occurring) days from the Hendersonville Rain Station. Bottom panel shows entire time series of Hendersonville precipitation for reference.

The idea that extremely low baseflow recession constants are associated with large hydrograph peaks caused by large individual precipitation events, specifically tropical storms and hurricanes occurring in the later summer and early fall appears to hold true. To investigate if a similar statement can be made about high baseflow recession constants and small hydrograph peaks the same analysis is carried out for high baseflow recession constants ($k > 0.98$).

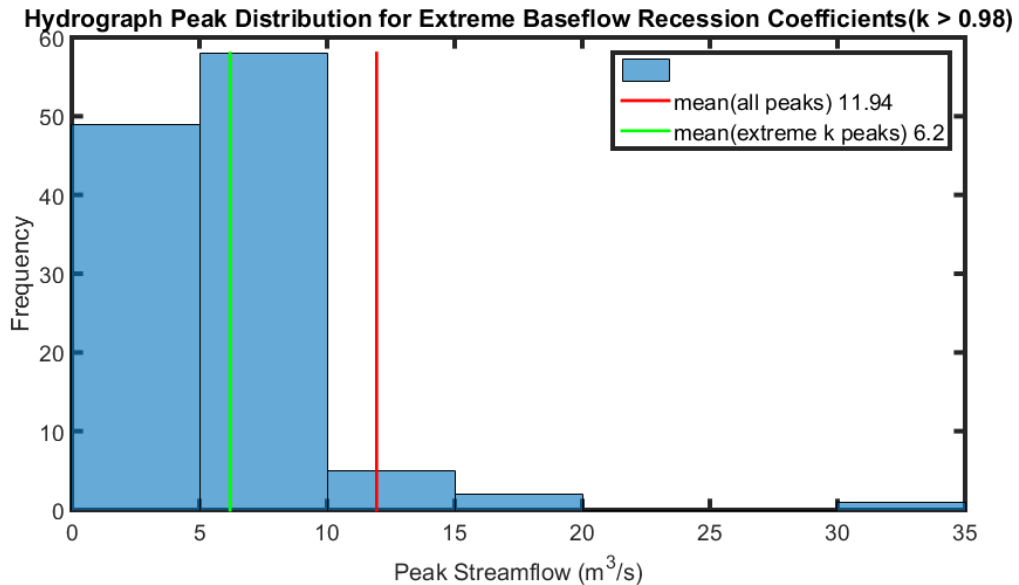


Figure 18: Distribution of streamflow peaks associated with high extreme baseflow recession constants (n=115).

The positive skew on the distribution of the largest baseflow recession constants show that lower hydrograph peaks are associated with higher baseflow recession constants. A lower hydrograph peak means that there is much smaller fraction of overall streamflow contribution from surface runoff and preceding precipitation. This would imply that a higher fraction of the streamflow in these cases is being contributed by baseflow.

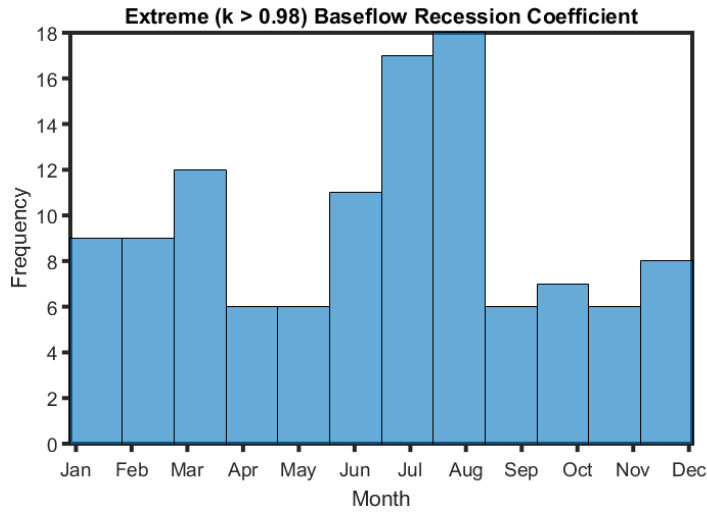


Figure 19: Intra-annual distribution of high baseflow recession constants. Higher values are associated with shallower hydrograph recession limbs and lower hydrograph peaks, and we see this in the high frequency during the summer (lower flow) months.

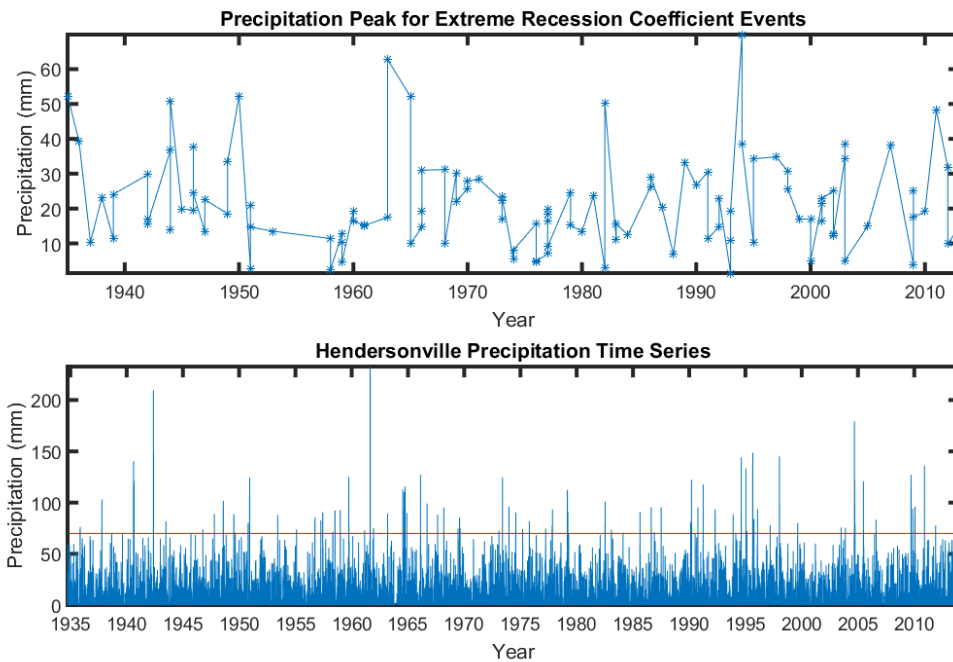


Figure 20: Top panel shows the precipitation peak associated with each high baseflow recession constant event. The red line in the bottom panel shows the maximum of the top panel in reference to the Hendersonville Rain Station time series.

The precipitation events associated with hydrograph peaks leading to baseflow recession constants greater than 0.98 are not unusually high as seen in the bottom panel of Fig. 20. Compared to the values in Fig. 17, these precipitation peak values are much smaller as expected, but they occur during wet (rainy) periods of high antecedent rainfall, and therefore high soil moisture conditions. In order to have a significant hydrograph with peak prominence greater than 1 m³/s (one of the criteria chosen to define hydrograph peaks) there has to be some influx of water to basin (precipitation).

2.3.2 Baseflow Estimation

2.3.2.1 Streamflow Filtering

Applying Eq. (1): $N=bA^{0.2}$ to the Mills River USGS stream gauge location, with $b=1$ and $A=66.7$ mi², the number of days after the peak to apply the first filter is $N=2.32$ days, but when applied to the daily data will be rounded to 2 days. In the literature, the filter window is $2N-1$ days wide, where $2N$ is rounded to the nearest odd integer so that the window can be centered on a data point. In this case $2N = 4.64$ rounded to 5 days and thus the sliding interval is four days wide.

$$Y(t) = \min(Q(t-2) : Q(t+2)) \quad (\text{Eq. 5})$$

For the second pass-filter to obtain the baseflow contribution, the minimum value from the resulting sliding interval filter for the entire water year (October 1 – September 30) is used.

$$Q_b(t) = \min(Y(t=\text{October 1}) : Y(t=\text{September 30})) \quad (\text{Eq. 6})$$

The necessity for applying a second filter can be visualized in Fig. 21, 22, and 23. After the first filter is applied, much of the new time series still has strong peaks corresponding to fast interflow response which are typical in this region (Tao and Barros, 2013). The baseflow response time series is generally expected to gradually rise underneath a streamflow peak as seen in Fig. 21 below.

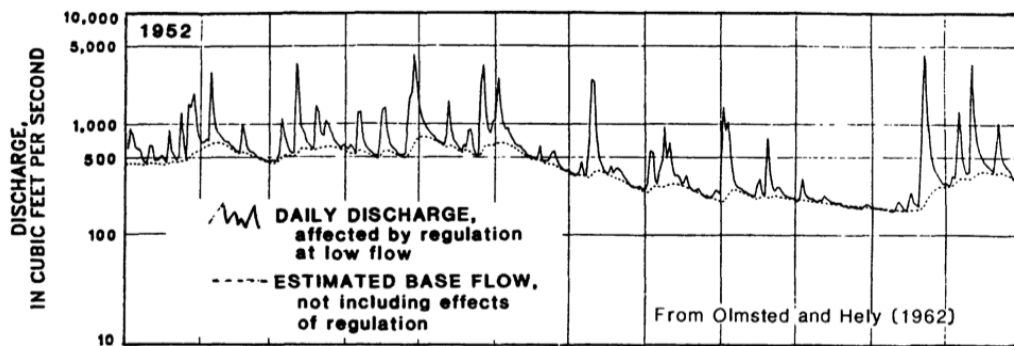


Figure 21: Example of a graphically estimated baseflow time series by hand (White and Sloto, 1990). The estimated baseflow does not have flashy peaks like the streamflow time series, but rather a much slower and gradual response.

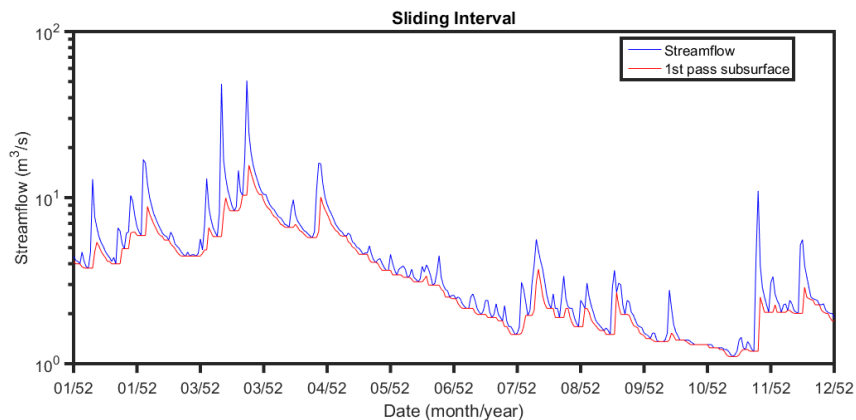


Figure 22: Applying the first sliding filter to the Mills River streamflow data yields the time series in red. Compared with the shape of the estimated baseflow in Fig. 20, the new time series is not representative of a slow groundwater response, having distinct peaks under many of the streamflow hydrograph peaks, but rather interflow from surface-subsurface interactions. Y axis is in log scale for comparison to Fig. 21.

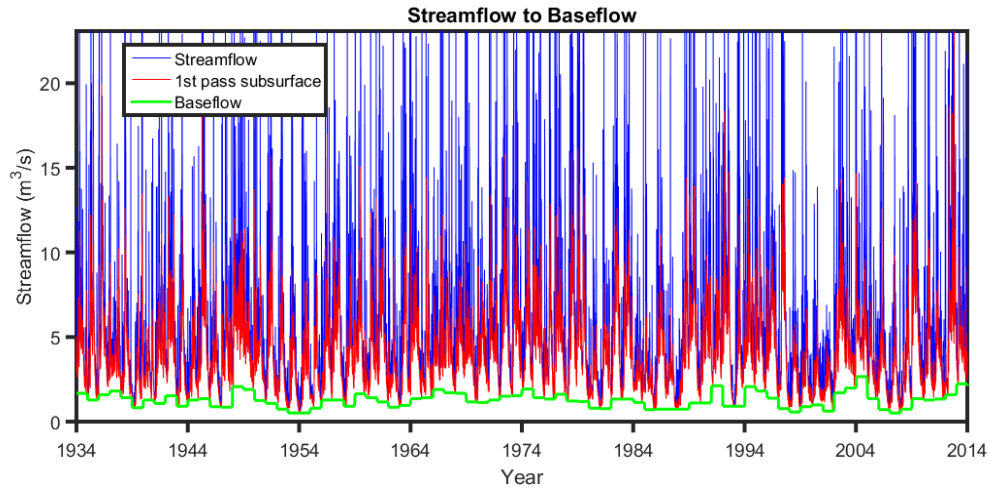


Figure 23: The lower end of the streamflow time series and the progression going from streamflow to subsurface flow and to estimated baseflow.

A baseflow time series should have some reaction to a hydrograph peak and also rejoin the streamflow hydrograph once the recession limb is finished (Murphy et al., 2009). Taking a minimum value from a fixed interval (White and Sloto, 1990) ensures that the baseflow estimation does not severely underestimate the baseflow, a weakness previously identified in the Chapman (1999) filter (Murphy et al., 2009).

2.3.2.2 Time Series Analysis

Baseflow groundwater contributions to streamflow are much slower processes than those that tend to govern streamflow and subsurface flow variability (Linsley, 1958). Wavelet analysis was performed as in Torrence and Compo (1998) to investigate the temporal variability and to identify possible non-stationarity in baseflow, subsurface/interflow contribution, and streamflow proper using standardized time-series ($\text{anomaly} = \frac{x - \text{mean}(x)}{\sqrt{\text{variance}(x)}}$).

Scale averaged wavelet power as defined by Torrence and Compo (1998):

$$\overline{W}_n^2 = \frac{\delta j \delta t}{C_\delta} \sum_{j=j_1}^{j_2} \frac{|W_n(s_j)|^2}{s_j} \quad (\text{Eq. 7})$$

$|W_n(s)|^2$ is the power spectrum at different scales (s). δj is a factor that dictates the scale resolution (chosen as 0.25), and C_δ is a reconstruction factor specific to each wavelet form; $C_\delta = 0.776$ for the Morlet wavelet. δt is time step of 1 day because the data is daily in temporal resolution. To allow the juxtaposition of streamflow from watersheds of different sizes, each scale-averaged series are normalized by σ^2 of the original series, which leads to a $(\sigma^2 \delta j \delta t) / C_\delta$ factor in front of the weighted sum of the wavelet power spectrum (Torrence and Compo, 1998). For 1-20 year scale averaged variance the scale (s) ranges from 1 to 20 years (365.25 to 20*365.25 due to the daily time step).

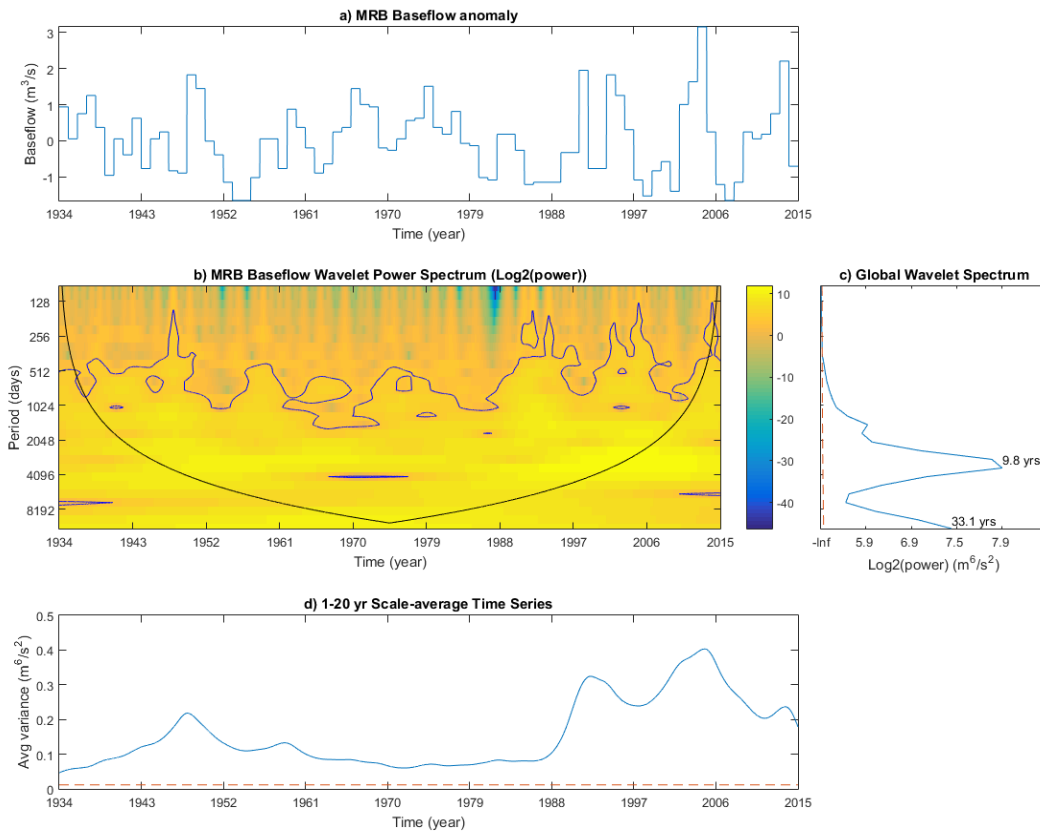


Figure 24: Wavelet analysis of MRB baseflow anomaly. The main things to note are the global wavelet spectrum peak at 9.8 years and the variation of the scale averaged variance.

The data indicates that droughts or periods of low flow are becoming more common after the relatively wet period in the 1960's and 1970's (see Fig. 24(a)), with periods of low flow (significant negative anomalies) in the early and late 1980's, late 1990's and mid-late 2000's. If this signal is being picked up in the slowest response flow, then a similar increase in variance post 1970 with multiple droughts should also be evident in the interflow and streamflow anomalies.

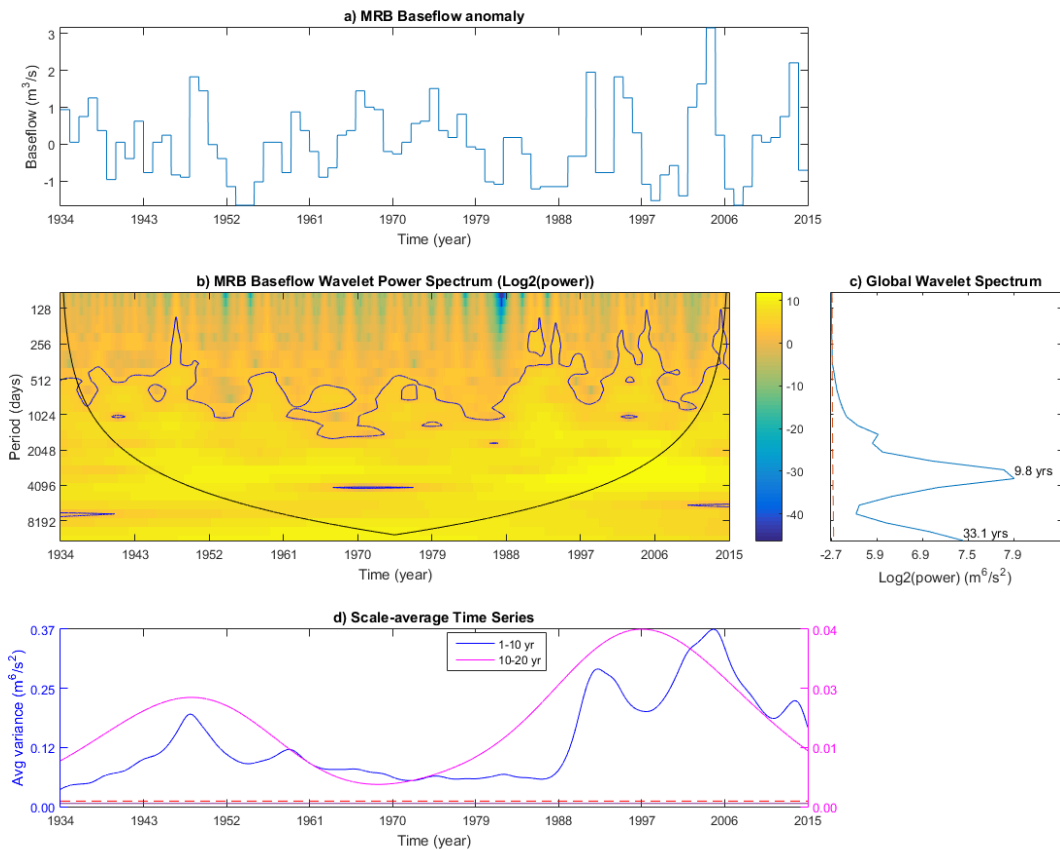


Figure 25: Wavelet analysis of MRB baseflow normalized by the standard deviation. Difference from Fig. 24 is in the scale average time series, split between 1-10 year and 10-20 year. 1-10 year accounts for nearly all of the variance.

When the 1-20 year scale averaged variance is divided into two parts (1-10 year and 10-20 year scale averages) in Fig. 25, it is apparent that the decadal signal is dominant, that is the variance at 9.8 years (less than 10 years) is the overwhelming contributor to the 1-20 year scale average variance. Note the scale of the y axes in Fig. 25(d), with the 1-10 year scale average being an order of magnitude greater than that of the 10-20 year scale average.

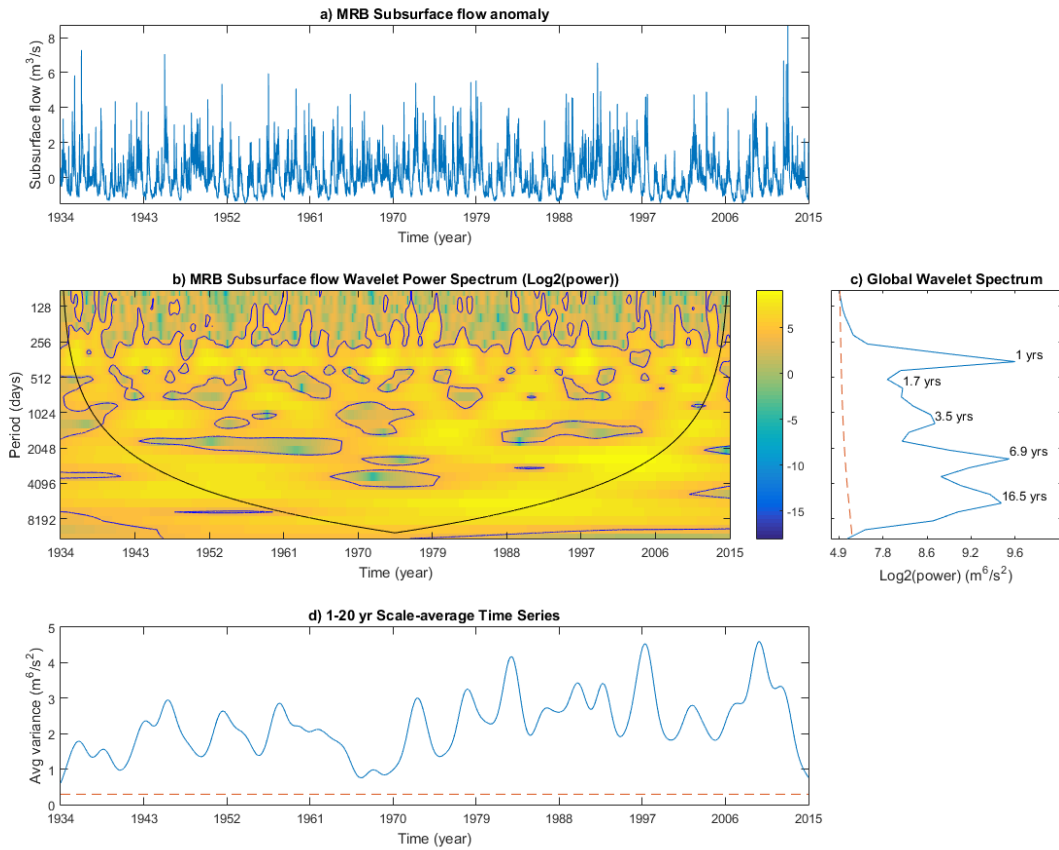


Figure 26: Wavelet analysis of MRB subsurface flow anomaly. Note the global wavelet spectrum peaks at 1 and 6.9 years (annual variability and ENSO time scales) and the variation of the scale averaged variance.

In addition to the evidence of ENSO variability (3.5-6.9 year global spectrum peaks) signal inspection of Fig. 26 reveals an increase in the variance mean after 1970, which we attribute in part to a change in the synoptic weather patterns in the Atlantic for different phases of the AMO (Atlantic Multidecadal Oscillation) climate index: trending positively since 1970. The relationship between the scales of streamflow variability and climate variability as described by various climate indices will be further explored in Chapter 5.

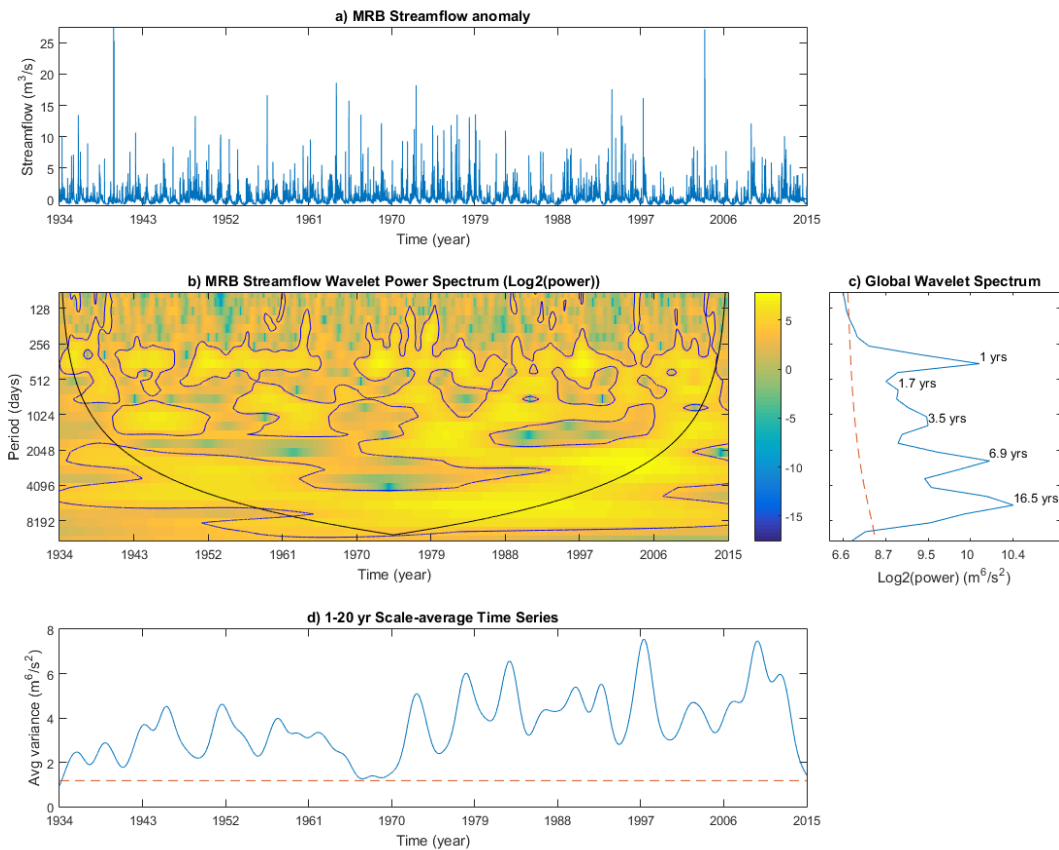


Figure 27: Wavelet analysis of MRB streamflow normalized by the standard deviation. The main things to note are the global wavelet spectrum peak at 1 and 6.9 years (annual variability and ENSO time scales) and the variation of the scale average variance.

Figures 24-27 show that baseflow variability takes place on significantly longer timescales than does streamflow or interflow. Baseflow in the MRB exhibits strong decadal (9.8 years) variability according to the global wavelet spectra shown in Fig. 24 and 25. Figures 26 and 27 show the same signatures, which is indicative of the similar short term response of subsurface/interflow and streamflow. The variance of the baseflow is much lower than that of the streamflow and subsurface flow when looked at

together in Fig. 28, though not negligible especially in the context of the relative magnitude of baseflow (see Fig. 29).

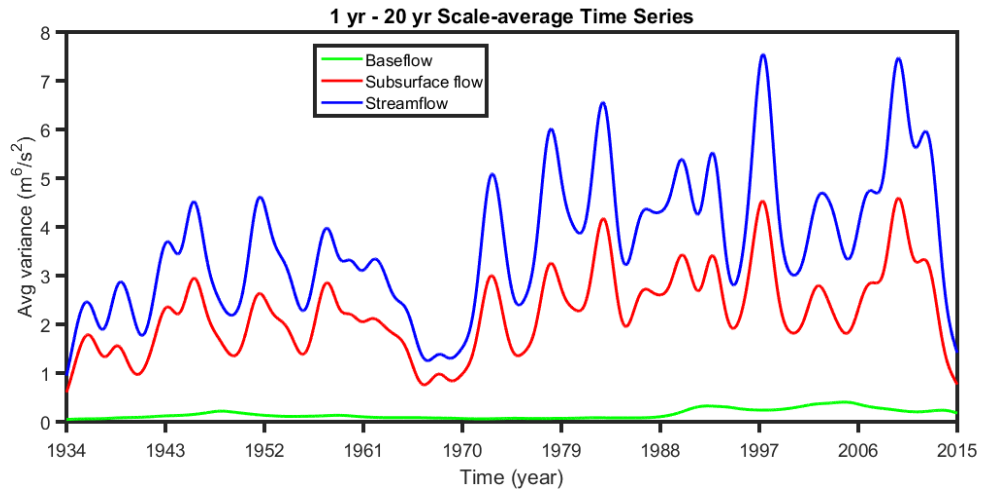


Figure 28: The 1-20 year scaled average variance of Mills River streamflow, subsurface flow, and baseflow.

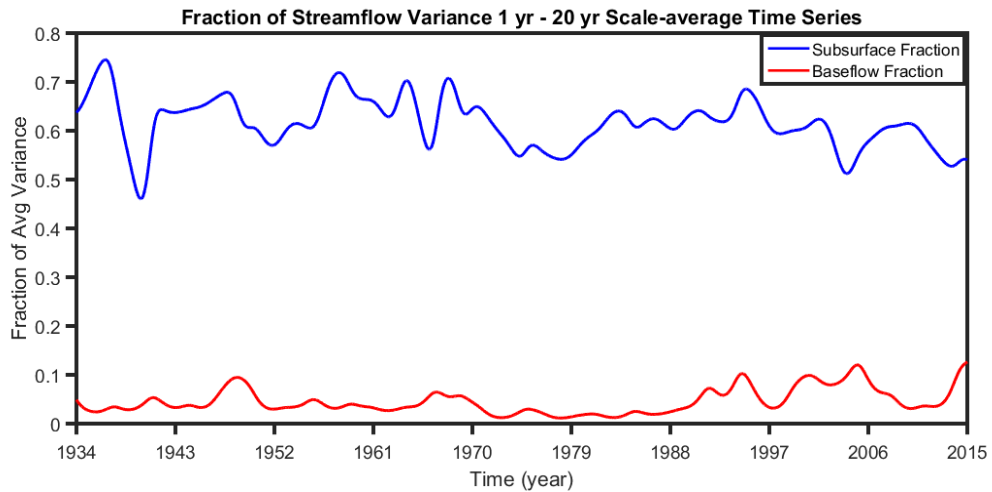


Figure 29: Baseflow generally accounts for very little of the overall streamflow variance, but a few cases, it appears to peak when subsurface variance decreases and accounts for a more significant portion of the streamflow scale average variance.

The similarity and almost identical behavior of the streamflow and interflow time series provides further justification for the double-filtering of the streamflow time

series because the goal is to obtain an estimate of baseflow, which varies on much longer time scales than streamflow, but the once filtered interflow varies on the same time scales as the streamflow, and therefore would not qualify as an accurate estimate of baseflow.

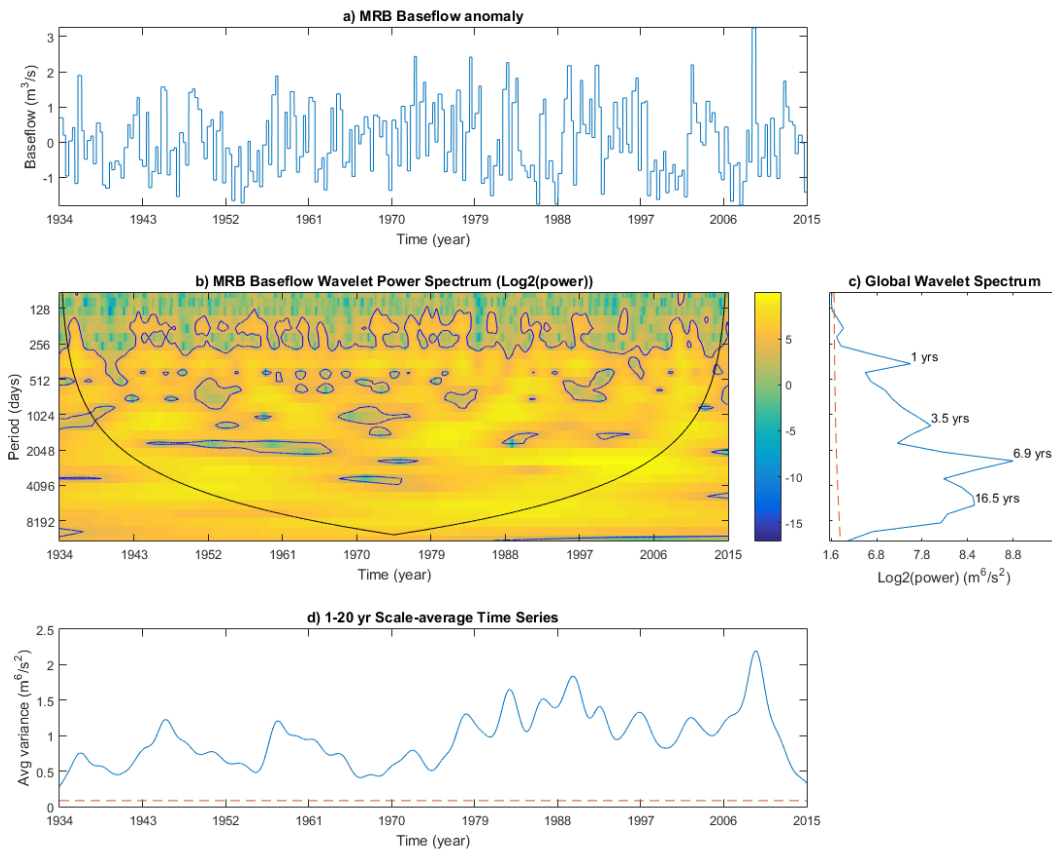


Figure 30: MRB seasonal baseflow wavelet analysis. Seasons of April, May, June (amj), July, August, Spetember, October (jaso), and November, December, January, February, and March (ndjfm) were used to separate the hurricane season from typical weather in the spring and early summer. Baseflow was initially calculated on a monthly basis (via an altered Eq. 6 using monthly minimum instead of water year minimum) and then averaged according to the seasons just listed. An ENSO (6.9 years) associated peak in the global spectrum is very pronounced and especially strong in the second half of the time series, looking at 30(b).

It is apparent from the wavelet analyses that the amount of variability visible in any of the baseflow, interflow, and streamflow time series has increased significantly in the post 1970 period as compared to pre 1970, with the large negative anomalies coinciding with severe droughts in the region during 1999-2002 and 2007-2008, which had significant impacts on agriculture and general water use (Davis, 2015; Weaver 2002).

2.3.3 Instream Flow and Combined Demand

A minimum instream flow requirement serves as a baseline for water demand in the form of aquatic ecosystem demand (Richter et al., 2003). By adding the water demand for human consumption, a combined demand from the river is found (Gleick, 1998). The level of sustainability of how the Mills River is used can be assessed by comparing streamflow upstream of the WTPs at the USGS gauge with total demand for the river (downstream human demand plus ecosystem demand). Human use in the MRB downstream of the USGS station can be estimated by the sum of the withdrawals from the river by the Hendersonville and Asheville Water Treatment Plants. In MRB the cooperation between members of the local government and municipalities allows for some semblance of an instream flow requirement to be implemented in practice (Mead, 2002; Mills River Partnership, 2015). The HWTP and the local branch of the US Forest Service have an understanding of what instream flow must be maintained. There were recommendations made (Mead, 2002) with suggested instream values for two locations below the headwater catchment reservoirs, one for the main branch of the river at the

USGS gauge, and one for below the WTPs themselves. While there were numerous suggestions and recommendations from NCDENR (North Carolina Department of Environment and Natural Resources) and Mead (2002) an agreement between HWTP and the US Forest Service is that if the daily mean of USGS gauge upstream from HWTP goes below 50 cfs, the HWTP will cut its upstream reservoir intake down close to 0, so that more of the headwaters can reach the rest of the basin.

The presence of the endangered Appalachian Elktoe Mussel in the MRB also facilitated the adoption and implementation of loose guidelines as it pertains to minimum ecological flow requirements. The mussel only adds to the awareness of the region, where water quality is already a priority due to a series of past water quality issues due to rapid development (Riverlink, <http://riverlink.org/learn/about-riverlink/history-of-french-broad-river/>). The HWTP monitors the upstream USGS gauge to make sure there that they are not taking too much water from their headwater reservoirs. This loose guideline of 50 cfs at the USGS gauge serves as instream flow requirement or environmental flow (McKay, 2015). For comparison, the 7Q10, 7Q2 and 50cfs requirements are marked in Fig. 31. Note how the 50 cfs requirement is equivalent to the 7Q2 or the bi-annual hydrologic drought, thus a very stringent criterion in practice.

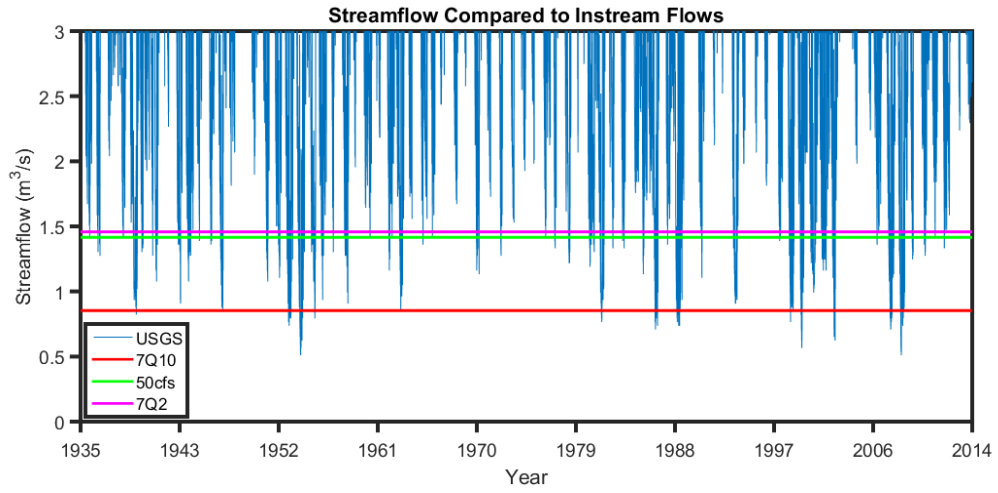


Figure 31: The lower portion of the Mills River streamflow time series and three potential instream flow requirements (7Q10, 50cfs, and 7Q2). 50 cfs (1,416 m³/s) is the current threshold used by HWTP. Changing the instream flow requirement can change the appearance of how sustainable an area is.

3. Model Evaluation

The DCHM used here is a physically based, fully distributed, and uncalibrated high-resolution (250m and 5 minute) model with combined surface–subsurface physics (Yildiz and Barros, 2007; Tao and Barros, 2013 2016). The DCHM was originally a column model used for investigating land–atmosphere interactions (Barros, 1995), and has evolved over the years into a distributed hydrologic model solving the combined water and energy balance equations including combined surface–subsurface interactions (Devonec and Barros, 2002, Yildiz, 2001, Yildiz and Barros, 2005, Yildiz and Barros, 2007 and Yildiz and Barros, 2009). The DCHM consists of three combined modules: a vertical Land Surface Hydrology Model (LSHM), a two-dimensional Surface Flow Routing Model (SFRM), and a two-dimensional Lateral Subsurface Flow Routing Model (LSFRM). There is no interaction between the local and regional groundwater systems. At each location, the vertical soil column consists of both an unsaturated zone and a conditionally saturated zone. The unsaturated zone is discretized into four layers, of which the 1st layer is the superficial soil zone at the land–atmosphere interface, the 2nd and 3rd layers are root layers, and the 4th deep layer varies in time in response to changes in the water table. The saturated layer is defined by the water table. Overland flow is estimated either from rainfall excess (Horton) mechanism or saturation excess (Dunne) mechanism for each grid element at each time step and routed by the SFRM, (Yildiz and Barros, 2007). Subsurface flow, comprised of interflow and baseflow, is then laterally

routed by the LSFRM. A more detailed description of the model can be found in (Devonec and Barros, 2002, Yildiz, 2001, Yildiz and Barros, 2005, Yildiz and Barros, 2007 and Yildiz and Barros, 2009).

Since there are no observations available to specify the initial soil moisture distribution in the basin, 1-year long simulations are repeated sequentially until there are no significant differences between streamflow simulations between one year and the next. These are called “spin-up” simulations and the goal is to reach internal equilibrium and consistency among all soil moisture stores. In most of the DCHM runs four to five spinup periods were executed, and then the fifth or sixth run was taken as the actual model output. In this case only the 2008 water year is being examined due to its historic drought levels. Due to the high resolution and resulting computation time of the model (5 minute time step, 250m x 250m grid) the same period (October 1, 2007 – September 30, 2008) is run multiple times with the same atmospheric forcing data each time, and the ending hydrologic conditions of the previous spinup are used as initial conditions for the subsequent run. The fact that there is only local groundwater interaction and no regional scale groundwater interactions in the model likely has an impact on baseflow estimation due to the physiography and hydrogeology of the basin and its relationship to the region as a whole. Specifically, long-range transport via fractures is not represented. It is hypothesized that such long-range transport takes

place in the aftermath of severe storms such as tropical cyclones, which is less of a concern in this study since it was a drought year.

3.1 Precipitation

Atmospheric forcing data were derived from the North American Regional Reanalysis (NARR), and precipitation was generated from NCEP/EMC 4KM Gridded Data Stage IV datasets. All the datasets were first extracted from original data sources, re-projected to UTM and bi-linearly interpolated to the domain grid system at 250m x 250m as described by Tao and Barros (2014a,b). The input precipitation is the fundamental driver of a hydrology model providing an input of water to the system. Accurately estimating this input precipitation can be difficult due to limited spatial density of rain gauge stations, especially in mountainous terrain. There were two rain gauges used to interpolate the Stage IV precipitation data down to 250m x 250m scales (see Fig. 32 below). These two rain gauge locations had the longest consistent period of record available in the region (1876 and 1899 starting dates) and had nearly complete records, which is why they were chosen. Both gauge stations are under 700m elevation, which is a problem because the headwaters of the MRB where it rains the most (McGill Associates, 2012) are upwards of 1700m on the eastern slopes of the Appalachians, and therefore orographic enhancement effects are not captured by the rain gauges. On the other hand, the radar scan from Greenville, SC overshoots shallow precipitation, and thus miss low level precipitation that is significant in this region (e.g. Wilson and Barros,

2015), while ground clutter effects affect the precipitation estimates at high elevation. Therefore, heavy precipitation in the upper MRB is likely underestimated both at high elevations and light to moderate rainfall conditions at lower elevations.

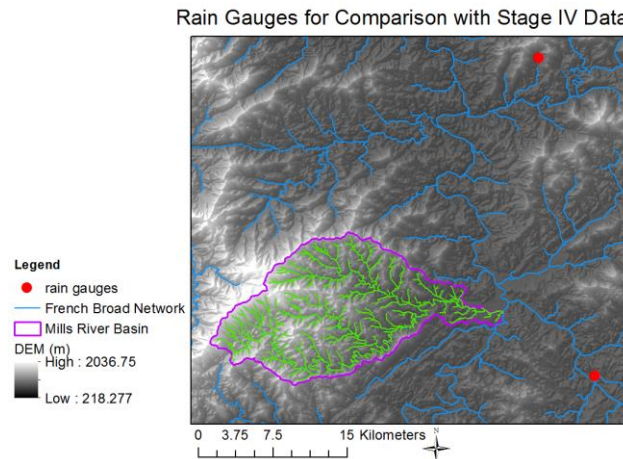


Figure 32: Rain gauge locations. The northern station is in Asheville (<http://www.ncdc.noaa.gov/cdo-web/datasets/GHCND/stations/GHCND:USW00013872/detail>) and the southern station is in Hendersonville (<http://climate.ncsu.edu/cronos/?station=313976&temporal=D>)

The input precipitation is still able to capture the general gradient of precipitation for a large event as seen in Fig. 33 below.

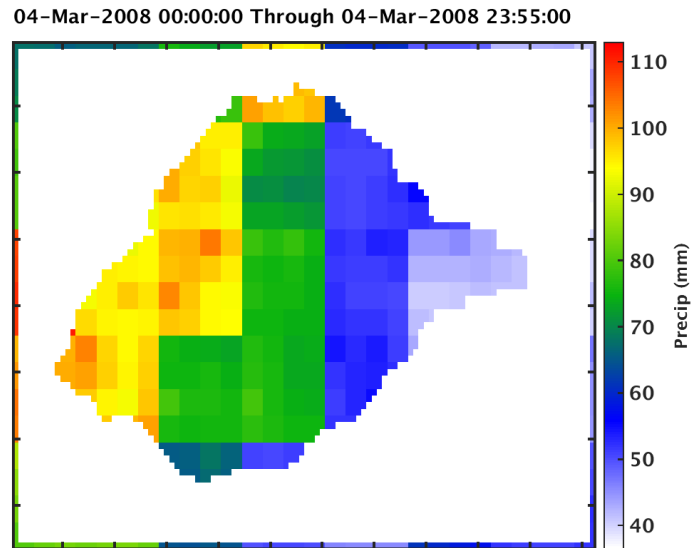


Figure 33: Cumulative precipitation over a single day during a large precipitation event in March 2008. Notice the gradient going from high precipitation to low as you go from high elevations to low (west to east). The general gradient is in line with what would be expected and has been observed (McGill Associates, 2012). If these values are overestimated from the observed it would explain the overestimation of hydrograph peaks that will be seen in section 3.2.

3.2 Streamflow

Streamflow is the measure of water availability from the perspective of surface water (the other perspective being groundwater) and for many municipalities rivers or lakes and reservoirs fed by rivers are the primary sources of water supply. Note that all model outputs in this section are taken from a model run using five periods of spin-up for the 2008 water year. Figure 34 shows where the streamflow response output from the DCHM is captured well compared to the actual USGS gauge measurements and where the model differs from measurement.

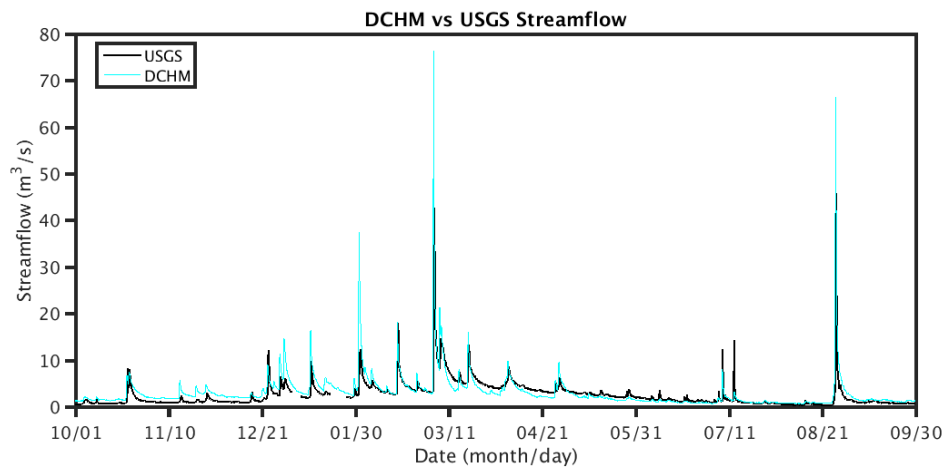


Figure 34: 2008 Water Year. 15 minute interval streamflow data from Mills River USGS station compared with 5 minute interval DCHM model output streamflow aggregated to 15 minute interval.

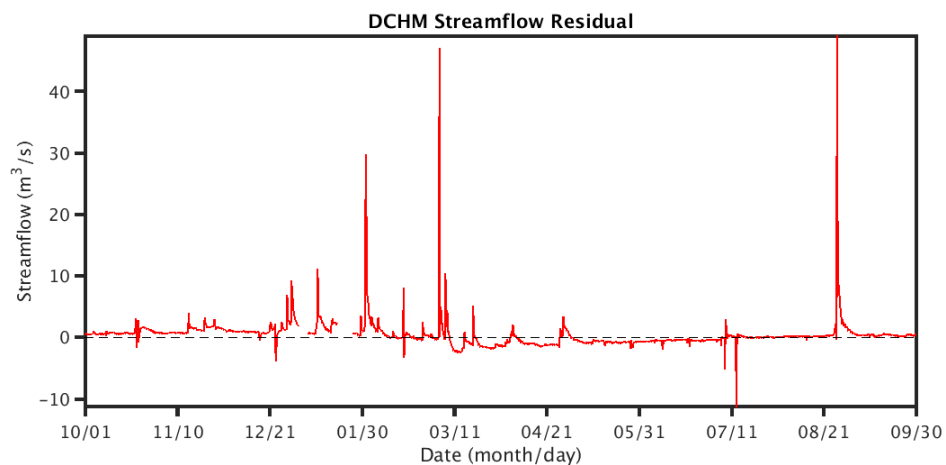


Figure 35: Residual of time series from figure 34 (DCHM output – USGS observation). 1.58% of the residual is more than 5 m³/s away from the accepted value and 0.54% is more than 10m³/s away from the accepted value.

The model does well estimating streamflow for the vast majority of the period of interest. In a couple of places the peak streamflow associated with precipitation events is severely overestimated, shown by a peak in residual (see Fig. 35), but this can be attributed to a precipitation input issue rather than a streamflow routing issue within

the model. One of the main takeaways is that the model is able to accurately obtain the low streamflow during the summer months (residual is close to zero from May on excluding three precipitation events), which is of particular interest if further modeling of low flow and drought scenarios is the goal.

To evaluate both model output and the filtered method from Eq. 5 and 6 we will compare interflow and baseflow from model output with calculated interflow and baseflow obtained from the filtering process. For Eq. 6 here we will use the minimum monthly value instead of the minimum value from the entire water year because here only the 2008 water year is being looked at and the filtered estimate would just be a constant value using Eq. 6 as it is written (water year minimum).

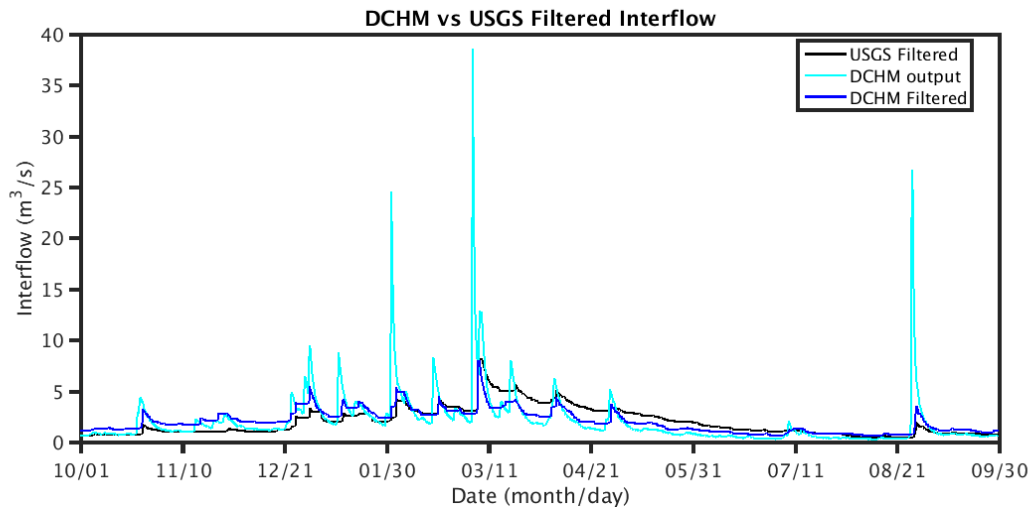


Figure 36: Shown are the USGS and DCHM time series resulting from the first filter application (Eq. 5), as well as the interflow from DCHM output. Interflow in the model output varies a great deal more than the filtered results in response to precipitation events. Looking at the shape of the peaks from the filtered time series they are still not indicative of a slow response, as they are still flashy.

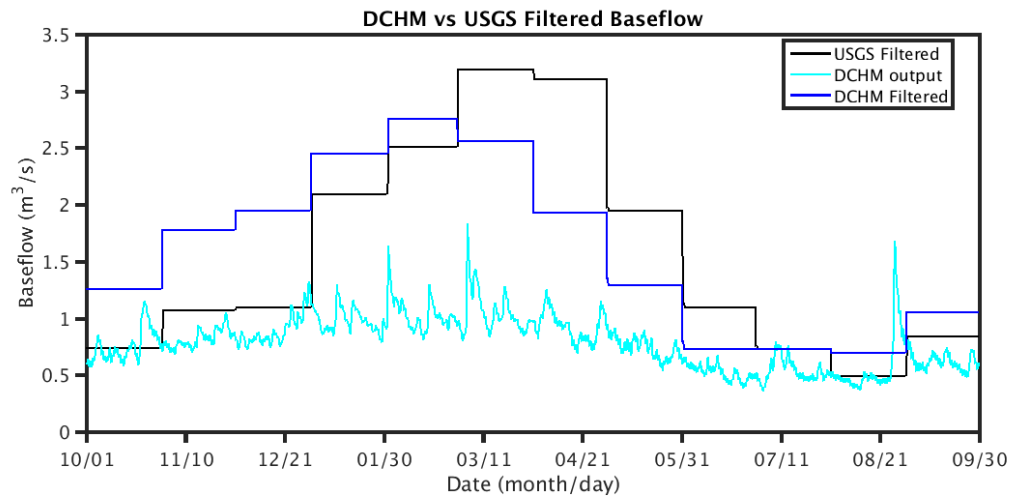


Figure 37: Shown are the USGS and DCHM time series resulting from the second filter application (Eq. 6 using monthly minimum), as well as the baseflow output from DCHM. The DCHM baseflow output is still lower in most cases than the twice filtered time series.

The twice filtered data are much closer to the baseflow output than would be if only 1 filter was applied via the WS90 method. This could mean that one filter is not enough and that estimating baseflow after one filter application is still incorporating interflow response, or that the DCHM is underestimating baseflow and groundwater contribution. It could be that the model does a good job separating interflow and baseflow and that the deep groundwater response is better represented by the model output and twice filtered time series. Baseflow output is underestimated by the DCHM because of the representation of subsurface hydraulic properties, and soil and hydrogeologic heterogeneities, and because it does not take into account regional groundwater connectivity. The impacts of regional groundwater in the Appalachians are

discussed by Brun and Barros (2014), Trapp Jr. and Horn (1997), Lloyd Jr. and Lyke (1995) and will be discussed in Chapter 5.

If a hydrology model is able to predict a water availability in the form of streamflow output given reasonable precipitation input that would be a useful tool for municipalities, decision makers, or prospective businesses to assess how their area might be affected by changing precipitation patterns and therefore be able to adjust when needed.

3.3 Other Parameters

Adapting a model to a specific basin requires adjustment of parameters that often vary from one river basin to the next. One such parameter is maximum channel width, which defines how wide any portion of the stream network may be. With the Mills River being a smaller and narrower river, the maximum channel width was estimated to be 30 meters from google maps. Changing the maximum channel width, in this case making the channel width smaller compared to a previous run, led to changes in streamflow given the same volume of water passing through (see Fig. 38 below). Making the channel width smaller and more realistic for MRB actually improve the timing of the hydrograph peaks as compared to a maximum channel width of 50m. The 30m width time series seen in blue peaks prior to the 50m width time series seen in magenta. It is clear in the first peak in Fig. 38 that the change in response time using 30m is more in line with the USGS stream gauge.

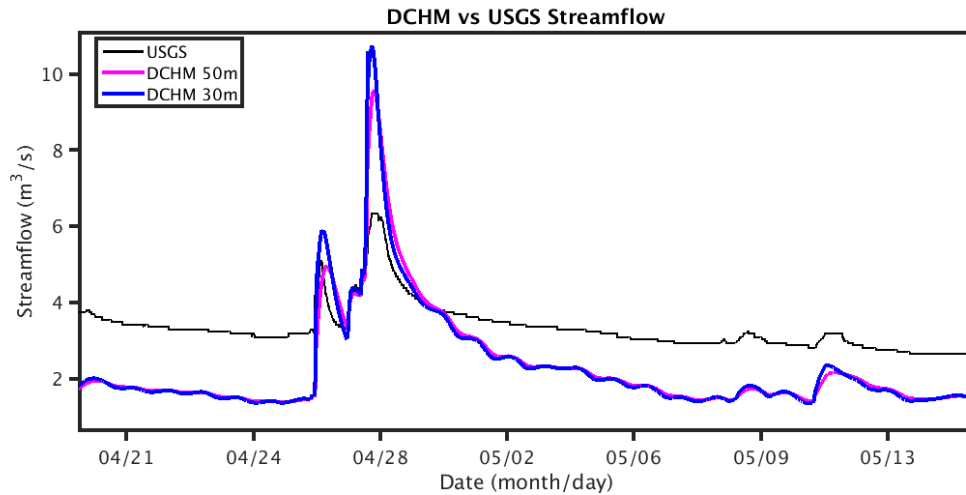


Figure 38: Two sets of model outputs seen in magenta and blue. Decreasing the maximum channel width from 50m to 30m is correct in that it is a more accurate representation of the Mills River and as expected gives a higher peak streamflow.

The spatial distribution of channel width in the MRB is seen below. The headwater streams are smaller and serve as tributaries to the two main forks of the Mills River (north and south), which then combine to form the Mills River in the lower section of the basin.

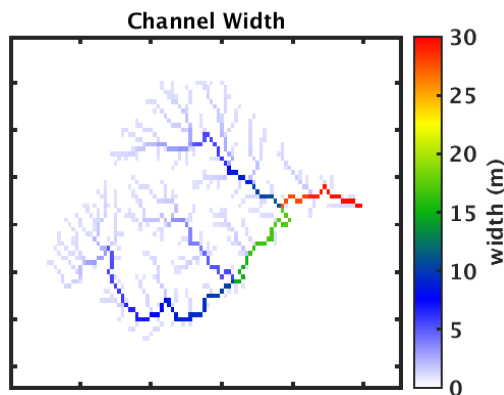


Figure 39: Channel width distribution in MRB. Most of the basin is comprised of smaller headwater streams, only becoming larger once the topographic relief decreases in the eastern portion of the basin.

Changing the coefficient that determines the magnitude of subsurface routing conductivity has implications on the lower portion of the hydrograph while surface runoff is associated with most of the upper peaks of the hydrograph.

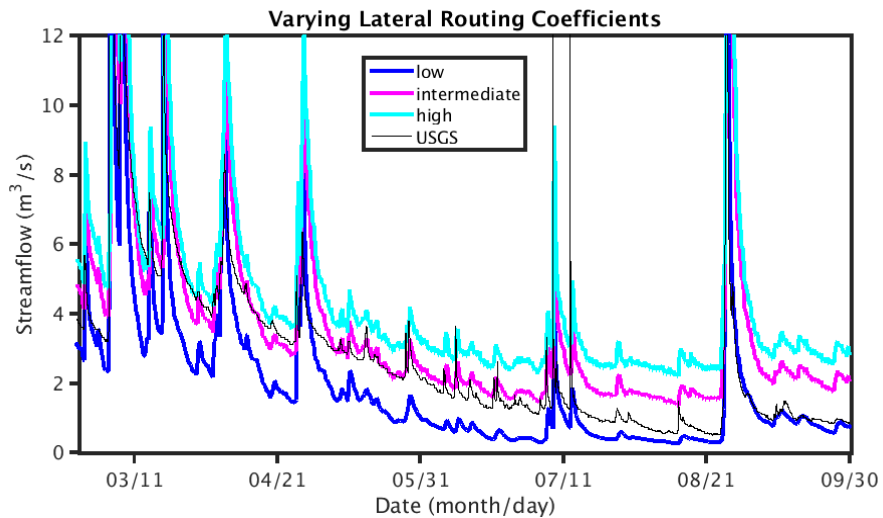


Figure 40: Changing the subsurface routing will have a significant effect on the location of the lower end of the hydrograph. There are three coefficients changed in each scenario (one for soil layer 2, one for soil layer 3, and one for soil layer 4). High (Run2) = 2000, 3, 0.5. Intermediate (Run4) = 1000, 1.5, 0.15. Low (Run 3) = 100, 0.5, 0.05. Runs are listed in Table 2 below.

Looking at Fig. 40, the intermediate routing coefficient gives a better estimate of streamflow than the low routing coefficient prior to the two large precipitation events in July and late August, but after the precipitation events the low routing coefficient gives a more accurate estimation of streamflow. The difference in streamflow estimation between the two different runs decreases over a period of recession, but increases following a precipitation event. This behavior is seen in the soil moisture for layers 2 and

3 with agreement increasing (difference decreasing) throughout a recession period, but increased difference after an influx of water (Fig. 41).

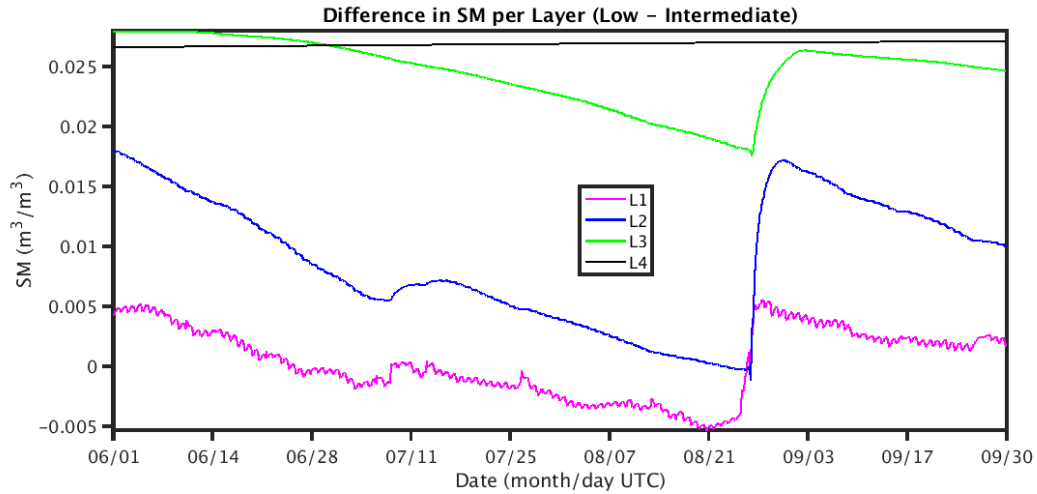


Figure 41: The difference in soil moisture for each of the four soil layers (intermediate routing – low routing). Calculated as the basin average of soil moisture at each time step and then subtracted. Note that Tropical Storm Fay occurred in late August, which is the reason for the significant increase for layers 1, 2, and 3.

Layer 4 exhibits almost no change over the four month period shown in Fig. 41 due to the slow response that is characteristic of deeper soil layers and resulting baseflow. A greater routing coefficient means faster subsurface routing and that less water is stored in the ground or moves slowly within the ground but rather moves out to the channel faster, which is why streamflow at the USGS gauge pixel is generally higher for a larger routing coefficients (Fig. 40). The set of coefficients used to obtain Fig. 34 and 35 were from Run 5 (see Table 2) with coefficients in between that of the low and intermediate coefficients used in Fig. 40 because the low coefficients appear to chronically underestimate streamflow and the intermediate coefficients result in higher

than anticipated streamflow near the end of the time series, which should not be the case because the model should adjust well and do a better job capturing an accurate response by the end of the run.

Table 2: Specific of some of the DCHM runs with results present in this section. Lateral routing coefficients are used to change the rate of subsurface routing. LB means base layer.

	Max channel width (m)	Lateral routing coefficients (L2,L3,LB)	Total runs (Spins +output)
Run1	50	100, 0.5, 0.05	5
Run2	30	2000, 3.0, 0.3	5
Run3	30	100, 0.5, 0.05	5
Run4	30	1000, 1.5, 0.15	5
Run5	30	500, 1.0, 0.1	6

Different routing coefficients will have different effects on streamflow, interflow, and baseflow at different time scales. Faster routing will lead to more streamflow at shorter time scales because water will follow gradients to the channel faster, but lower routing will lead to more soil moisture in deeper layers over longer time scales (Fig. 42) because less water is being diverted to the river channel and is given time to percolate down through the layers.

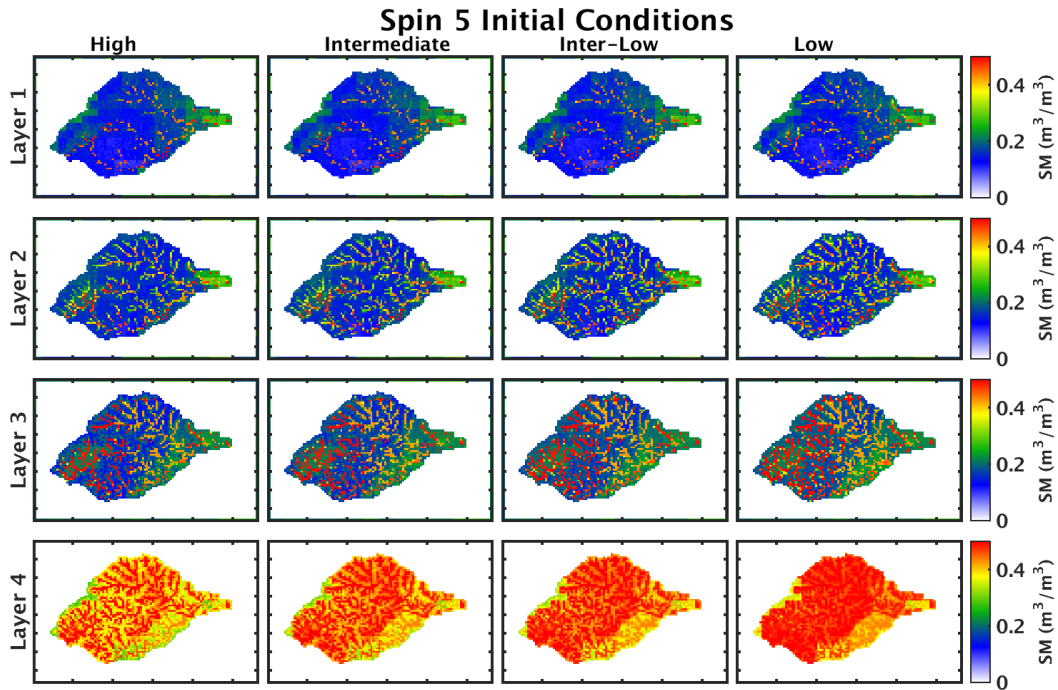


Figure 42: Varying soil moisture conditions after four spins using different lateral routing coefficients. High (Run 2), Intermediate (Run 4), Inter-Low (Run 5), and Low (Run 3) from Table 2. Notice how layer 4 is most noticeably different because the higher the lateral routing, the more water that will make its way to the stream network. The 4 years of spin prior to this figure is enough time to have differentiation between the base layers (layer 4).

Soil moisture and associated subsurface movement of water are what control the replenishment of groundwater aquifers and affect baseflow. Changes in soil moisture at the lower layers are not obvious over weeks and months because of the much slower response that they exhibit (Fig. 43 below). However, it is possible to view the changes in soil moisture in the first and second soil layers due to precipitation or lack thereof.

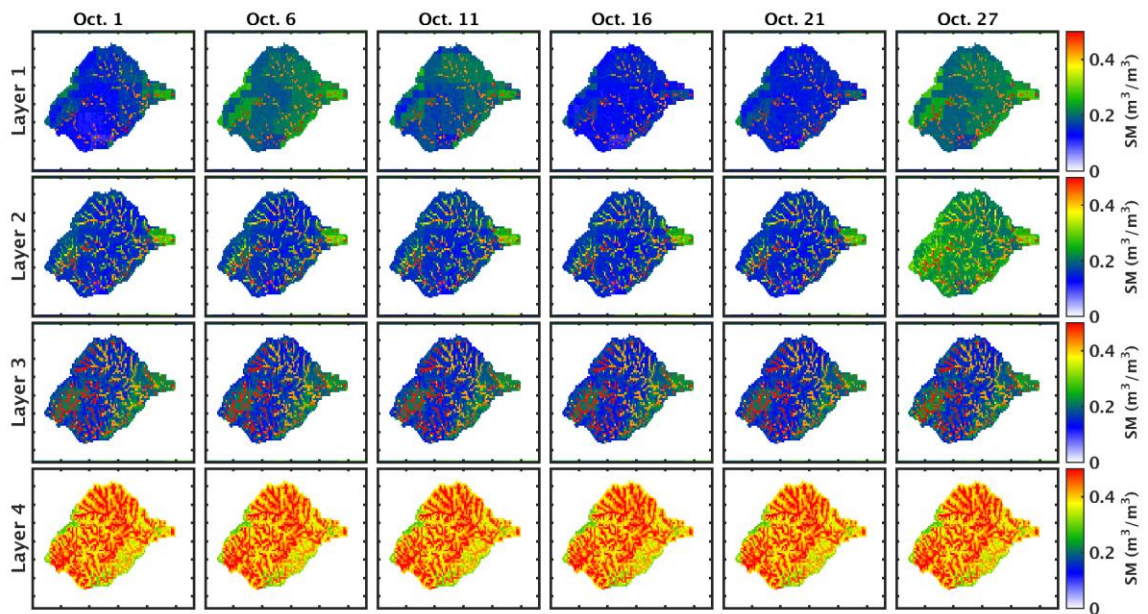


Figure 43: Over the course of October there is a period of little to no rain (mid to late October) and then a noticeable rainfall/streamflow response event near the end of the month (see Fig. 34 for hydrograph response). The change from October 16 to October 27 is very noticeable in the first two layers, but there is no visible change in layers three or four. This is due to the fact that the upper layers respond at shorter time scales while lower layers respond at much longer time scales.

4. Evidence of Combined Natural and Human Systems

4.1 Sustainability

The sustainability of the MRB will be assessed based on the ability of available streamflow to meet combined demand. Combined demand is defined as natural demand (minimum ecological flow requirement: 50 cfs) plus human demand. The USGS gauge will be used to measure the upstream water availability here so that human demand is defined as water use downstream of the gauge itself. HWTP and AWTP have intakes downstream of the gauge (Fig. 4) and account for the human demand used in this section. We see that the addition of water municipalities over time leads to an increase in water supply vulnerability with respect to natural and human demand.

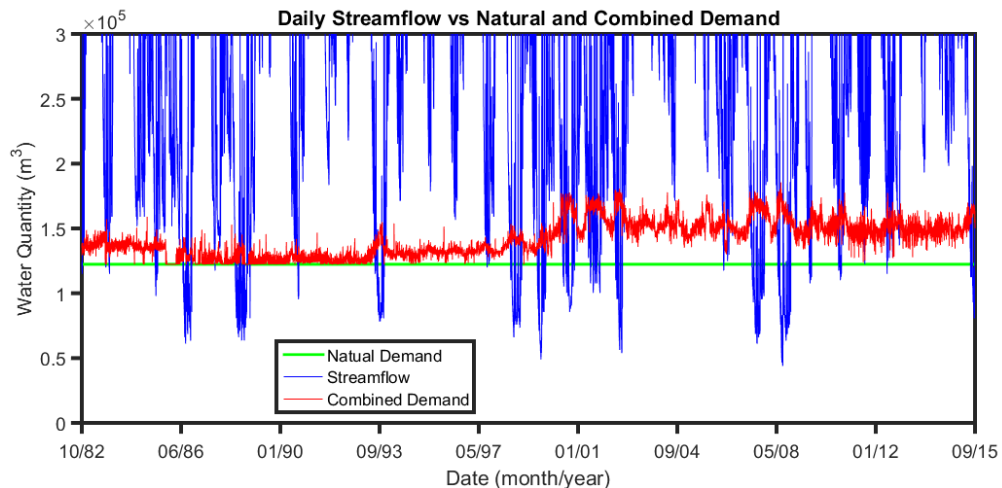


Figure 44: Daily Streamflow compared to natural and combined demand. Note that all values are aggregated to m³/day. Natural demand is defined by 50 cfs, which is the value below which the HWTP alters its uptake pattern. Combined demand is defined as the amount of water withdrawn from the river downstream of the USGS gauge plus natural demand.

With the addition of the AWTP in 2000, there is a visible jump in combined demand (Fig. 44). The different levels of human influence on sustainability is evident in both Fig. 45 and 46 below. In Fig. 45, from 2000-2015 what actually occurred is marked in red as both HWTP and AWTP were operational, but if only HWTP was taken into account (marked in green), the number of unsustainable days would have been lower (see Fig. A2 for AWTP data calculation).

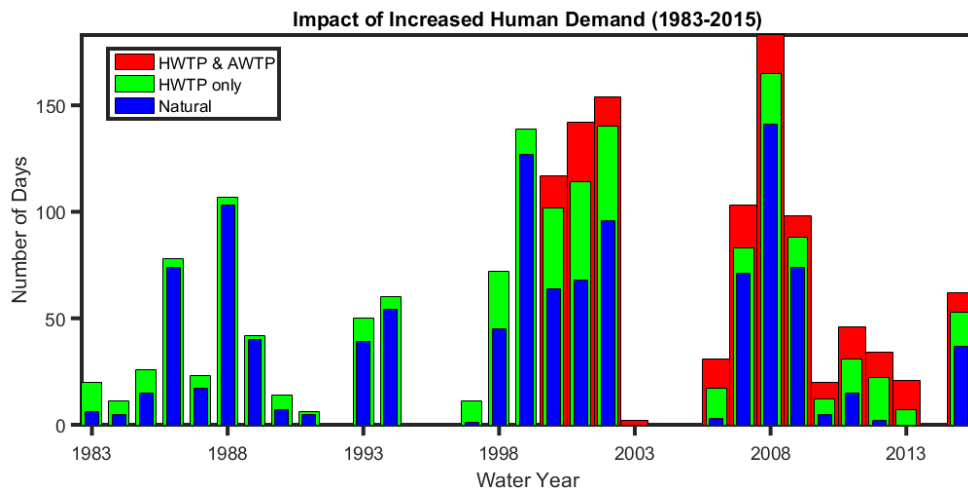


Figure 45: Introduction of human demand (HWTP only) in 1982 and increased human demand (HWTP&AWTP) in 2000 increases the number of unsustainable days within a given water year. Note that AWTP did not open until 2000 and HWTP data was not consistent until 1982. 2008 was an especially dry year and is reflected in the figure.

The results of Fig. 45 make sense as one less WTP withdrawing water should result in less days of combined demand exceeding available streamflow. The blue bar shows the number of unsustainable days that would have occurred due only to breaching the ecological minimum flow requirement. Figure 46 shows the vulnerability of the MRB when predisposed to naturally dry conditions. In each case shown there is a

moderate to severe drought according to the Palmer Drought Severity Index (PDSI), which can be seen by the significant number of unsustainable days based solely on the natural demand exceeding the available streamflow, without any addition from human demand. The driest years with PDSI < -3 all have more than 70 naturally occurring unsustainable days.

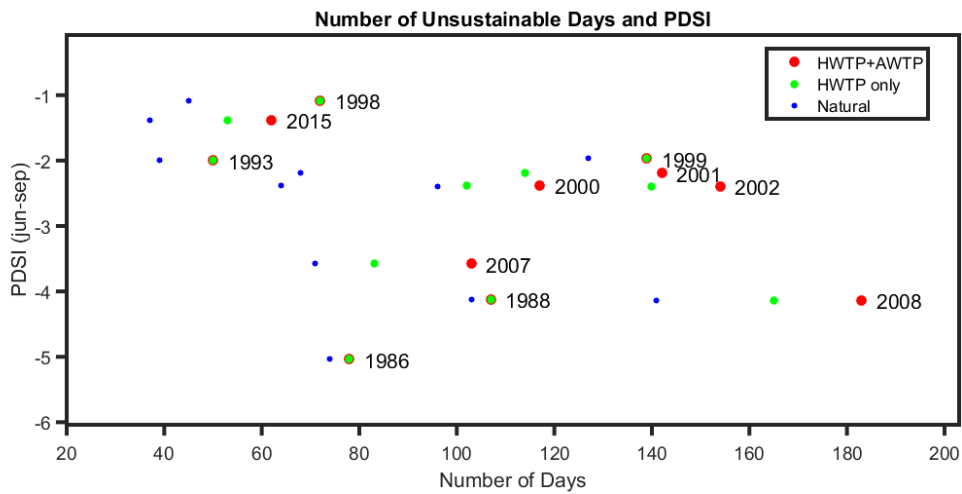


Figure 46: The effect of combining human demand with natural demand can be seen in the difference between the blue, green, and red data points. Prior to 2000 the green and red points will be identical because there was no additional water treatment plant open yet. PDSI is the Palmer Drought Severity Index, calculated for NC climate division 1 for a four month period June-September (<http://www.ncdc.noaa.gov/cag/>).

The addition of one WTP increases the risk of stressing the system and then the addition of a second WTP (indicative of increased LULC change and population growth) leads to even higher rates of unsustainable days per year (see Table 3 below). This increase over time and development is visible in Fig. 46, moving from left to right as natural demand progresses to HWTP only and then eventually both WTPs. Table 3 delivers two main points, first on the impact of choosing what the minimum instream

flow requirement is (i.e. 7Q2, 7Q10, or other) and second on the impact of different levels of human influence. Choosing a larger minimum ecological flow requirement may end up giving the appearance of having more unsustainable days, but will likely lead to better awareness and management in a more sustainable manner due to the improved management and conservation efforts needed to meet the more stringent requirement. For example in Table 3 if HWTP had used the 7Q10 streamflow value as opposed to the daily mean of 50 cfs as their instream flow requirement, their number of unsustainable would have been far fewer despite using the same amount of water. In fact, if the instream flow requirement were 7Q10, they could actually have used more water and still had far fewer unsustainable days than they accrued with the 50 cfs instream flow requirement.

Table 3: Unsustainable days per year for (50 cfs, 7Q2, and 7Q10) in that order for each of the given time periods and different levels of human demand. Note that combined (both) takes into account both WTPs. HWTP data starts in the 1983 water year, AWTP in 2000, hence the N/A's in some places. Yellow highlighted periods is the actual combined demand during that given period. The orange highlighted period is the overall average for the entire period (all 3 yellow periods). All other values are what the numbers would have been if that level of human demand had theoretically occurred.

	Natural	Combined (HWTP)	Combined (AWTP)	Combined (both)
1935-2015 (81 yrs)	(27.1, 30.5, 4.0)	(31.8, 34.7, 4.7)	(29.1, 32.1, 5.8)	(34.0, 36.9, 11.0)
1935-1982 (48 yrs)	(22.5, 25.9, 2.8)	N/A	N/A	N/A
1983-1999 (17 yrs)	(31.6, 34.2, 5.2)	(38.8, 40.6, 15.1)	N/A	N/A
2000-2015 (16 yrs)	(36.0, 40.3, 6.3)	(52.1, 54.9, 18.6)	(46.3, 48.4, 15.4)	(63.3, 66.1, 31.6)
1983-2015 (33 yrs)	(33.8, 37.2, 5.7)	(45.2, 47.5, 7.5)	(38.8, 41.1, 10.2)	(50.7, 53.0, 23.1)

Looking at combined demand with different levels of human demand there is the obvious progression of increased human involvement leading to more unsustainable days per year. The three yellow highlighted counts show the increase over time as the Mills River went from natural demand to having the HWTP and finally to having HWTP and AWTP. From Table 3 there is also an insight into the longer term trend of water availability in the region comparing the average number of unsustainable days per year that would occur if you only take into account natural/ecosystem demand. For the three distinct periods of 1935-1982, 1983-1999, and 2000-2015 there is a significant increase in the number of naturally occurring unsustainable days per year across all three levels of instream flow requirements. Under the assumption that this estimate of natural demand is fully uncombined from human demand, then one could assert that there is progressively less water available via natural processes from 1935-2015, but from Fig. 47 it appears to be more so 1975-2009.

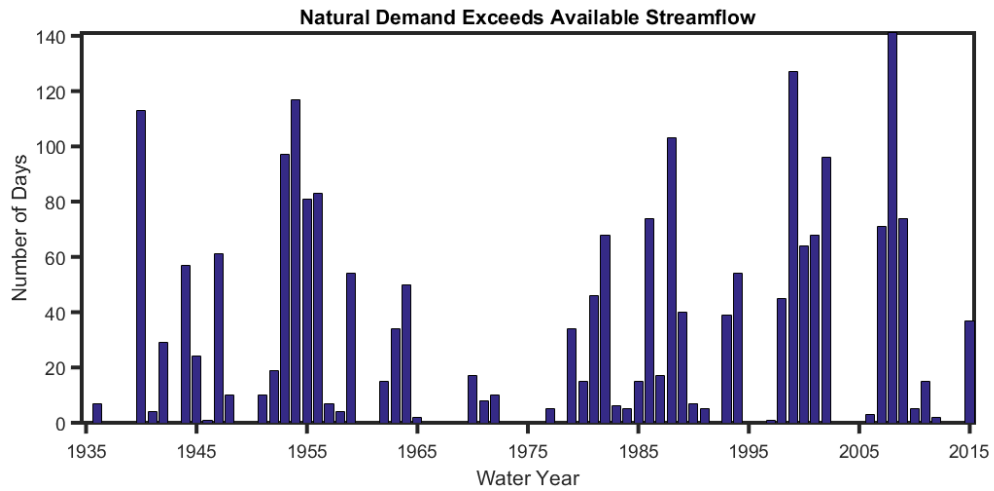


Figure 47: Distribution of naturally occurring unsustainable days. Note that 2008 (severe drought) is the tallest peak. There appears to be a longer term trend getting wetter from 1940-1975 and then drier from 1975 on.

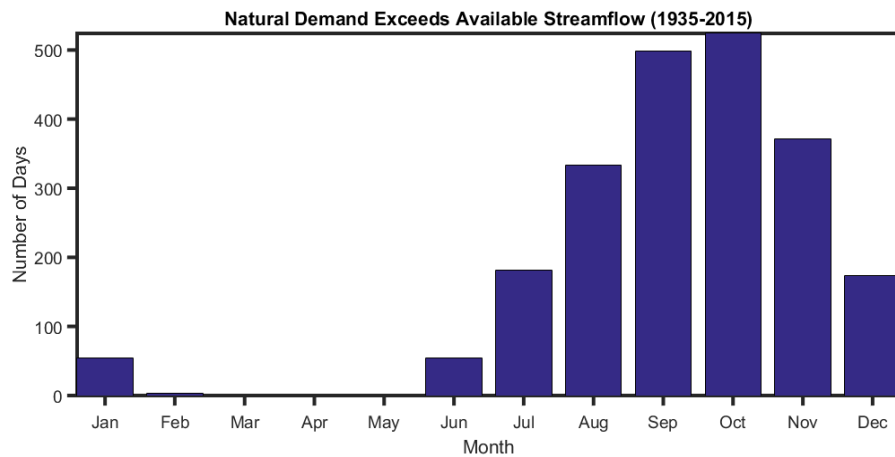


Figure 48: Distribution of naturally occurring unsustainable days. As expected the months with the higher frequencies occur during the lower values of streamflow on average.

The distribution of natural demand exceeding minimum instream flow shows that within the last 30 years there have been more periods of low flow while the distribution of unsustainable days across time of year follows an expected distribution

with frequencies highest during the time of year when the hydrograph is in recession and at its lowest flows (end of summer, early fall).

It should be noted that if 50 cfs at the USGS gauge were truly a minimum ecological requirement, then for the entire combined system to be considered sustainable the minimum flow should really be 50 cfs plus downstream human demand. In a severe drought year (based on 2008 water year data) the WTPs added 16 cfs to this requirement bringing the total minimum flow requirement to 66 cfs at the USGS gauge. For a wet year (2010 water year) the WTPs added 12.8 cfs to the minimum flow requirement bringing the total minimum flow requirement to 62.8 cfs.

The minimum instream flow requirement followed by HWTP leads to changes in behavior when the available streamflow is below the level of this requirement. The HWTP will in effect shut off its headwater reservoir intakes and rely solely on the downstream river intake (Fig. 4). This can potentially have a negative impact on the quality of the pre-treated water as the headwaters of the basin are cleaner than the water downstream, and can lead to increased cost of treatment. It is important to have the instream flow requirement be sufficient for the ecosystem, but also taking into account the potential costs of days where the WTP has to shift its behavior and treatment. Looking at a range of minimum instream flow requirements (Fig. 49) defined as the mean daily streamflow at the USGS gauge, it is clear that there is a jump in days where HWTP would have to shift its operation. There is a big difference below and above the

30 cfs requirement in the average number of days per year of such occurrences. Mead (2002) from NCDENR made instream flow requirement suggestions on a monthly and seasonal basis such that only July-December had requirements and those requirements ranged by month from 30-42 cfs. HWTP uses 50 cfs as the threshold, which is actually more stringent of a requirement and favors the ecosystem over potential WTP costs of breaching the threshold.

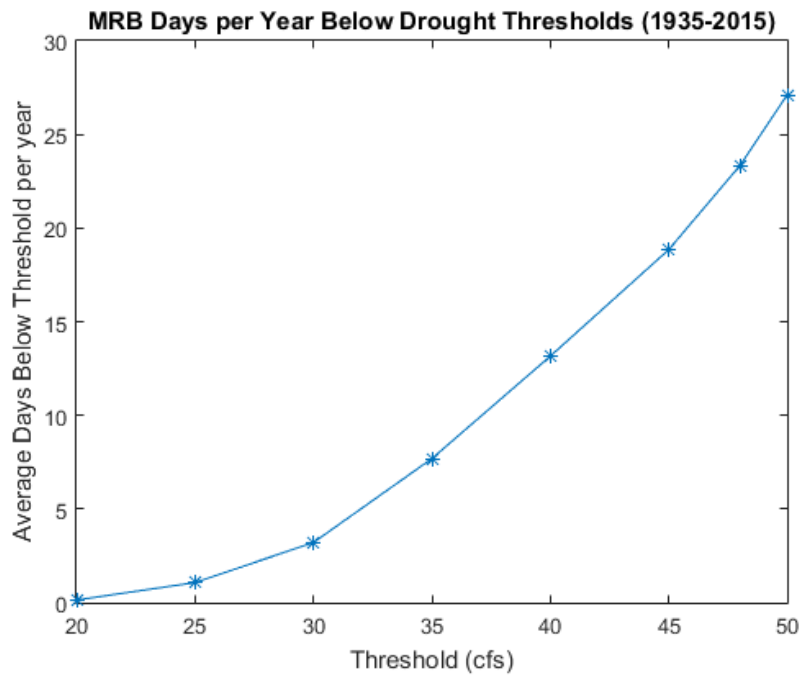


Figure 49: Average number of days per year where observed mean daily streamflow is below the instream flow requirement threshold.

Setting up a minimum ecological flow requirement and thus a metric of sustainability is important to make sure that day to day demand is met (Richter et al., 2003). From a longer term water budget assessment, it appears that the Mills River is being used sustainably at the annual time scale. It is important to note that due to time

constraints for this thesis project, the model was not initialized at equilibrium. Tao and Barros (2014) reported that it was necessary to spin up the model for a total of about twenty to thirty five-years in order to achieve stability in model performance, whereas here only five repetitions of the same year, and a particularly dry year were used for spin-up. In addition, a general baseline representation of the deep soil horizons and water table depth was used, which implies very significant gradients between the characteristic time-scales of lateral water transport in the top soil layers that cause excessive numerical diffusion (the model is run with a time-step of 5 minutes, and the vertical discretization is of the same order of magnitude of the horizontal discretization for the deep soil layer, even as the hydraulic conductivities differ by orders of magnitude with depth). This results in mass balance closure errors that vary from year to year during spin-up. The cumulative natural water balance in the model is:

$$\text{Model Imbalance} = P - R - ET - \Delta S_{sm} = -78.5 \text{ mm} \quad (\text{Eq. 8})$$

Cumulative human impact over the course of the 2008 water year is calculated as:

$$-RW_w - GW_w + Ret = \Delta S_h = -90.8 \text{ mm} \quad (\text{Eq. 9})$$

P=precipitation, R=runoff, ET=evapotranspiration, ΔS_{sm} =soil water content change, RW_w =river water withdrawal, GW_w =groundwater withdrawal Ret=return to natural system, ΔS_h =change in water storage (human only). All assumptions and detailed calculations for human demand can be found in Appendix B. The impact of human

water use on the system is within the model water balance closure uncertainty as model imbalance and ΔS_h are on the same order of magnitude.

The model imbalance errors using the five spin-up repetitions is 7.4% when divided by the input precipitation. This is excessive. By contrast the model imbalance at the end of spin 2 was less than 1%, but the performance for peak discharge was inferior to using the five spin ups. Thus, further work is needed to examine the representation of deep soil layers including the vertical discretization, followed by model initialization spanning regionally relevant time-scales and including an adequate range of year-to-year climate variability including wet years.

4.2 Streamflow and Baseflow Time Series Signatures

In order to determine if the increase in naturally occurring unsustainable days is part of a longer multi decadal trend or just natural variation, plotting naturally occurring unsustainable days with precipitation should show if these are all related to meteorological drought conditions.

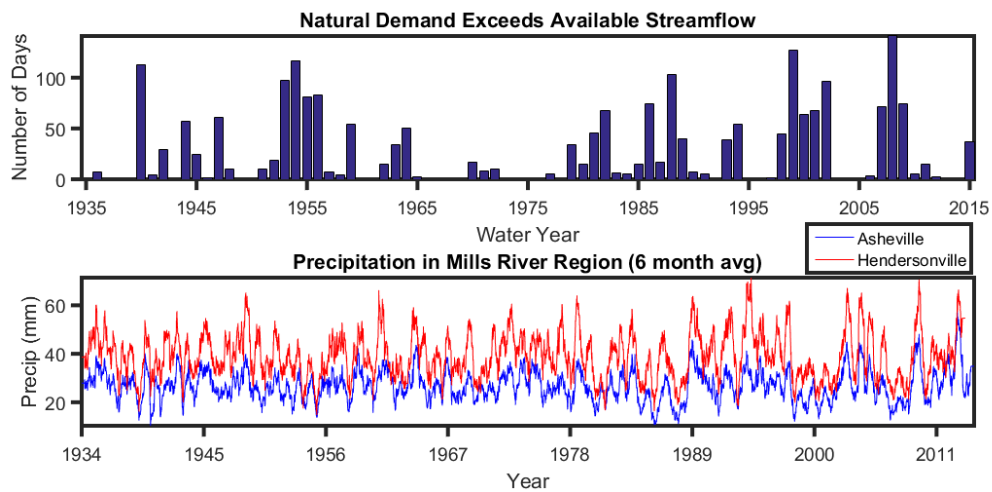


Figure 50: Distribution of naturally occurring unsustainable days. Two nearby precipitation station records (smoothed to six month average). Almost every multiyear trough in the precipitation data corresponds to a cluster of high frequency years of unsustainable days (meteorological drought conditions).

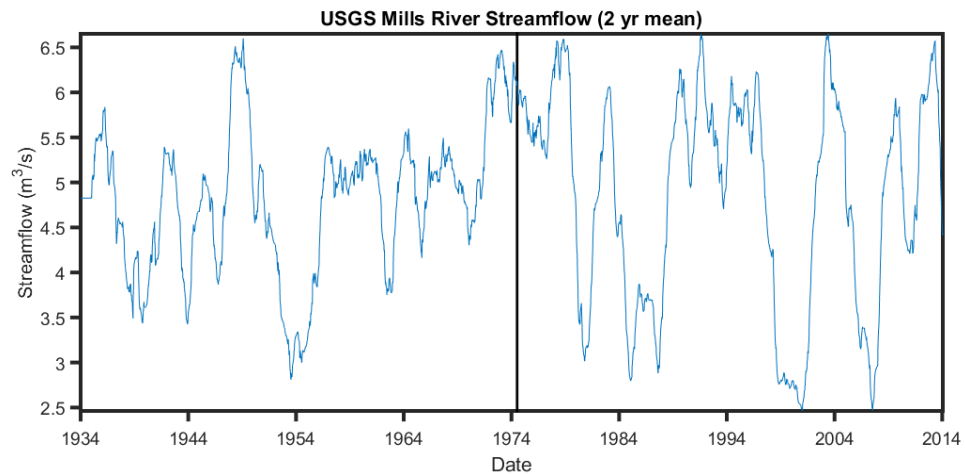


Figure 51: Two year running mean of Mills River streamflow to explore any differences before and after 1975 (4/1/1975 is the midpoint of the data). There is minimal difference in the mean before and after 4/1/1975 (4.80 vs 4.85), but there is a large change in variance (0.63 vs 1.40). This is evident in the much larger swings between periods of high and low streamflow post 1975.

In order to explore the nature of the divergent behavior of natural exceedances from 1975 out in both direction, the two year running mean streamflow time series was constructed to see the larger trends over multiple years. The overall trend of streamflow does not change over time which means that in terms of long term trend, the amount of water available in the Mills River is not changing a great deal, but the more than doubling of variance between the two halves of the data suggest that periods of low flow and drought have recently been a major concern for those involved in water management and any type of activity reliant upon freshwater supply. This shift in variance since the mid 1970's can be attributed to shifts in precipitation variability and was not isolated to the MRB, but rather common to the entire Southeast U.S. (Wang et al., 2010). In that study, two periods (1948-1977 and 1978-2007) for the entire Southeast U.S. exhibited very different behavior with regard to precipitation variability, similar to the patterns seen in Fig. 51. In the first period there were two wet and two dry summers exceeding one standard deviation, while in the second period there were six wet and five dry summers. It was also shown that the variance of multiple precipitation indices have been steadily increasing since 1970. The trend in intense precipitation has been linked to increasing greenhouse gas concentrations (Groisman et al., 2005). If this increase in variability is indeed linked to greenhouse gas concentrations then there is little to no reason to suspect that this pattern of extreme precipitation and thus extreme

streamflow will not continue as greenhouse gas concentrations continue to increase in coming decades (Meinshausen et al., 2009).

Agriculture in the MRB is prevalent and in the most recent decade there have been a number of extreme drought years (Schlenker, 2009) that caused a large downturn in agricultural yield and thus had an impact on food prices and availability of certain goods. The drought of 2007-2008 cost North Carolina's agriculture an estimated \$573 million in damages and 79% of water customers (over 5 million people) faced water use restrictions (Davis, 2015). Both the 2007-2008 and 1998-2002 severe droughts in North Carolina were characterized by lack of rain as meteorological droughts (Weaver, 2002).

To explore the increase in overall unsustainable days over time as it relates to increased human presence in the region, population data can be used as an indicator of human demand on the Mills River, as the cities of Hendersonville and Asheville both have WTPs on the river, but did not always. As populations of Henderson and Buncombe Counties, as well as that of the cities of Hendersonville and Asheville have grown and continue to grow (Fig. 1 and 2), the increased demand on water has and will lead to changes in the interactions between municipalities and the MRB. It becomes increasingly difficult to manage growing human demand sustainably during periods of drought as human water demand is often highest during the periods of low natural streamflow in the summer months from increased water use for both residential and for agricultural purposes in response to high summer temperatures (Battisti, 2009). As seen

in Fig. 52 below, not only did the addition of a second WTP to the MRB in 2000 lead to increased unsustainable days, but the years 1999-2002 and 2007-2008 were periods of intense drought in the region, which was only exacerbated by the newly increased human presence.

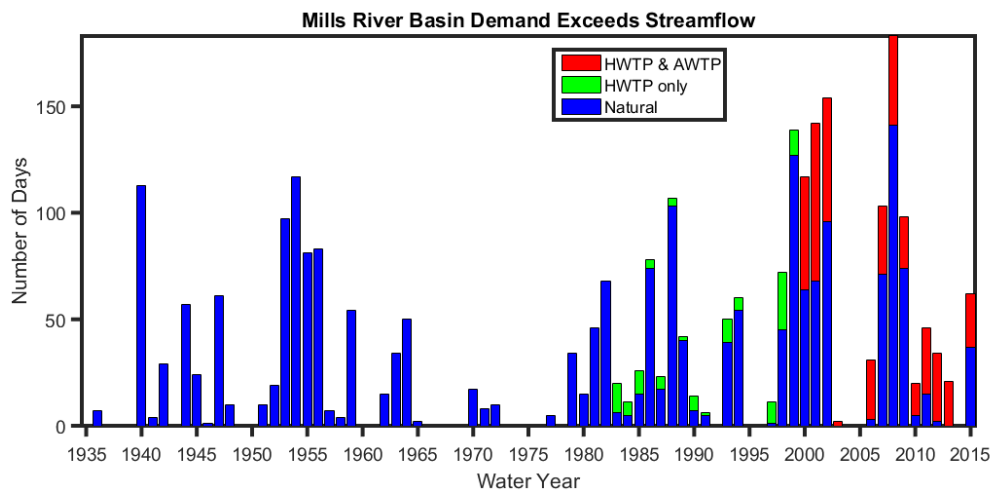


Figure 52: Unsustainable days over time of the Mills River with different levels of human influence over time, first with the addition of HWTP and then AWTP. The number of unsustainable days that would have occurred given zero human demand is shown in blue.

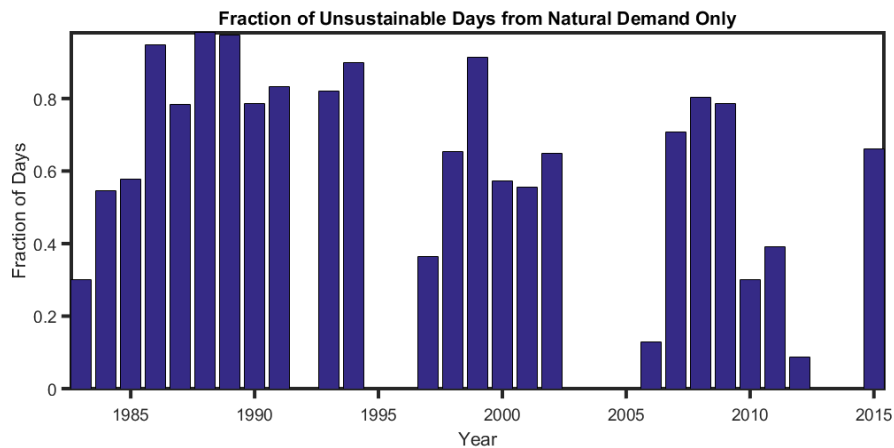


Figure 53: Fraction of unsustainable days attributed to natural demand only. Natural demand (50 cfs instream flow requirement) is still the main driver of unsustainability, but there are some years where that is not the case.

The HWTP has a permit to withdraw 14.2 million gallons per day and is expanding to 18 million gallons per day, receiving a permit to set up a secondary river intake that will be located on the French Broad River, of which the Mills River is a tributary (Mead, 2002). The local governing bodies in Mills River, cooperation between stakeholders, and public awareness of the importance of water quality and water availability in the region should help to ensure that the Mills River is managed properly in a holistically beneficial manner (Mills River Partnership, 2015). It should be noted that AWTP has a smaller capacity than HWTP, but does not adhere to any instream flow requirements. After the addition of AWTP the number of exceedances attributable to additional human demand greatly increased from the years prior when there was only HWTP present (Fig. 45 and 52). As human demand has increased over time it is not

surprising to see a number of recent years where the fraction of unsustainable days attributed to natural demand only is relatively low compared to previous years (Fig. 53).

Separating streamflow into contributing parts (runoff, interflow, and baseflow) we should expect to see strong dependence on baseflow in the summer and early fall months. Figure 54 shows this strong dependence on baseflow, and also that subsurface flow all together (interflow and baseflow) mostly control the overall streamflow except during times of precipitation events marked by peaks in runoff.

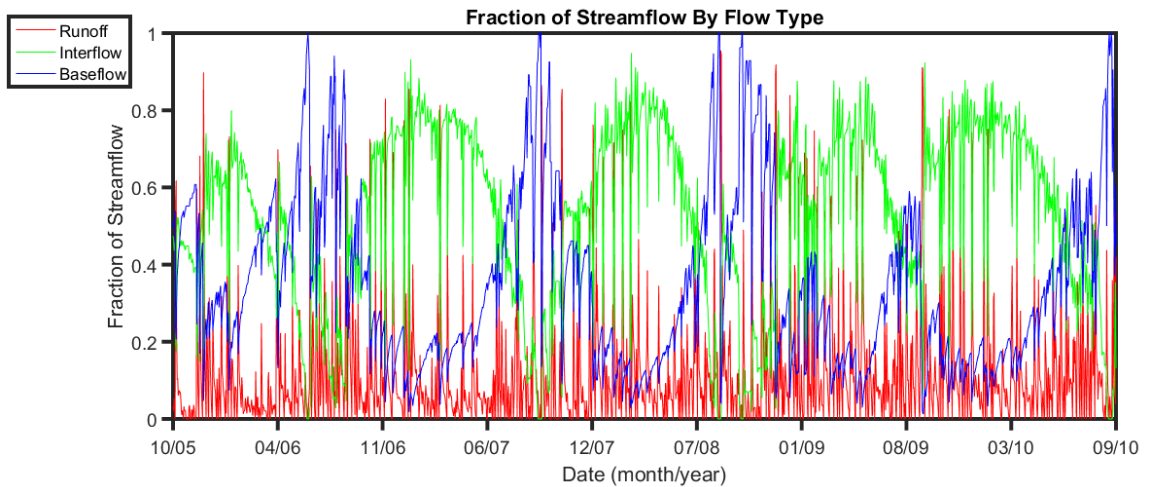


Figure 54: Contribution to streamflow by component of streamflow. It is evident that baseflow is consistently the overwhelming contributor to streamflow in the periods of low streamflow during the summer and fall. The baseflow time series used was calculated by Eq. 5 and 6. Interflow was calculated by Eq. 5. Runoff is the difference between streamflow and interflow.

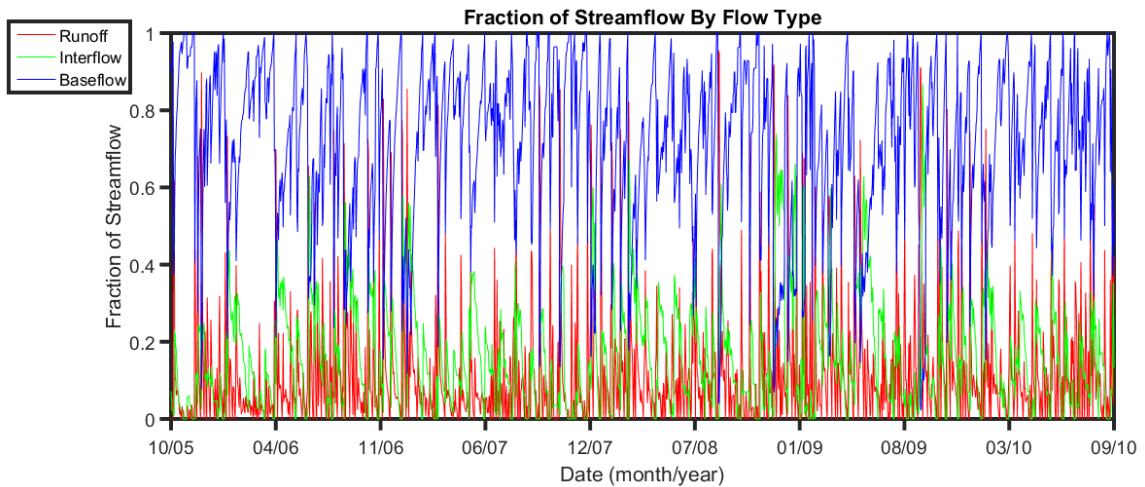


Figure 55: Contribution to streamflow by component of streamflow. The difference from Fig. 54 is an alteration to Eq. 6. Instead of taking the minimum value for the entire water year, the minimum value per month was used instead. This takes away some of the previously calculated interflow and attributes it instead to baseflow.

Looking at Fig. 55 it is evident that baseflow is major contributor to streamflow, which is not surprising because the MRB consists of smaller order streams and has topographic relief therefore local regime baseflow as a fraction of streamflow will be greater (Faye and Mayer, 1990). Other streamflow and baseflow studies of the southeast U.S. have been found to have a wide range of annual average baseflow contribution ranging from 16 to 92 percent (Bachman et al., 1998). Using Eq. 6 with minimum per water year (Fig. 54) the mean baseflow contribution is 37%, while using minimum per month (Fig. 55) the mean baseflow contribution is 70%. This disparity is due to the difference between filter interval width and leads to a difference in assigning what is interflow and what is baseflow. In both cases it is shown that in the lower streamflow months baseflow becomes the main contributor to overall streamflow. It is difficult to

regulate groundwater (Hobbs Jr., 2013; Dellapenna, 2003; Scophocleous, 1997) but in basins where baseflow is a major contributor to water availability in periods of drought (Peters et al., 2005; Van Loon and Laaha, 2015) it would appear prudent to manage and be aware of groundwater systems in addition to stream networks.

5. Characterization of Hydrogeological Heterogeneity based on Baseflow Variability

The diverse physiography and topography of North Carolina can lead to a variety of subsurface responses based on the hydrogeology of the region. Brun and Barros (2014) showed that different physiographic regions (as defined by USGS) will have different subsurface responses to precipitation events. This would lead one to think that baseflow will behave differently depending on the physiographic region and associated subsurface response to water input from precipitation events. The physiographic regions looked at here include the Coastal Plain, Piedmont Province, Blue Ridge Province, Valley and Ridge Province, and Appalachian Plateau Province. The Coastal Plain is mostly underlain by semiconsolidated to unconsolidated sediments that consist of silt, clay, and sand, with some gravel and lignite. Some consolidated beds of limestone and sandstone are present. The Piedmont Province is an area of varied topography that ranges from lowlands to peaks and ridges of moderate altitude and relief. The metamorphic and igneous rocks of this region have been sheared, fractured, and folded with some sedimentary basins of shale, sandstone, and conglomerate also in the province. The mountain belt of the Blue Ridge Province consists mostly of igneous and metamorphic rocks but also includes small areas of sedimentary rocks. The Valley and Ridge Province is characterized by layered sedimentary rock that has been complexly folded and locally thrust faulted. As the result of repeated cycles of uplift and

erosion, resistant layers of well-cemented sandstone and conglomerate form elongated mountain ridges and less resistant, easily eroded layers of limestone, dolomite, and shale form valleys. The Appalachian Plateau Province is underlain by rocks that are continuous with those of the Valley and Ridge Province, but in the Appalachian Plateau the layered rocks are nearly flat-lying or gently tilted and warped, rather than being intensively folded and faulted. In the Piedmont and Blue Ridge Provinces almost all water recharge is from precipitation that enters aquifers through porous regolith. Much of the recharge moves laterally through the regolith and discharges to nearby streams after a storm event, but some of the water moves downward until it reaches bedrock and enters fractures in crystalline rocks and sandstones. In crystalline-rock areas, the regolith and fractures in the bedrock serve as the principal places for the storage transmission of water (Trapp Jr. and Horn, 1997; Lloyd Jr. and Lyke, 1995).

To examine how baseflow varies between physiographic regions, USGS stream gauges from 34N-37N, 74W-88W were selected. Gauges with more than 3% of their length of record accounted for by missing data (most missing data occurred in the early history of these gauges) were truncated from the beginning of record until missing data accounted for only 3% of the record. From there, only stations with length of record of at least 20,000 days (54.7 years) and with an end of record of 9/30/2015 or later were kept. This led to the selection of 126 suitable USGS stream gauge stations (see Table 4). The beginning of record for selected stations were all 10/1/1961 or prior, and the first October

1 in the period of record was used as the start date and 9/30/2015 was used as the end date to remain consistent and have only full water years in the period of analysis.

Table 4: USGS stream gauge stations used. Station number as seen in figures going forward, numbered from west to east. Start date is the start date used in the proceeding analysis for complete water years (October 1-September 30). End date used for all sites was 9/30/2015.

Station number	USGS ID	Latitude	Longitude	Drainage area (mi ²)	start date
1	03604000	35.496	-87.833	447	10/1/1920
2	03434500	36.122	-87.099	683	10/1/1925
3	03599500	35.618	-87.032	1208	10/1/1920
4	03433500	36.055	-86.929	409	10/1/1920
5	02450000	34.012	-86.737	358	10/1/1928
6	03598000	35.480	-86.499	481	10/1/1934
7	03574500	34.624	-86.306	320	10/1/1936
8	03421000	35.708	-85.732	640	10/1/1924
9	02398000	34.466	-85.336	192	10/1/1937
10	02388500	34.298	-85.138	2115	10/1/1939
11	02395980	34.232	-85.117	1801	10/1/1938
12	02387500	34.577	-84.942	1602	10/1/1893
13	02387000	34.667	-84.928	687	10/1/1937
14	02383500	34.564	-84.833	831	10/1/1939
15	02385800	34.717	-84.770	64	10/1/1960
16	02394000	34.163	-84.741	1122	10/1/1938
17	03540500	35.983	-84.558	764	10/1/1927
18	02392000	34.240	-84.495	613	10/1/1936
19	02334430	34.157	-84.079	1040	10/1/1942
20	03550000	35.139	-83.981	104	10/1/1914
21	02333500	34.528	-83.940	153	10/1/1940
22	03498500	35.786	-83.885	269	10/1/1951
23	02331600	34.541	-83.623	315	10/1/1957
24	03504000	35.128	-83.619	51.9	10/1/1940
25	03503000	35.336	-83.527	436	10/1/1944
26	03513000	35.428	-83.447	655	10/1/1897
27	03528000	36.425	-83.398	1474	10/1/1919
28	03500240	35.159	-83.394	57.1	10/1/1961
29	03500000	35.150	-83.380	140	10/1/1944
30	03512000	35.461	-83.354	184	10/1/1945
31	02177000	34.814	-83.306	207	10/1/1939
32	03455000	35.982	-83.161	1858	10/1/1920
33	03531500	36.662	-83.095	319	10/1/1931
34	03459500	35.635	-82.990	350	10/1/1927
35	03491000	36.426	-82.952	47.3	10/1/1957
36	03455500	35.396	-82.938	27.6	10/1/1954

37	03456500	35.462	-82.870	51.5	10/1/1954
38	03456991	35.522	-82.848	130	10/1/1928
39	03439000	35.143	-82.825	67.9	10/1/1935
40	03453500	35.786	-82.661	1332	10/1/1942
41	03443000	35.299	-82.624	296	10/1/1920
42	03446000	35.398	-82.595	66.7	10/1/1934
43	03451500	35.609	-82.578	945	10/1/1895
44	03451000	35.568	-82.545	130	10/1/1934
45	03465500	36.176	-82.457	805	10/1/1920
46	02163500	34.392	-82.223	580	10/1/1939
47	03463300	35.831	-82.184	43.3	10/1/1957
48	03524000	36.945	-82.155	533	10/1/1920
49	03478400	36.632	-82.134	26.9	10/1/1957
50	02149000	35.423	-82.112	79	10/1/1951
51	02154500	35.121	-81.986	116	10/1/1930
52	02138500	35.796	-81.891	66.7	10/1/1922
53	02167000	34.175	-81.864	1360	10/1/1926
54	03473000	36.652	-81.844	303	10/1/1931
55	03479000	36.239	-81.822	92.1	10/1/1940
56	03488000	36.897	-81.746	221	10/1/1920
57	02151500	35.211	-81.698	875	10/1/1925
58	02152100	35.493	-81.682	60.5	10/1/1959
59	03471500	36.760	-81.631	76.6	10/1/1942
60	02111000	35.991	-81.558	28.8	10/1/1939
61	02156500	34.595	-81.421	2790	10/1/1938
62	03161000	36.393	-81.407	205	10/1/1924
63	02143000	35.684	-81.403	83.2	10/1/1942
64	02143500	35.421	-81.265	69.2	10/1/1951
65	02144000	35.306	-81.235	31.8	10/1/1953
66	02111500	36.175	-81.169	89.2	10/1/1939
67	02112000	36.153	-81.146	504	10/1/1920
68	02169000	34.014	-81.088	2520	10/1/1925
69	03164000	36.647	-80.979	1141	10/1/1929
70	02146000	34.985	-80.974	3050	10/1/1942
71	03165000	36.646	-80.919	39.4	10/1/1944
72	03167000	36.939	-80.887	258	10/1/1927
73	03168000	36.938	-80.746	2212	10/1/1929
74	02118500	36.001	-80.746	155	10/1/1951
75	02148000	34.245	-80.654	5070	10/1/1929
76	02114450	36.299	-80.415	42.8	10/1/1960
77	02130900	34.514	-80.183	108	10/1/1959
78	02126000	35.149	-80.176	1372	10/1/1929
79	02130910	34.397	-80.150	173	10/1/1960
80	02072000	36.781	-80.025	215	10/1/1946
81	02072500	36.770	-80.001	259	10/1/1939
82	02093800	36.173	-79.953	20.6	10/1/1955
83	02129000	34.946	-79.870	6863	10/1/1927
84	02128000	35.387	-79.831	106	10/1/1954
85	02071000	36.413	-79.826	1053	10/1/1940

86	02074000	36.526	-79.766	538	10/1/1939
87	02132000	34.052	-79.754	1030	10/1/1929
88	02100500	35.726	-79.656	349	10/1/1923
89	02094500	36.173	-79.614	131	10/1/1928
90	02131000	34.204	-79.548	8830	10/1/1938
91	02133500	35.061	-79.494	183	10/1/1939
92	02096500	36.087	-79.366	606	10/1/1928
93	02135000	34.057	-79.247	2790	10/1/1942
94	02102000	35.627	-79.116	1434	10/1/1930
95	02075500	36.642	-79.089	2587	10/1/1950
96	02134500	34.443	-78.960	1228	10/1/1929
97	02077000	36.777	-78.916	547	10/1/1929
98	02085500	36.183	-78.879	149	10/1/1925
99	02105500	34.836	-78.824	4852	10/1/1937
100	02102500	35.406	-78.813	3464	10/1/1924
101	02066000	36.915	-78.741	2966	10/1/1950
102	02088000	35.571	-78.591	83.5	10/1/1939
103	02081500	36.194	-78.583	167	10/1/1939
104	02109500	34.095	-78.548	680	10/1/1939
105	02087500	35.647	-78.405	1150	10/1/1927
106	02051000	36.997	-78.350	56	10/1/1946
107	02106500	34.755	-78.289	676	10/1/1951
108	02088500	35.511	-78.160	232	10/1/1930
109	02089000	35.338	-77.998	2399	10/1/1930
110	02082950	36.183	-77.876	177	10/1/1959
111	02108000	34.829	-77.832	599	10/1/1940
112	02051500	36.717	-77.832	552	10/1/1929
113	02091000	35.489	-77.806	80.4	10/1/1954
114	02044500	36.983	-77.800	317	10/1/1950
115	02083000	36.151	-77.693	526	10/1/1926
116	02080500	36.460	-77.634	8384	10/1/1912
117	02089500	35.258	-77.586	2692	10/1/1930
118	02091500	35.429	-77.583	733	10/1/1929
119	02052000	36.690	-77.541	744	10/1/1951
120	02083500	35.894	-77.533	2183	10/1/1931
121	02092500	35.064	-77.461	168	10/1/1951
122	02045500	36.900	-77.400	577	10/1/1930
123	02047000	36.770	-77.166	1441	10/1/1941
124	02053200	36.371	-77.026	225	10/1/1958
125	02053500	36.280	-76.999	63.3	10/1/1950
126	02049500	36.763	-76.898	613	10/1/1944

USGS Stations with common period of record 1962-2015 water years
within 34N-37N, 75W-88W

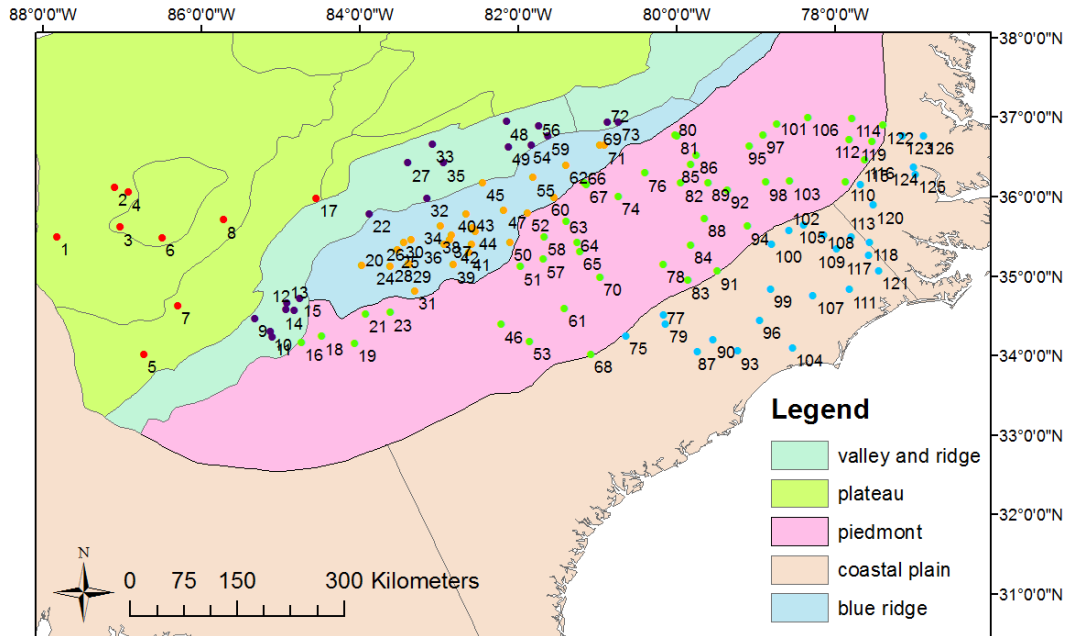


Figure 56: USGS streamflow gauge sites with at least 54 years of data, divided by physiographic regions as defined by USGS (n=126 sites). Note that the stations are numbered from 1 to 126 by longitude (west to east).

The same algorithms (Eq. 5, 6) that yielded the baseflow time series seen in Fig. 23 and the subsequent wavelet analysis seen in Fig. 24 were run for each of the streamflow time series of the 126 selected stations. One of the results is the scale averaged variance of the station's baseflow (Fig. 24(d) for example). Each of these variances were normalized by dividing the time series by the maximum value to have a range of [0 1].

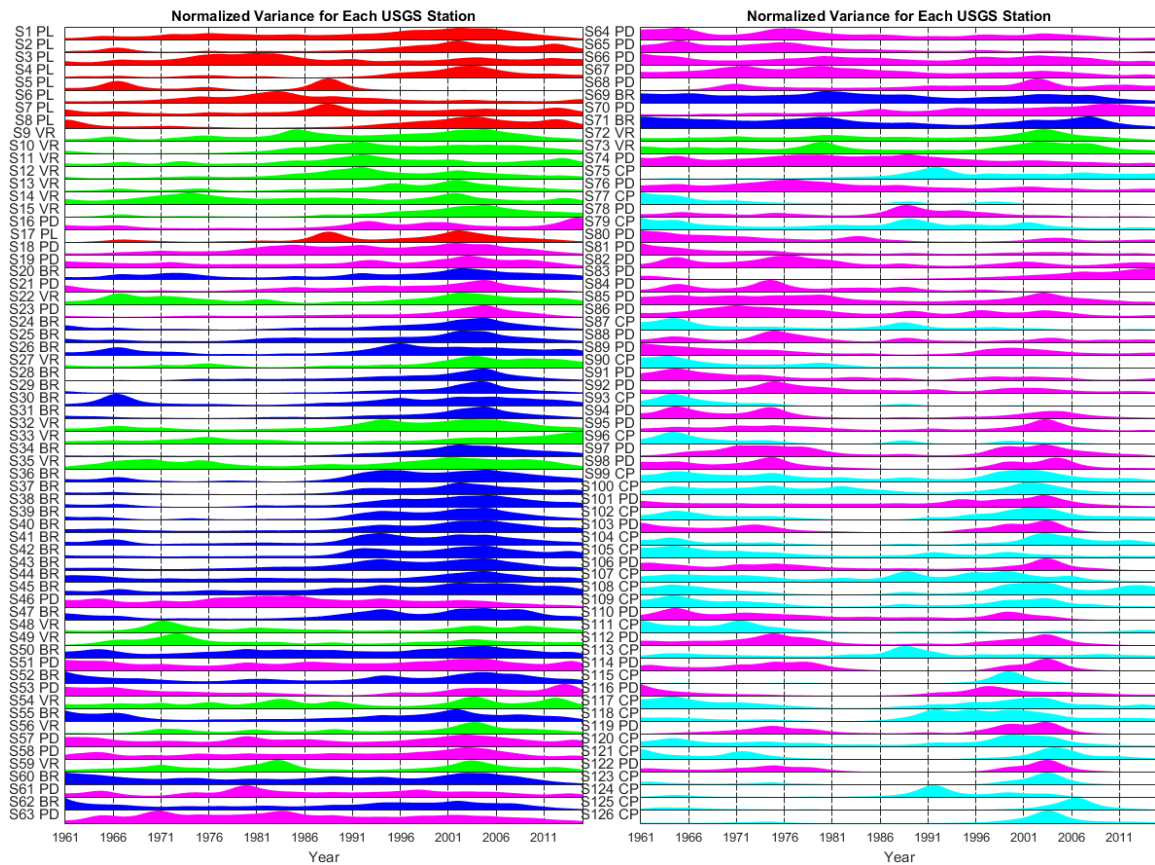


Figure 57: Normalized baseflow variance for the 126 stations in question. Red denotes Plateau region, green Valley Ridge, blue Blue Ridge, magenta Piedmont, and cyan Coastal Plain. Note that Mills River is Station 42 (Blue Ridge).

Looking at all of the stations' normalized variances, color coded by physiographic region, allows for the categorization of baseflow response due to physiographic region and longitudinal location. The signal from most of the Blue Ridge stations are very similar with higher variance later in the time series and very little in the earlier portion, but most of the Blue Ridge stations numbered 45 and below are in a similar geographic region. If you examine the response of Blue Ridge stations outside of this main cluster (stations numbered 50 and above) there is a similarity in response between them, but a

much different response than the Blue Ridge stations 45 and under. This is one example where geographic location and thus the local precipitation and river basin have more of an effect on baseflow variability than the physiographic classification and subsequent subsurface properties. An example of physiographic region and associated subsurface properties having more control over baseflow variability than location is evident when comparing a number of Coastal Plain and Piedmont stations. Many of the Coastal Plain stations exhibit similar responses to one another with high variability either in the 1960's or late 1990's-early 2000's. While a number of Piedmont stations are located near the Coastal Plain, most have a bimodal response with peaks in the 1970's and 2000's. This difference can either be attributed to varying subsurface responses to the same meteorological events, or differences in river basins and thus direction of routing. The easternmost Blue Ridge stations (50, 52, 55, 60, 62, 69, and 71) all have a similar normalized variance distribution (Fig. 57) and are actually more similar to those of the nearby Piedmont stations than the other Blue Ridge stations. This makes sense when you look at Fig. 56 as these station are actually along the border of the Blue Ridge and Piedmont Provinces. The fact that there are a number of stations within the same physiographic region that have very different responses suggests that further reclassification is necessary to group these stations properly.

USGS Stations with common period of record 1962-2015 water years within 34N-37N, 75W-88W

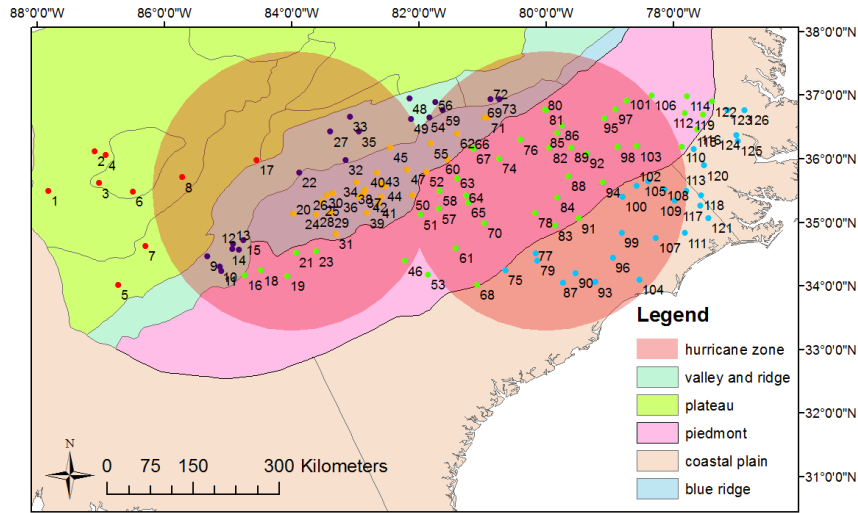


Figure 58: Zones used to search for tracks of hurricanes and tropical storms through the National Hurricane Center (<https://coast.noaa.gov/hurricanes/>). 200 km radius (max), centered at 35.5 N, 80W and 35.5N, 84W.

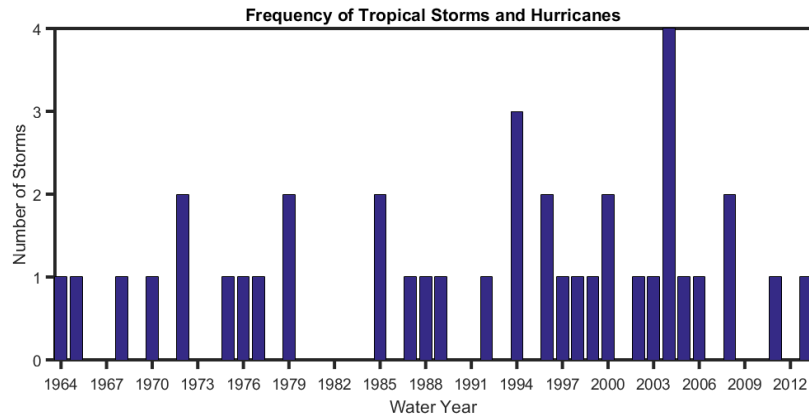


Figure 59: Temporal distribution of tropical storm and hurricane tracks passing through the selected zone seen in Fig. 58.

Most of the Blue Ridge stations have very similar signatures near 2004, which was the year with the most hurricanes or tropical storms in this period of record

(National Hurricane Center). The storms from 2004 led to a large signal in the variance at most stations in the region due to the unusually high amount of precipitation received. Almost every station other than the block of stations numbered 74-93 have an increased level of variability in the early 2000's centered around 2004. Looking at the storm tracks of the four tropical storms and hurricanes from that year explains why. The block of stations numbered 74-93 are mainly in the eastern Piedmont and southwestern Coastal Plain and are in the gap between the tracks of Jeanne and Gaston (Fig. 60) and not in a region of steep transition where groundwater would be transported over longer distances from other locations at higher elevations, as is in the Blue Ridge for example.

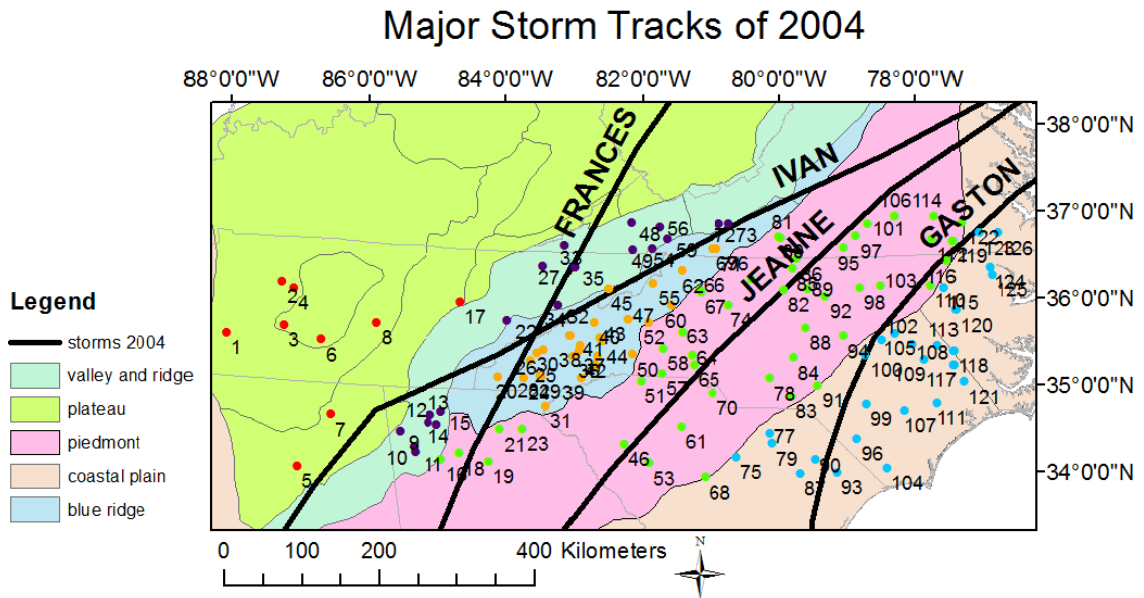


Figure 60: Storm tracks of major hurricanes and tropical storms of 2004. Geographic location and thus proximity to storms can also help to explain differences in baseflow response.

The order of the stations going from west to east jumps between physiographic regions, but it would be ideal to find a cross section where from west to east the stations go from one physiographic region to the next, without any overlap so a transect is defined (see Fig. 61).

USGS Stations with common period of record 1962-2015 water years within given transect of physiographic regions

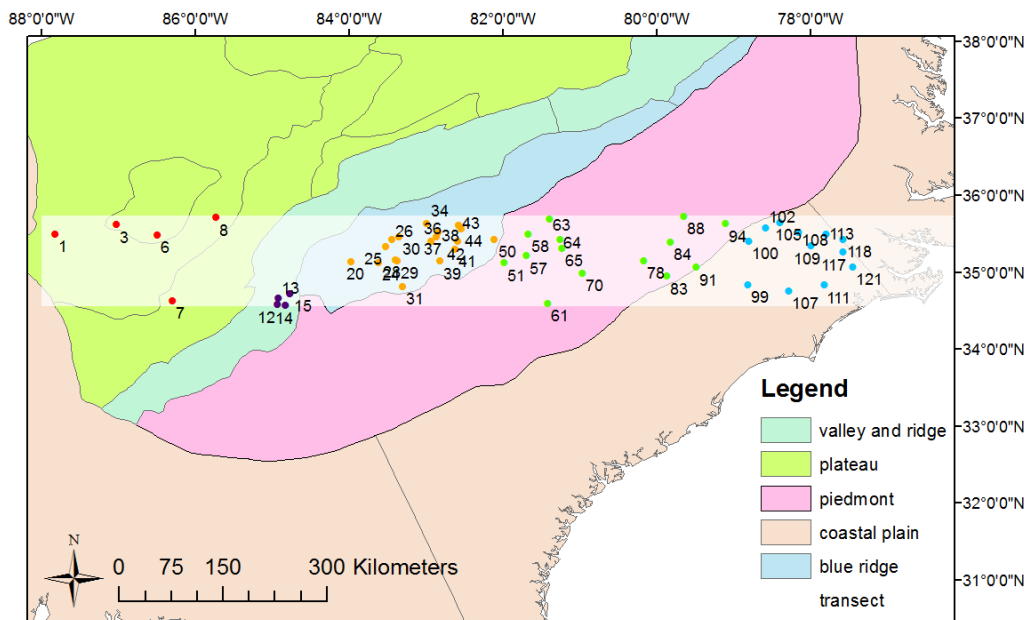


Figure 61: The transect shown in white creates a set of stations such that the stations progress from one physiographic region to the next as you change longitude.

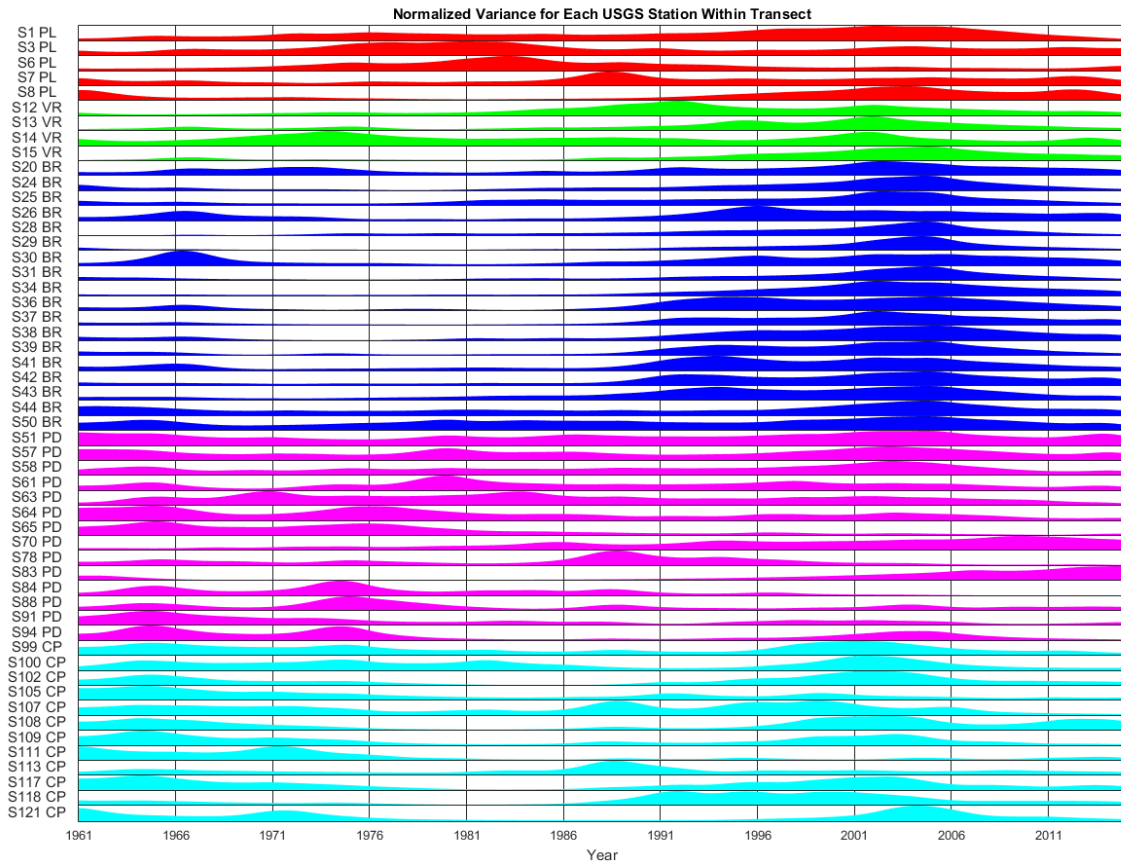


Figure 62: Normalized baseflow variance for the 53 stations within the transect defined in Fig. 61. Red denotes Plateau region, green Valley Ridge, blue Blue Ridge, magenta Piedmont, and cyan Coastal Plain.

The fact that 2004, a year marked by extreme precipitation events, exhibits the vast majority of variance for most of the Blue Ridge stations suggests that the Blue Ridge has a generally high amount of baseflow to start with and takes a series of extremely large precipitation event to register a significant signal in variance. This is in contrast with the Piedmont and Coastal Plain stations where the variance is spread out more so than for the Blue Ridge stations which means that either baseflow was extraordinarily high for the Blue Ridge in the years surrounding 2004 or that the Piedmont and Coastal

Plain generally exhibit more mild levels of baseflow such that the generally wet periods (1960's and 1970's) are able to produce above average baseflow and thus a signature in Fig. 62. It is known that local baseflow contribution as a fraction of total streamflow tends to be greater in regions of topographic relief and areas of lower stream orders and headwaters, both of which are more characteristic of the Blue Ridge than the eastern Piedmont Province and certainly the Coastal Plain (Faye and Mayer, 1990; Priest, 2004).

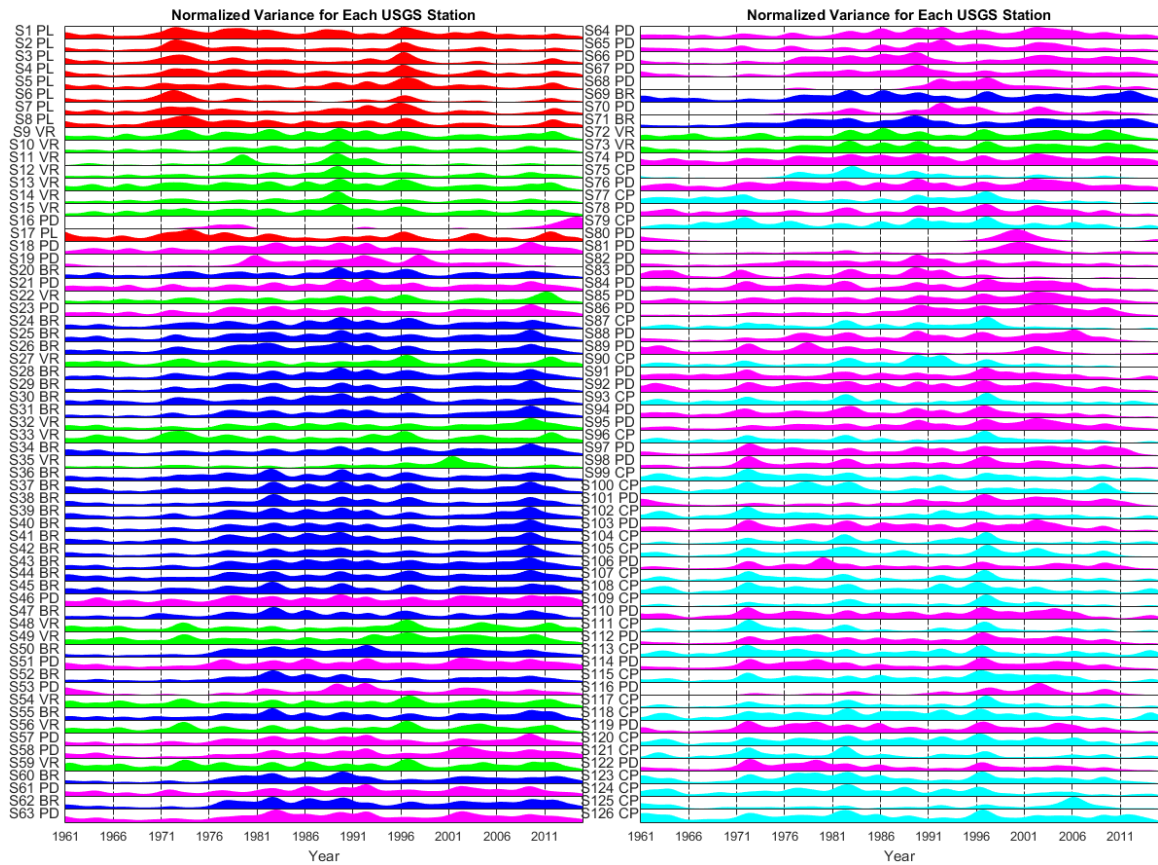


Figure 63: Normalized scaled averaged variance of seasonal baseflow for the 126 stations in question. Red denotes Plateau region, green Valley Ridge, blue Blue Ridge, magenta Piedmont, and cyan Coastal Plain. Note that Mills River is Station 42 (Blue Ridge). The baseflow used here is seasonal as opposed to per water year (see Fig. 30 for explanation of seasonal baseflow calculation).

Seasonal baseflow has more variability than annual baseflow as is shown by the increased number of peaks in Fig. 63 compared to Fig. 57. The potential impact of subsurface geology can be seen here in the similarity of response from stations 43-74, which include stations from the eastern Blue Ridge, eastern Valley and Ridge, and western Piedmont Provinces. The same six features appear for each station: peaks in roughly 1983, 1986, 1990, 1997, and two elongated peaks near 2004 and 2010. These stations are all located in a similar section of the Appalachian Mountains and it is likely that they are regionally connected via subsurface features such as fractures (Brun and Barros, 2014).

Empirical Orthogonal Function (EOF) and Principal Component Analysis (PCA) (Bjornsson and Venegas, 1997) are used to analyze the variability of a single field including spatial patterns of variability and time variation, as well as the importance of each pattern. Using normalized baseflow time series for each station ($\text{baseflow}/\text{max}(\text{baseflow})$) the EOF/PC analysis was performed. Principal component 1 is the eigenvector of the largest corresponding eigenvalue obtained from the EOF analysis. It is the component that explains the largest portion of variance amongst the mean time series of all 126 stations. Figure A3 shows that PC 1 and the mean normalized baseflow of all 126 stations are very much in agreement as expected and has a correlation of 0.98. PC 1 accounts for 37% of variance, PC 2 10.77%, and PC 3 9.79%. The time series of PC 1,

PC 2, and spatial distribution of EOF 3 provide some insight into what the controlling factors of baseflow variability might be.

The time series of PC 1 is very similar to that of the precipitation anomaly time series seen below (Fig. 64) with expansion coefficient peaks and troughs corresponding to specific peaks and troughs in the precipitation time series. It can be claimed that the amount of precipitation accounts for 37% of the variance in normalized baseflow.

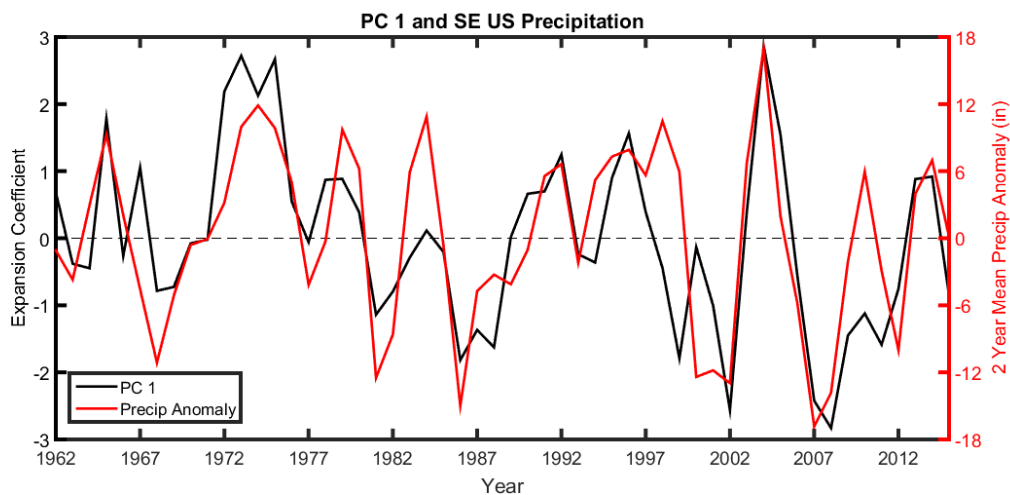


Figure 64: SE US precipitation anomaly (<http://www.ncdc.noaa.gov/cag/>) and PC 1. The anomaly was calculated from a two year average of precipitation. For example the precipitation anomaly for 1963 is from the two year mean precipitation for 10/1961 - 9/1963. PC 1 for 1963 is a measure of the 1963 water year (10/1962 - 9/1963). The two year precipitation average is important because large storms occurring in September will have significant impact on baseflow in October. This captures both precipitation during the respective water year as well as the antecedent precipitation that has a future impact on slow response baseflow.

Looking at Fig. 65-67 it appears that the magnitude of the EOF depends on whether storm tracks go through the station's location or not. Notice how the smaller blue circles in the Blue Ridge Province and smaller black circles in the Piedmont

Province have fewer storm tracks over them compared to the stations in the Coastal Plain or the western portion of the Appalachians, where the magnitude of the EOFs are generally larger.

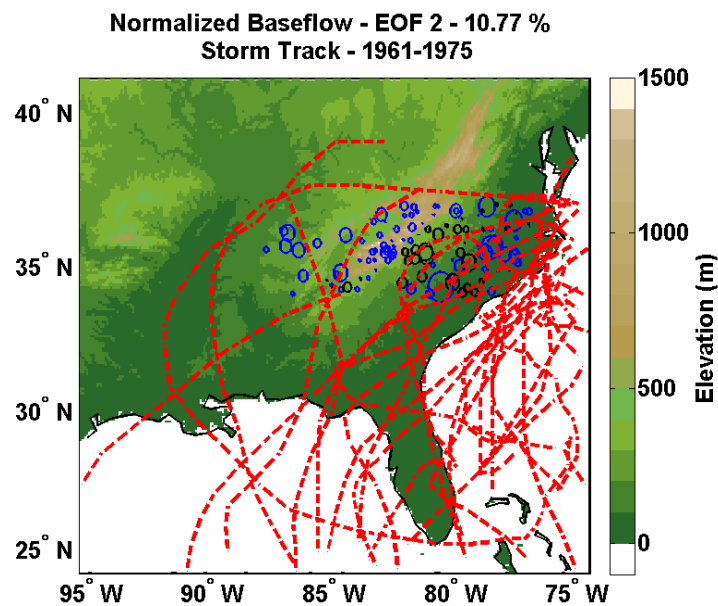


Figure 65: Hurricane and tropical storm tracks during 1961-1975 plotted with EOF 2. Note that EOF 2 is calculated for the entire period (1961-2015). Notice the lack of storm tracks over the eastern Blue Ridge and western Piedmont Provinces. Scarcity of storm tracks during this generally wet period, especially the early 1970's, is in line with the idea that the wet early 1970's were a result of high precipitation, but not due to impact of tropical storms and hurricanes.

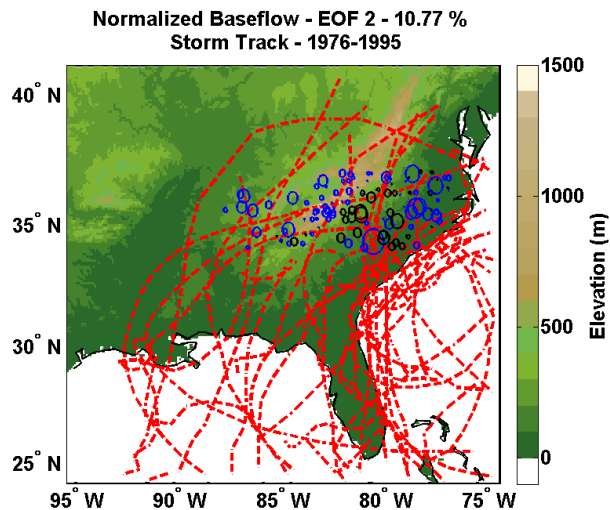


Figure 66: Hurricane and tropical storm tracks during 1976-1995 plotted with EOF 2. Note that EOF 2 is calculated for the entire period (1961-2015). Notice the lack of storm tracks over the eastern Blue Ridge and western Piedmont Provinces compared to the western Appalachians and Coastal Plain.

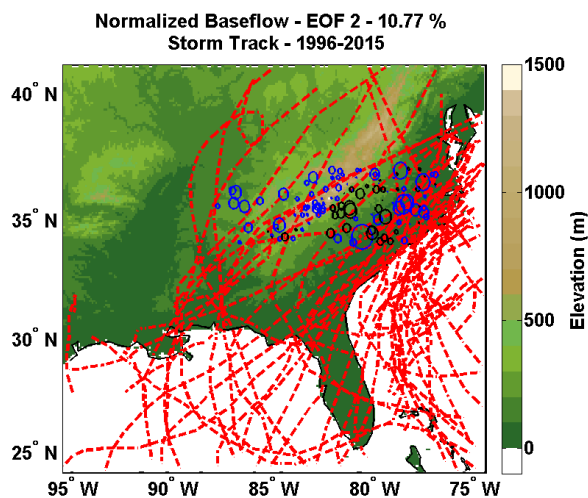


Figure 67: Hurricane and tropical storm tracks during 1996-2015 plotted with EOF 2. Note that EOF 2 is calculated for the entire period (1961-2015). Notice the lack of storm tracks over the eastern Blue Ridge and western Piedmont Provinces compared to the western Appalachians and Coastal Plain. Also this period has many more storms over the Appalachians than in Fig. 65 and 66. The higher number of large storms over the Appalachians during this period is in line with idea that some of the more recent wet years (2004 in particular) were heavily impacted by tropical storms and hurricanes.

Comparing the Principal Components time series to various climate indices exploring possible teleconnections, it is apparent that PC 2 and AMO (Atlantic Multidecadal Oscillation) are related (see Fig. 68 below).

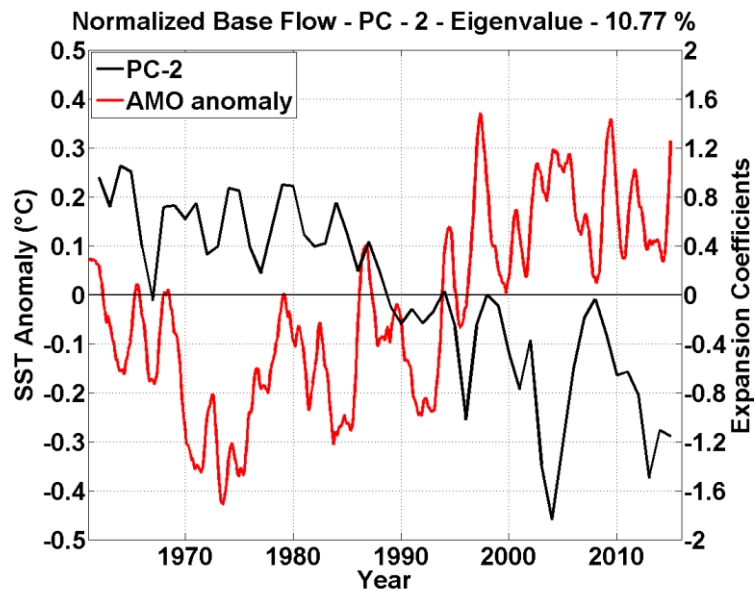


Figure 68: AMO 12 month running average SST anomaly and PC 2 for normalized baseflow. Inverse relationship both long and short term is evident. Monthly AMO data (unsmoothed) from <http://www.esrl.noaa.gov/psd/data/timeseries/AMO/>.

Since 1970, the AMO has been trending in a positive manner and PC 2 has been doing the opposite, trending negatively in the long term. In the shorter time scales, PC 2 and AMO also appear to be inversely related. The PC 2 time series has extreme negative values during years of multiple hurricanes and tropical storms, while having values close to zero for years of drought. It has been shown that a positive AMO phase is related to an increased number of tropical storms and hurricanes due to a warmer Atlantic Ocean (McCabe et al., 2004; Curtis, 2008; Maxwell et al., 2013; Labotka et al.,

2015). Positive AMO in conjunction with cold Pacific Decadal Oscillation (PDO) controls the majority (52%) of variability of North American droughts and is associated with drought in the Southern Appalachians (McCabe et al., 2004; Curtis, 2008; Mo et al, 2009). Comparing the time series of PC 1 and PC 2 it is evident that the large precipitation years associated with tropical storms and hurricanes have extreme values in both PC 1 and PC 2 (opposite sign), while periods of high precipitation associated with a generally wet period of time (early to mid 1970's) do not have a large signature in PC 2, but do in PC 1. For most of the recent droughts (1999, 2002, 2007-2008) the low values of PC 1 are associated with near zero values of PC 2.

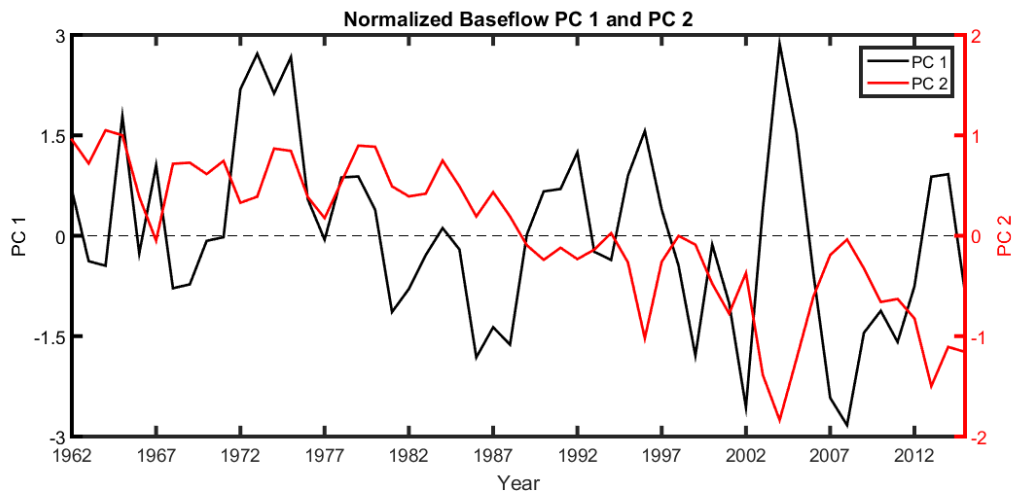


Figure 69: Time series of PC 1 and PC 2. PC 2 trending negatively over the length of the time series and becomes more extreme in most recent decades. Strong negative values of PC 2 can be associated with years heavily influenced by passing tropical storms and hurricanes.

To evaluate what factor is third most important in controlling normalized baseflow looking at the spatial plot of EOF 3 shows a dichotomy among the stations.

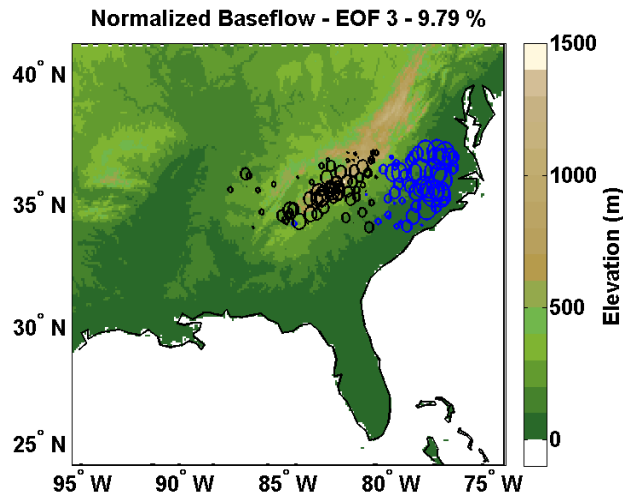


Figure 70: Normalized baseflow EOF 3 spatial distribution. Blue is negative while black it positive and the size of the circle indicates magnitude of variability.

Looking at Fig. 70 it appears that there is a relation between the sign of EOF 3 and either physiographic region or topography/elevation.

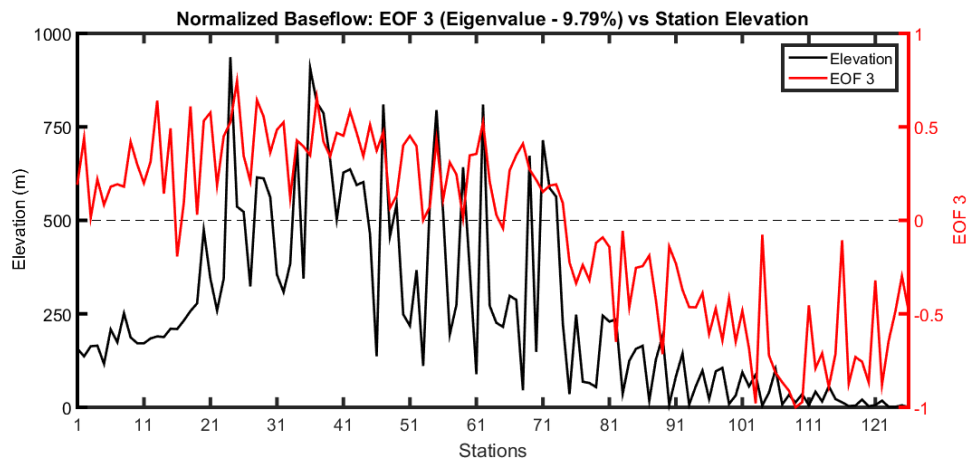


Figure 71: EOF 3 and elevation of 126 stations. Stations in the western portion that are mostly in mountainous terrain in the Blue Ridge and Valley and Ridge Provinces have non-stationarity and variability in the same direction, while stations 75 and above located in the eastern portion of the Piedmont Province and Coastal Plain exhibit non-stationarity in the same direction (opposite to that of the western stations).

The difference in topographic relief or underlying rock type and subsequent differences in aquifer behavior could explain this dichotomy. The transition of the EOF from positive to negative occurs exactly where there is a notable drop off in station elevation. At higher elevations baseflow is likely to fluctuate more so than at lower elevations simply because water is less likely to sit locally, but rather move with the topographic gradient downhill (Priest, 2004). This differs from lower elevation streams that have may have a lower fraction of local baseflow contributing to total streamflow than the upper elevation stations do, but can also have longer term baseflow contribution from incoming nonlocal sources at higher elevation (Winter, 1998; Faye and Mayer, 1990). In the Coastal Plain and the topographically low eastern region of the Piedmont Province aquifers are in carbonate rocks and sandstone, while in the mountainous portion of the Piedmont Province and Blue Ridge Province are largely metamorphic and igneous rocks. The Valley and Ridge province is largely folded and thrust faulted sandstone, while the Appalachian Plateau is also sandstone but layered instead (Trapp Jr. and Horn, 1997). If elevation and topographic relief were the sole influences on normalized baseflow variance in the third principal component then the first 20 stations should have had a negative EOF response similar to the more eastern stations that are also at lower elevations, but they do not. The first 20 stations EOF 3 responses are in the same positive regime as those in the mountains, which tells you that the underlying geology and physiographic region has some impact. It appears that there

is a fundamental difference between the Coastal Plain and eastern section of the Piedmont Province and the rest of physiographic regions in question looking at Fig. 71. Metamorphic and igneous rocks that underlie most of the Blue Ridge and western Piedmont Provinces are consolidated crystalline rocks. Other underlying rock of the physiographic regions other than the Coastal Plain includes consolidated sedimentary rock from older geologic periods such as the Paleozoic or Precambrian. The older the rock, the better consolidated it is. The eastern Piedmont Province and Coastal Plain consist of semi consolidated and unconsolidated sedimentary rock from younger geologic periods such as the Cretaceous or Quaternary (Trapp Jr. and Horn, 1997), (see Fig. A4 for geology). This distinction would in fact lead to a difference in behavior and response of baseflow due to the difference in movement of groundwater depending on whether an aquifer is classified as consolidated or unconsolidated (Bachman et al., 1998). Fractures that occur in crystalline and consolidated rock provide a faster mode of transport for baseflow (Wendland, 2009) especially in regions with topographic relief, but can also favor less baseflow contribution as a fraction of total streamflow because such bedrock is less permeable (depending on the nature of the fracture) and the slope favors increased runoff. The impact of the unconsolidated silt and clay (low permeability) of the Coastal Plain, and thus an even slower baseflow response than in the Blue Ridge where there is an elevation gradient and fracturing, is visible in Fig. 57 and 62. The Blue Ridge Province stations have the majority of the variance concentrated

in one or two large peaks, whereas the Coastal Plain stations have more spread out and elongated periods of higher variance (decades as opposed to several years). An anomalous baseflow event in the Blue Ridge Province is shorter lived (years) than in the Coastal Plain (decade) due to the shorter amount of time it takes for groundwater to move through fractures on an elevation gradient than it does to move through silt and clay at almost no elevation gradient. Combining classification based on physiographic region and underlying geology (Bachman et al., 1998; Bloomfield et al., 2009) would likely provide greater insight to variable baseflow response.

6. Conclusions

The main contributions of this thesis are 1) baseflow estimation from discharge observations that is physically meaningful, readily reproducible, and takes into account the characteristic hydrology of the individual basin in question; 2) associating strong patterns of variability in baseflow with climate phenomena (i.e. ENSO), decadal variability, and frequencies of hurricanes and tropical storms; 3) elucidating the importance of treating the MRB as a combined system with built in natural demand in the form of an instream flow requirement and how that allows stakeholders in the basin to assess their current level of sustainable use; 4) exploring the use of a physically-based model to link stream water availability with water states in the watershed, especially during periods of little rain; 5) the determination of the major influences on regional baseflow variability.

The main contributor of variance to normalized baseflow among the 126 stations was found to be the presence of precipitation or lack of precipitation. The second contributing factor was the relationship between summer precipitation and the frequency and trajectory of tropical cyclones. The third contributor was found to be the hydrogeology of the station location including elevation and topographic relief, physiographic region, and underlying geology.

With increasing human presence, impact, and the resulting increase in water demand in combination with potential changes in precipitation, there may be an

increased interest in analyzing water availability from the point of view of drought and the associated controlling baseflow as well as combined natural and human demand in order to ensure continued water security.

6.1 Limitations

Some limitations with regard to the model simulations with the DCHM derive from the short duration (1 water year) simulation (October 1, 2007 – September 30, 2008), thus not actually reproducing interannual variability as in Tao and Barros (2014a,b). The accuracy of the precipitation input data is a key source of uncertainty and places a limit on how accurate the model can get each hydrograph peak and recession. The DCHM also only takes into account local groundwater interactions and the location of the MRB relative to other river basins suggests that there should be some sort of regional groundwater interaction with basins located at higher elevations in the Blue Ridge Province. A limitation of the unsustainable days and level of human interaction known or unknown is that there are stakeholders on the river in between the USGS gauge location and the WTP locations so the amount that reaches the WTPs may not be exactly what it was at the USGS gauge. General estimation of human demand is inexact due to a lack of complete data on every source or sink of water (surface and subsurface) in the MRB. Groundwater withdrawals are largely unknown for the region with installations in the basin since 2000 on record, but the vast majority of groundwater wells have been in place long before then.

6.2 Contributions

Using a combination of filters to obtain a baseflow estimate based solely on aquifer/groundwater contribution as opposed to what is normally estimated as baseflow after one graphical filter pass ensures that only the groundwater contribution is taken into account, and not any deeper interflow. The algorithm for baseflow separation was developed for the Mills River, but was able to be readily applied to the other 125 stations in the greater region. Using baseflow response and long term variability to classify hydrologic regimes would be one contribution. The streamflow in Mills River has become much more extreme with multiple extended periods of low flow in recent decades. This would suggest that there has been a shift in climate. Determining a metric by which a basin's level of sustainability with regard to water use can also be applied to other basins. The main thing is to establish a reasonable minimum instream flow requirement so that there is a combination of natural and human systems, with the natural system having a baseline requirement.

The differing definitions of baseflow can impact what method of baseflow separation is deemed appropriate. Here the baseflow that was of interest was solely the groundwater contribution to streamflow, which was the reason for using a second filter and seeking lower estimates than the one filter WS90 method that defines baseflow as groundwater and lower subsurface layer contributions to streamflow. By the strict

definition of groundwater contributions only, these lower layer contributions would qualify as interflow.

Attributing the variance of normalized baseflow to precipitation contributions, tropical cyclone tracks, and physiography and hydrogeology can help to understand what the response of groundwater aquifers in different areas will be under future scenarios and determine if certain aquifers are more resilient to changes in extreme events (droughts and tropical storms).

6.3 Recommendations for Potential Future Work

Some recommendations for future work on the subject at hand would include interpolating the Stage IV precipitation data using other gauge stations in the MRB region to try to mitigate error and uncertainty in input data that is then translated to uncertainty and error in output. Another piece of future work would include reclassifying clusters of similar stations based on what larger river basin the station is a member of in combination with geology, physiography, and geography.

Appendix A

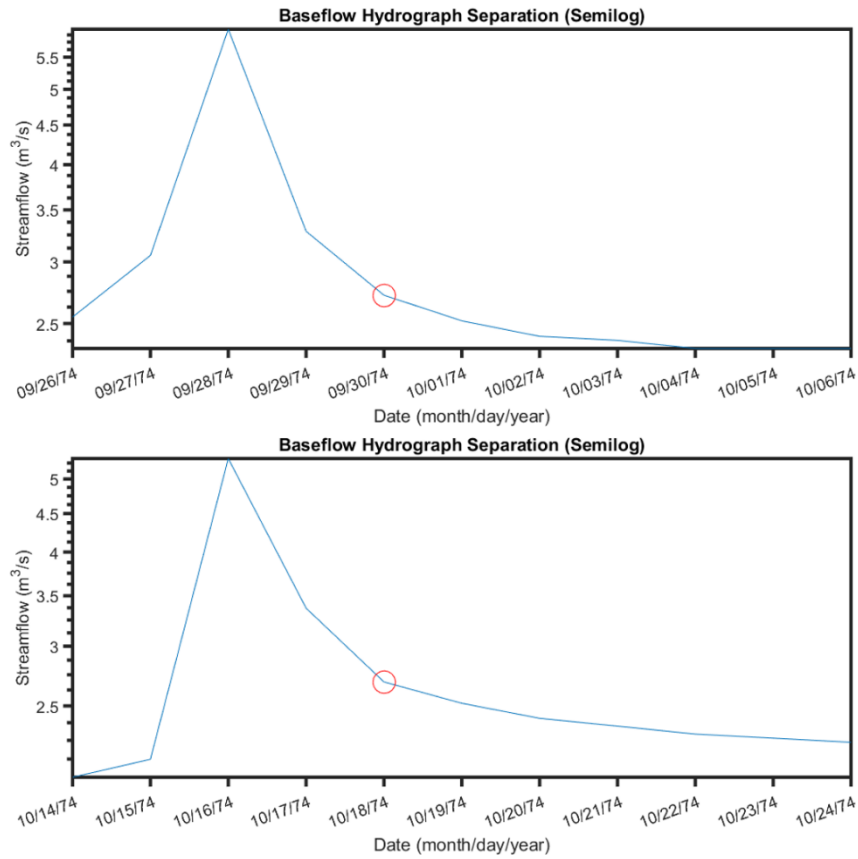


Figure A1: Semi logarithmic plot of two example hydrographs (seen in Fig. 5). The red circle marks the second change in slope of the hydrograph after the peak. This marks the beginning of the baseflow recession curve. The red circles are also the points calculated as N days after the peak, which shows that the chosen recession period definition is in agreement with the graphical definition of the start of the baseflow recession curve.

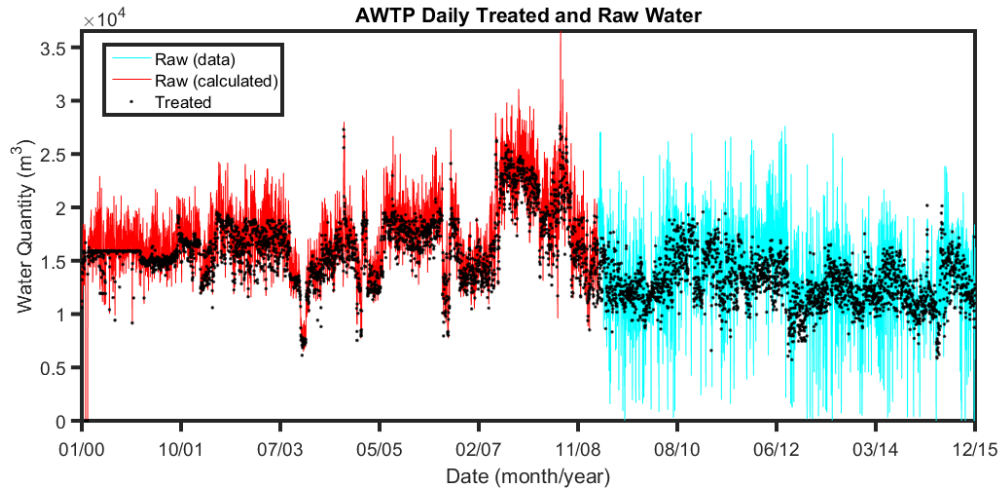


Figure A2: Asheville Water Treatment Plant river uptake data. WTP daily quantity of water treated data available for length of record (2000-2015), but raw water withdrawn from Mills River only available for 2009-2015 (cyan color). Average ratio per day of year between treated and raw water for 2009-2015 was calculated and the applied to treated data for 2000-2009 to obtain an estimate for raw water (red color).

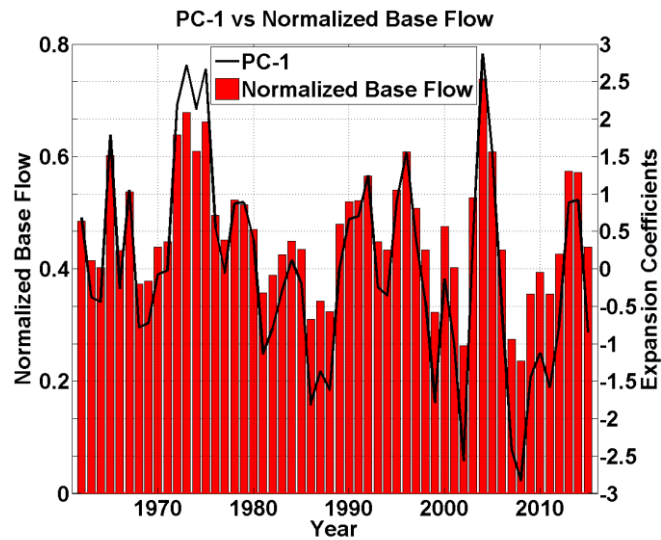


Figure A3: The principal components are calculated from the mean time series of normalized baseflow of all 126 stations. It is expected that PC 1 would be in agreement with most of the mean time series since it captures most of the variance. The regions where there is not perfect agreement can be explained by PC 2 and 3.

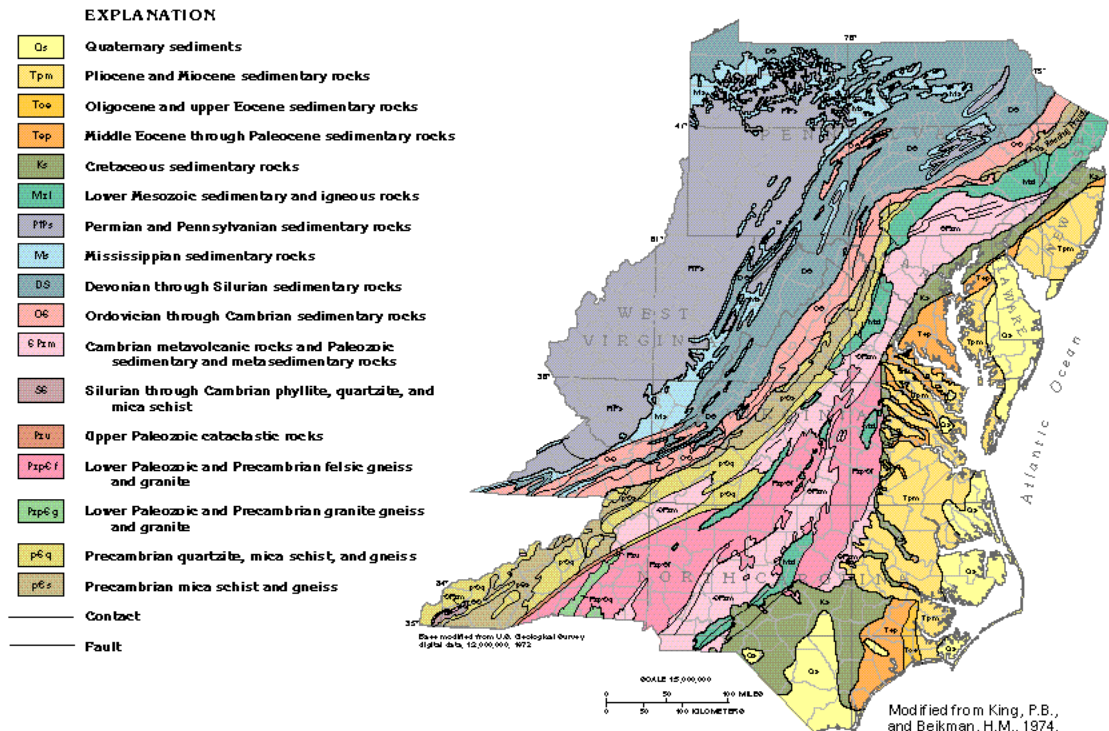


Figure 8. A simplified geologic map shows the extent of the major rock units in Segment 11. Glacial and alluvial deposits in the northern and western parts of the segment are not mapped.

Figure A4: Underlying geology (focusing on North Carolina here). Note that age increases as you go down the explanation of colors. Older rocks (more consolidated) are in the western and central part of the state where the mountainous regions are. Younger rocks (less consolidated) are located in the eastern portion of the state. This accounts for some of the difference in variability and timing of baseflow at different stations throughout the region.

Appendix B

Human demand for 2008 Water Year (drought year) (Eq. 9)

$-RW_w - GW_w + \text{Loss/return}$

Calculation of river water withdrawal, $RW_w = \text{HWTP} + \text{AWTP}$

HWTP (all 3 intakes) = 8,441,600 m³

AWTP = 8,052,500 m³

$RW_w = 8,441,600 \text{ m}^3 + 8,052,500 \text{ m}^3 = 16,494,100 \text{ m}^3$

Calculation of groundwater withdrawal, $GW_w = \text{Agriculture} + \text{Residential} + \text{other}$

Calculation of agricultural groundwater.

2,562 acres of agricultural land in MRB (Mills River Partnership, Inc., 2015).

Henderson County data (USDA, 2012) states that 27.4% of agricultural land is wooded, therefore farmable land = $.726 * 2,562 = 1,860$ acres.

Drip irrigation is commonly used (Kirby Johnson).

1,000 gal/acre/day drip irrigation (Stanley and Clark, 2004; Swistock, 2016).

Crops in MRB consist of corn, tomatoes, and peppers, assume a growing season of four months (120 days).

$(1,860 \text{ acres}) * (1,000 \text{ gal/acre-day}) * (0.00378541 \text{ m}^3/\text{gal}) * (120 \text{ days}) = 844,903 \text{ m}^3$

Calculation of residential groundwater

2876 residents in MRB (McGill Associates, 2012). 2.5 people per household in Mills River, 1150 residences in MRB. Mills River is 45% rural, 55% urban, assume urban residents receive piped water and do not use groundwater wells and only consider 45% of residences (518). Typical residence in the area uses 200 gallons/day (NCDENR, Andrew Moore, Brett Laverdy, personal correspondence).

$(518 \text{ residences}) * (200 \text{ gal/residence-day}) * (0.00378541 \text{ m}^3/\text{gal}) * (366 \text{ days}) = 143,141 \text{ m}^3$

Other

HWTP pumps out 20 gal/min of groundwater to keep the large holding tank from floating due to high groundwater levels.

$(20 \text{ gal/min}) * (1440 \text{ min/day}) * (0.00378541 \text{ m}^3/\text{gal}) * (366 \text{ days}) = 39,901 \text{ m}^3$

$GW_w = 844,903 \text{ m}^3 + 143,141 \text{ m}^3 + 39,901 \text{ m}^3 = 1,027,945 \text{ m}^3$

Loss/return

HWTP uses 180,000-200,000 gallons/day for testing and then releases back to the river.

$(190,000 \text{ gal/day}) * (0.00378541 \text{ m}^3/\text{gal}) * (366 \text{ days}) = 263,237 \text{ m}^3$

It was calculated that Hendersonville Water Municipality loses ~25% of water due to pipe leakages, but the vast majority of pipeline is outside the MRB and thus almost all losses would not be returned to MRB, which is why this factor is not estimated here. Wastewater contributions are not taken into account.

$-RW_w - GW_w + \text{Loss/return}$, based on Eq. 9.

$-16,494,100 \text{ m}^3 - 1,027,945 \text{ m}^3 + 263,237 \text{ m}^3 = -17,258,808 \text{ m}^3$ (human influence on entire basin)

Convert to per unit area.

$-17,258,808 \text{ m}^3 / (190.1 \text{ km}^2 * 1000 \text{ m/km} * 1000 \text{ m/km}) = -0.090788 \text{ meters} = -90.8 \text{ mm per unit area.}$

Bibliography

- Arnold, J. G., Allen, P. M., Muttiah, R. and Bernhardt, G. (1995), "Automated Base Flow Separation and Recession Analysis Techniques," *Ground Water*, 33: 1010–1018.
- Arnold, J.G. and Allen, P.M. (1999), "Automated Methods for Estimating Baseflow and Ground Water Recharge From Streamflow Records," *JAWRA Journal of the American Water Resources Association*, 35: 411–424.
- Bachman, L.J., Lindsey, B.D., Brakebill, J.W., and Powars, D.S. (1998). "Ground-water discharge and base-flow nitrate loads of nontidal streams, and their relation to a hydrogeomorphic classification of the Chesapeake Bay watershed, middle Atlantic coast" (p. 72). US Department of the Interior, US Geological Survey.
- Barros, A. P. (1995). "Adaptive multilevel modeling of land-atmosphere interactions." *Journal of climate*, 8(9), 2144-2160.
- Barros, A. (2013), "Orographic Precipitation, Freshwater Resources, and Climate Vulnerabilities in Mountainous Regions," in *Climate Vulnerability*, ed. Roger Pielke, pp. 57-78, Academic Press, Oxford.
- Battisti, D.S., and Naylor, R.L. (2009). "Historical Warnings of Future Food Insecurity with Unprecedented Seasonal Heat. *Science*, 323(5911): 240-244.
- Bjornsson, H., and S. A. Venegas. (1997). "A manual for EOF and SVD analyses of climatic data." *CCGCR Report 97*, no. 1: 112-134.
- Bloomfield, J.P., Allen, D.J., and Griffiths, K. J. (2009). "Examining geological controls on baseflow index (BFI) using regression analysis: An illustration from the Thames Basin," UK. *Journal of Hydrology*, 373(1), 164-176.
- Blume, T., Zehe, E., and Bronstert, A. (2007). "Rainfall—Runoff Response, Event-based Runoff Coefficients and Hydrograph Separation." *Hydrological Sciences Journal*, 52(5): 843-862.
- Brun, J. and Barros, A. (2014), "Mapping the role of tropical cyclones on the hydroclimate of the southeast United States: 2002–2011," *Int. J. Climatol.* 34: 494–517
- Caruso, B.S. (2000), "Evaluation of low-flow frequency analysis methods." *Journal of Hydrology New Zealand*, 39(1): 19-47.

- Caruso, B.S., Rademaker, M., Balme, A., and Cochrane, T.A. (2013), "Flood modelling in a high country mountain catchment, New Zealand: comparing statistical and deterministic model estimates for ecological flows," *Hydrological Sciences Journal*, 58 (2): 1–14.
- Chapman, T. (1999), "A comparison of algorithms for stream flow recession and baseflow separation," *Hydrol. Process.*, 13: 701–714.
- Curtis, Scott. "The Atlantic multidecadal oscillation and extreme daily precipitation over the US and Mexico during the hurricane season." *Climate Dynamics* 30.4 (2008): 343-351.
- Dai, Z.J., Chu, A., Du, J.Z., Stive, M., and Hong, Y. (2010). "Assessment of Extreme Drought and Human Interference on Baseflow of the Yangtze River." *Hydrological Processes*, 24(6): 749-757.
- Davis, C. (2015) "NC Extremes: 2007's Drought Emerged Quickly, Affected Millions in NC" State Climate Office of North Carolina.
- Dellapenna, J.W. (2003). "Adapting Riparian Tights to the Twenty-First Century." *W. Va. L. Rev.*, 106, 539.
- Devonec, E., & Barros, A. P. (2002). "Exploring the transferability of a land-surface hydrology model." *Journal of Hydrology*, 265(1), 258-282.
- Eckhardt, K. (2008). "A Comparison of Baseflow Indices, which were Calculated with Seven Different Baseflow Separation Methods." *Journal of Hydrology*, 352(1): 168-173.
- Faye, R.E., and Mayer, G.C. (1990). "Ground-water flow and stream-aquifer relations in the northern coastal plain of Georgia and adjacent parts of Alabama and South Carolina" (No. 88-4143). US Geological Survey; Books and Open-File Reports Section [distributor].
- Fraley, S., and Simmons, J. W. (2006). "An Assessment of Selected Rare Mussel Populations in Western North Carolina Following Extraordinary Floods of September 2004." *North Carolina Wildlife Resources Commission*.
- Gleick, P. H. (1998). "Water in Crisis: Paths to Sustainable Water Use," *Ecological applications*, 8(3): 571-579.

- Gossling, S. (2001) "The Consequences of Tourism for Sustainable Water Use on a Tropical Island: Zanzibar, Tanzania," *Environmental Management*, 61(2): 179-191.
- Groisman, P.Y., Knight, R.W., Easterling, D.R., Karl, T.R., Hegerl, G.C., and Razuvaev, V.N. (2005). "Trends in Intense Precipitation in the Climate Record. *Journal of climate*, 18(9): 1326-1350.
- Grumbine, R.E. (1994) "What is Ecosystem Management?" *Conservation Biology*, 8(1): 27-38.
- Grumbine, R.E. (1997) "Refelctions on 'What is Ecosystem Management?'" *Conservation Biology*, 11(1): 41-47.
- Hao, L., Sun, G., Liu, Y., and Qian, H. (2015), "Integrated Modeling of Water Supply and Demand under Management Options and Climate Change Scenarios in Chifeng City, China." *Journal of the American Water Resources Association*, 51(3): 655-671.
- Hobbs Jr, G.J. (2013). "Reviving the Public Ownership, Antispeculation, and Beneficial Use Moorings of Prior Appropriation Water Law." *U. Colo. L. Rev.*, 84, 97.
- Jarvis, J.D. (2011). "Water Quality in the Upper Little Tennessee River and its Potential Effects on the Appalachian Elktoe Mussel (*ALASMIDONTA RAVENELIANA*) (Doctoral dissertation, Western Carolina University).
- King, P.B., and Beikman, H.M., (1974). Geologic map of the United States: U.S. Geological Survey, scale 1:2,500,000, 3 sheets.
- Labotka, D.M., Grissino-Mayer, H.D., Mora, C.I., and Johnson, E.J. (2015). "Patterns of moisture source and climate variability in the southeastern United States: a four-century seasonally resolved tree-ring oxygen-isotope record." *Climate Dynamics*, 46(7): 2145-2154.
- Leu, M., Hanser, S.E., and Knick, S.T. (2008). "The Human Footprint in the West: A Large-Scale Analysis of Anthropogenic Impacts." *Ecological Applications*, 18(5): 1119-1139.
- Linsley, R. K., Kohler, M.A., and Paulhus, J.L.H. (1958). *Hydrology for Engineers*. New York: McGraw-Hill, Print.
- Lloyd Jr., O.B., and Lyke, W.L. (1995). Hydrologic Atlas 730-K. U.S. Geological Survey.

- Loucks, D., Stakhiv, E., and Martin, L. (2000). "SUSTAINABLE WATER RESOURCES MANAGEMENT." *J. Water Resour. Plann. Manage.*, 126:2(43), 43-47.
- Lyne, V. and Hollick, M. (1979), "Stochastic time-variable rainfall-runoff modelling", Proceedings of the Hydrology and Water Resources Symposium, Perth, 10-12 September, Institution of Engineers National Conference Publication, No. 79(10): 89-92.
- Maxwell, J.T., Ortengren, J.T., Knapp, P.A., and Soulé, P. T. (2013). "Tropical cyclones and drought amelioration in the Gulf and southeastern coastal United States." *Journal of Climate*, 26(21), 8440-8452.
- McCabe, G.J., Palecki, M.A., and Betancourt, J. L. (2004). "Pacific and Atlantic Ocean influences on multidecadal drought frequency in the United States." *Proceedings of the National Academy of Sciences*, 101(12), 4136-4141.
- McGill Associates, (2012), A Review of the 2002 Mills River Watershed Management Strategy, Ten Years Later (MRWMS).
- McKay, S. Kyle, (2015), "Quantifying Tradeoffs Associated with Hydrologic Environmental Flow Methods," *Journal of the American Water Resources Association*, 1-11.
- Mead, J. (2002). "Proposed Conditions for Expansion of Hendersonville's Intake on the Mills River." NCDENR (North Carolina Department of Environmental and Natural Resources), Division of Water Resources.
- Meinshausen, M., Meinshausen, N., Hare, W., Raper, S.C., Frieler, K., Knutti, R., Frame, D.J and Allen, M.R. (2009). "Greenhouse-gas Emission Targets for Limiting Global Warming to 2 C." *Nature*, 458(7242): 1158-1162.
- Mesinger, F., DiMego, G., Kalnay, E., Mitchell, K., Shafran, P. C., Ebisuzaki, W., Jovic, D., Woollen, J., Rogers, E., Berbery, E. H., Ek, M. B., Fan, Y., Grumbine, R., Higgins, W., Li, H., Lin, Y., Manikin, G., Parrish, D., and Shi, W. (2006) "North American regional reanalysis", *B. Am. Meteorol. Soc.*, 87: 343-360,
- Mills River Partnership, Inc. (2015), Mills River Integrated Watershed Management Plan and Source Water Protection Plan.
- Mo, K.C., Schemm, J.K.E., and Yoo, S.H. (2009). "Influence of ENSO and the Atlantic multidecadal oscillation on drought over the United States." *Journal of Climate*, 22(22), 5962-5982.

- Monticino, M., Acevedo, M., Callicott, B., Cogdill, T., and Lindquist, C. (2007) "Combined Human and Natural Systems: A Multi-Agent-Based Approach," *Environmental Modelling & Software*, 22 (5): 656–663.
- Murphy, R., Graszekiewicz, Z., Hill, P., Neal, B., Nathan, R., and Ladson, T. (2009), Australian Rainfall and Runoff Revision Project 7: Baseflow for Catchment Simulation. Stage 1 report – Volume 1 – Selection of Approach. Engineers Australia.
- Nathan, R. J. and McMahon, T.A. (1990), "Evaluation of automated techniques for base flow and recession analyses", *Water Resour. Res.*, 26(7): 1465–1473.
- National Hurricane Center <https://coast.noaa.gov/hurricanes/>
- Neves, R.J., Bogan, A.E., Williams, J.D., Ahlstedt, S.A., and Hartfield, P.W. (1997). "Status of Aquatic Mollusks in the Southeastern United States: A Downward Spiral of Diversity." *Aquatic fauna in peril: the southeastern perspective. Special Publication, 1*, 43-85.
- Nogueira, M., Barros, A., (2014). The Integrated Precipitation and Hydrology Experiment – Hydrologic Applications for the Southeast US (IPHEX-H4SE) Part III: High-Resolution Ensemble Rainfall Products. Report EPL-2013-IPHEX-H4SE-3, EPL/Duke University (Pub.), p. 80.
- Nogueira, M., Barros, A.P., (2015). Transient stochastic downscaling of quantitative precipitation estimates for hydrological applications. *J. Hydrol.* 529, 1407–1421.
- Pahl-Wostl, C., Mostert, E., and Tàbara, D. (2008). "The Growing Importance of Social Learning in Water Resources Management and Sustainability Science." *Ecology and Society*, 13 (1): 24.
- Peters, E., Van Lanen, H.A J., Torfs, P.J.J.F., and Bier, G. (2005). "Drought in groundwater—drought distribution and performance indicators." *Journal of Hydrology*, 306(1), 302-317.
- Pettyjohn, W.A., and Henning, R. (1979), "Preliminary Estimate of Ground-Water Recharge Rates, Related Streamflow and Water Quality in Ohio," Ohio State University Water Resources Center Project. Completion Report Number 552.
- Priest, S. (2004). Evaluation of ground-water contribution to streamflow in coastal Georgia and adjacent parts of Florida and South Carolina. US Department of the Interior, US Geological Survey.

- Raju, K.S., Duckstein, L., and Arondel, C. (2000) "Multicriterion Analysis for Sustainable Water Resources Planning: A Case Study in Spain," *Water Resources Management* 14(6): 435-456.
- Richter, B.D., Matthews, R., Harrison, D.L, and Wigington, R. (2003). "Ecologically Sustainable Water Management: Managing River Flows for Ecological Integrity," *Ecological Applications*, 13(1): 206–224.
- Richter, B.D. (2009), "Re-thinking environmental flows: from allocations and reserves to sustainability boundaries." *River Res. Applic.*, 26: 1052–1063.
- Richter, B. D., Davis, M. M., Apse, C., and Konrad, C. (2012). "A Presumptive Standard for Environmental Flow Protection. *River Research and Applications*, 28(8): 1312-1321.
- Riggs, H.C. (1972). Low flow investigations. Techniques of Water Resources Investigations of the USGS, Book 4, Hydrological Analysis and Interpretation, Washington DC, 18 pp.
- Risley, J.C. (1994). Estimating the Magnitude and Frequency of Low Flows of Streams in Massachusetts. USGS Water-Resources Investigations Report 94-4100, 34 pp.
- Riverlink. <http://riverlink.org/learn/about-riverlink/history-of-french-broad-river/>
- Schlenker W. and Roberts, M. (2009) "Nonlinear Temperature Effects Indicate Severe Damages to US Crop Yields under Climate Change". *Proceedings of the National Academy of Sciences* 106(37): 15,594– 15,598.
- Schwarz, G. and Alexander, R. (1995), "Soils data for the conterminous United States derived from the NRCS State Soil Geographic (STATSGO) data base," US Geological Survey Open-File Report, 95-449.
- Scophocleous, M. (1997) "Managing water resources systems: why "safe yield" is not sustainable." *Ground Water*, 35 (4) p. 561.
- Stanley, C.D., and Clark, G.A. (2004). "Water Requirements for Drip-irrigated Tomato Production in Southwest Florida". University of Florida Cooperative Extension Service, Institute of Food and Agricultural Sciences, EDIS.
- Swistock, Bryan (2016). Water System Planning—Estimating Water Needs. Penn State College of Agricultural Sciences

- Szilagyi, J., and Parlange, M.B. (1998). "Baseflow Separation Based on Analytical Solutions of the Boussinesq Equation. *Journal of Hydrology*, 204(1): 251-260.
- Tallaksen, L. M. (1995), "A Review of Baseflow Recession Analysis," *J. Hydrol.* 165: 349-37.
- Tao, H., Gemmer, M., Bai, Y., Su, B., and Mao, W. (2011). "Trends of Streamflow in the Tarim River Basin During the Past 50 Years: Human Impact or Climate Change?" *Journal of hydrology*, 400(1): 1-9.
- Tao, J., and Barros, A. P. (2013). "Prospects for flash flood forecasting in mountainous regions—An investigation of Tropical Storm Fay in the Southern Appalachians." *Journal of Hydrology*, 506, 69-89.
- Tao, J. and Barros, A.P., (2014a). The Integrated Precipitation and Hydrology Experiment. Part I: Quality High-Resolution Landscape Attributes Datasets. Report EPL-2013-IPHEX-H4SE-1, EPL/Duke University (Pub.), V.1., 60 pp. <http://dx.doi.org/10.7924/G8H41PBG>
- Tao, J. and Barros, A.P., (2014b). The Integrated Precipitation and Hydrology Experiment. Part II: Atmospheric Forcing and Topographic Corrections. Report EPL-2013-IPHEX-H4SE- 2, EPL/Duke University (Pub.), V.1., 80pp. <http://dx.doi.org/10.7924/G8RN35S6>
- Tao, J. and Barros, A.P. (2014c), "Combined prediction of flood response and debris flow initiation during warm- and cold-season events in the Southern Appalachians, USA," *Hydrol. Earth Syst. Sci.*, 18: 367–388.
- Tao, J., et al. Operational hydrological forecasting during the IPHEX-IOP campaign – Meet the challenge. *J. Hydrol.* (2016), <http://dx.doi.org/10.1016/j.jhydrol.2016.02.019>
- Tarlock, A.D. (2001). "Future of Prior Appropriation in the New West," *Natural Resources Journal*, 41, 769.
- Torrence, C. and Compo, G.P. (1998), "A practical guide to wavelet analysis." *Bull. Amer. Meteor. Soc.*, 79: 61–78.
- Trapp Jr., H., and Horn, M.A. (1997). Hydrologic Atlas 730-L. U.S. Geological Survey.
- United States Census Bureau. <http://factfinder.census.gov/faces/tableservices/jsf/pages/productview.xhtml?pid>

=PEP_2014_PEPANNRES&prodType=table
<http://www.census.gov/popest/data/intercensal/st-co/files/CO-EST2001-12-37.pdf>
<http://www.census.gov/popest/data/intercensal/county/tables/CO-EST00INT-01/CO-EST00INT-01-37.csv>
<https://www.census.gov/population/www/censusdata/PopulationofStatesandCountiesoftheUnitedStates1790-1990.pdf>
<http://www.census.gov/quickfacts/table/PST045215/3743260>

United States Department of Agriculture (USDA). (2012). Census of Agriculture - County Data USDA, National Agricultural Statistics Service. https://www.agcensus.usda.gov/Publications/2012/Full_Report/Volume_1,_Chapter_2_County_Level/North_Carolina/st37_2_001_001.pdf
https://www.agcensus.usda.gov/Publications/2012/Online_Resources/County_Profilefiles/North_Carolina/cp37089.pdf

Van Loon, A. F., & Laaha, G. (2015). "Hydrological drought severity explained by climate and catchment characteristics." *Journal of Hydrology*, 526, 3-14.

Viviroli D., Archer, D.R., Buyaert, W., Fowler, H.J., Greenwood, G.B., Hamlet, A.F., Huang, Y., Koboltschnig, G., Litaor, M.I., Lopez-Moreno, J.I., Lorentz, S., Schadler, B., Schreier, H., Schwaiger, K., Vuille, M., and Woods, R. (2011), "Climate Change and Mountain Water Resources: Overview, Recommendations for Research, Management and Policy." *Hydrol. Earth Syst. Sci.* 15: 471-504.

Vogel, R. M., and Kroll, C.N. (1992), "Regional geohydrologic-geomorphic relationships for the estimation of low-flow statistics", *Water Resour. Res.*, 28(9): 2451-2458.

Vorosmarty, C.J., Green, P., Salisbury, J., and Lammers, R.B. (2000). "Global Water Resources: Vulnerability from Climate Change and Population Growth," *Science*, 289, Issue 5477: 284-288.

Wang, H., Fu, R., Kumar, A., and Li, W. (2010). "Intensification of Summer Rainfall Variability in the Southeastern United States During Recent Decades." *Journal of Hydrometeorology*, 11(4): 1007-1018.

Weaver, J.C., (2002), "The drought of 1998-2002 in North Carolina—Precipitation and hydrologic conditions" U.S. Geological Survey Scientific Investigations Report 2005-5053, 88 p.

Wendland, F., Kunkel, R., Kunstmann, H., Lingemann, I., Knoche, R., and Tetzlaff, B. (2009). "Area differentiated analysis of impacts of climate change scenarios on ground-water resources in Northwestern Germany." *Wasser im Gartenbau*, 11.

- White, K. E., and Sloto, R. A., (1990), "Base-flow frequency characteristics of selected Pennsylvania streams" Water-Resources Investigations Report 90-4160, USGS.
- Wilson, A.M., and Barros, A.P. (2015). "Landform controls on low level moisture convergence and the diurnal cycle of warm season orographic rainfall in the Southern Appalachians." *Journal of Hydrology*, 531, 475-493.
- Winter, T. C. (Ed.). (1998). "Ground water and surface water: a single resource" (Vol. 1139). DIANE Publishing Inc.
- Wittenberg, H. (2003), "Effects of Season and Man-made Changes on Baseflow and Flow Recession: case studies." *Hydrol. Process.*, 17: 2113–2123.
- Wu, X., Jeuland, M., Sadoff, C., and Whittington, D. (2013), "Interdependence in Water Resource Development in the Ganges: An Economic Analysis. *Water Policy* 15:89-108.
- Yildiz, O., (2001). Assessment and Simulation of Hydrologic Extremes by a Physically Based Spatially Distributed Hydrologic Model. Ph.D. Thesis, The Pennsylvania State University, University Park, PA, USA.
- Yildiz, O., and Barros, A. P. (2005). "Climate variability, water resources, and hydrologic extremes—modeling the water and energy budgets." *Climate and Hydrology in Mountain Areas*, 291-306.
- Yildiz, O., & Barros, A. P. (2007). "Elucidating vegetation controls on the hydroclimatology of a mid-latitude basin." *Journal of hydrology*, 333(2), 431-448.
- Yıldız, O., & Barros, A. P. (2009). "Evaluating spatial variability and scale effects on hydrologic processes in a midsize river basin." *Scientific Research and Essays*, 4(4), 217-225.